Summer 2012

Diverse Sample Analysis and Sample Preparation Studies Utalizing AP - MALDI-TOF-MS

Sara May Kallop

DIVERSE SAMPLE ANALYSIS AND SAMPLE PREPARATION STUDIES UTILIZING AP-MALDI-TOF-MS

A Dissertation

Submitted to the Bayer School of Natural and Environmental Sciences

Duquesne University

In partial fulfillment of the requirements for

the degree of Doctor of Philosophy

By

Sara May Kallop

August 2012

DIVERSE SAMPLE ANALYSIS AND SAMPLE PREPARATION STUDIES UTILIZING AP-MALDI-TOF-MS

By

Sara May Kallop

June 5, 2012

_____	_____
Stephanie J. Wetzel Assistant Professor of Chemistry (Committee Chair)	H. M. 'Skip' Kingston Professor of Chemistry (Committee Member)
_____	_____
Ellen Gawalt Assistant Professor of Chemistry (Committee Member)	Maura Donahue Environmental Protection Agency (Committee Member)
_____	_____
David Seybert Dean, School Name Professor of Chemistry and Biochemistry	Ralph Wheeler Chair, Department of Chemistry and Biochemistry Professor of Chemistry

ABSTRACT

DIVERSE SAMPLE ANALYSIS AND SAMPLE PREPARATION STUDIES UTILIZING AP-MALDI-TOF-MS

By

Sara May Kallop

August 2012

Dissertation supervised by Stephanie J. Wetzel Ph.D.

Sample preparation and analysis for atmospheric pressure matrix assisted laser desorption ionization time of flight mass spectrometry (AP – MALDI-TOF-MS) was investigated. By investigating the effects that sample preparation has upon MALDI signal, better analysis can be carried out. The influence of sample deposition was studied by not only observing the signal intensity produced but also by quantitation. Isotope dilution mass spectrometry (IDMS) was used for the quantitation of three different analytes. The results indicated that not only was signal greatly affected by sample deposition but the effect on quantitation error was also statistically significant among the three different sample deposition techniques that were evaluated.

Components of sample preparation solution were studied using polyethylene glycol (PEG) and polystryrene (PS) of different weights. This study altered the amounts of matrix, analyte and cationizing agent that were used to make up each sample. Not only did the sample signal intensity greatly vary which had statistical significance but a shifting of the polymer sample peaks was also observed. This confirms that sample preparation is of extreme importance for MALDI analysis.

Carpet fibers, glutathione and cell wall extracts from the bacteria *Staphylococcus Epidermidis* were also studied by AP – MADLI-TOF-MS. These analytes were carefully studied to provide an accurate characterization of each. The diversity of the analytes studied highlights the incredible capabilities that MADLI possesses being able to analyze a range of analytes. Though the samples were diverse each one was able to be completely and comprehensively analyzed using AP – MALDI-TOF-MS.

DEDICATION

I would like to dedicate this work to the people who stood with me – though I could not stand. Those who believed in me whenever I didn't believe in myself:

To my parents who helped me heal and renew my spirit. To my sisters who always believed in me no matter how insurmountable my obstacles became. To my husband who held me up to stand, even when I could not stand myself. He offered me his endless love and support. To my advisors who had infinite patience with me and appreciated my potential even whenever it had been overshadowed by numerous infirmities. I would lastly like to dedicate this work to the select few doctors who didn't give up even when they were faced with anomalies that no textbook could predict. To the few that celebrated my achievements and wept with my hardships. To these remarkable people, to whom I owe so much, I would like to dedicate this work to you to all and offer my eternal gratitude.

ACKNOWLEDGEMENT

I would like to acknowledge a couple of the undergraduate students who have worked with me over the years. First I would like to acknowledge Shana Kilgore, who's tireless work on the carpet fiber project has helped me immensely. I would also like to acknowledge Antonette Cabauatan who found little ways to help and encourage me.

TABLE OF CONTENTS

Page

LIST OF TABLES

Page

LIST OF FIGURES

Page

LIST OF ABBREVIATIONS

AP – MALDI-TOF-MS: atmospheric pressure matrix assisted laser desorption ionization time of flight mass spectrometry

m/z: mass to charge ratio

ESI: electrospray ionization

NanoESI: nanoelectrospray ionization

APCI: atmospheric pressure chemical ionization

SPE: solid phase extraction

MALDI: matrix assisted laser desorption ionization

TOF: time of flight

MS: mass spectrometry

ArF laser: Argon Flouride laser

KrF laser: Krypton Flouride laser

XeCl laser: Xenon Chloride excimer laser

Nd:YAG laser: neodymium-doped yttrium aluminum garnet solid state laser

N_2 laser: nitrogen laser

ER:YAG laser: Erbium-doped Yttrium Aluminium garnet solid state laser

CO_2 laser: carbon dioxide laser

UV: ultraviolet light

IR: infrared light

Vis: visible light

OPO: optical parametric ocillators

n_m : molecular number density of the sample

L_p : depth of laser penetration

F_{th}: threshold of laser fluence that needs to be reached for the observation of the exponential release of molecules from the sample

E_v^*: the critical energy density of the surface layer

CT: the thermal energy density of the sample preceding laser irradiation

S_1: first excited singlet state

DHB: 2,5-dihydroxybenzoic acid

K: Kelvin

m/s: meter per second

kJ/mol: kilojoules per mole

MH^+: the protonated matrix

A: uncharged analyte

M: the neutral matrix

AH^+: is the protonated analyte

THAP: 2,4,6-trihydroxyacetophenone

GGH: tripeptide glycyl – glycyl – histidine

FT-ICR: Fourier transform ion cyclotron resonance

mbar: millibar

nm: nanometer

ΔG: change in Gibbs free energy

Na: sodium

K: potassium

Cu: copper

PS: polystyrene

eV: electron volts

CHCA: α-Cyano-4-hydroxycinnamic acid

DNA: Deoxyribonucleic acid

nL: nanoliter

D4: four deuterium atoms

C13: carbon 13

LC/MSD/TOF: liquid chromatography mass spectrometry detector time of flight

L/min: liters per minute

V: volts

° C: degrees Celsius

ESD: electrospray deposition

PEG: polyethylene glycol

kV: kilovolt

da: Dalton

RA: retinoic acid

THF: tetrahydrofuran

µL: microliter

µL/min: microliter per minute

ANOVA: analysis of variance

cts: counts

SEM: scanning electron microscope

amu: atomic mass unit

n: number of samples

IDMS: isotope dilution mass spectrometry

W_{sp}: the mass of the labeled standard

C: concentration of the labeled solution

W_s: the mass of the standard solution

R: experimentally measured ratio of sample to labeled standard

B_{sp}: the abundance of unlabeled element within the isotopically enriched standard

B: the probability that the enriched isotope will naturally occur within the non-enriched sample (natural abundance)

A: the natural abundance of the unenriched element that is being used as the isotopic label

µg/g: microgram per gram

SEC: size exclusion chromatography

NMR: nuclear magnetic resonance

MMD: molecular mass distribution

M_n: mass moments

RA: *All-trans*-retinoic acid

NaTFA: Trifluoroacetic acid sodium salt

AgTFA: Trifluoroacetic acid silver salt

MAC: matrix to analyte to cationizing agent

PD: polydispersity

NIST: National Institute of Standards and Technology

MSE: matrix suppression effect

PyGCMS: pyrolysis gas chromatography mass spectrometry

GCMS: gas chromatography mass spectrometry

FTIR: Fourier transform infrared spectroscopy

DCTB: (trans – 2 - [3 - (4 - tert-Butylphenyl) – 2 – methyl – 2 – propenylidene] malononitrile)

GSH: reduced glutathione

GSSG: oxidized glutathione

HPLC: high pressure liquid chromatography

ppm: parts per million

PS/A: polysaccharide/adhesin

PIA: polysaccharide intercellular adhesion

x g: times gravity

min: minute

Chapter 1

Introduction

1.1 Analysis Methods in Analytical Chemistry

Analytical chemistry seeks to discover the chemical and physical properties of different materials found throughout nature.[1] The methodology that is used for the analysis is strongly dependent upon the desired result, whether it is a qualitative or quantitative analysis.[1, 2] Qualitative analysis is an analysis that seeks to identify what components make up a sample, its identity and characteristics. Quantitative analysis not only seeks to identify a sample and its characteristics but also seeks to determine the quantity of the entire sample and the quantity of the sample's components.

Though there has been much advancement within the scientific community to enhance and give new abilities for analysis of our physical world, many shortcomings are still observed.[1] The very physical properties that we seek to elucidate hinder our attempts, as some analytical techniques require the sample to have certain volatility or the ability to be dissolved within an aqueous solution. Due to the diversity of the physical world, the techniques used to analyze it must be just as diverse. Mass spectrometry is an extremely useful technique for analysis. Mass spectrometry measures the mass of molecules that have been ionized reporting a mass to charge ratio (m/z). This m/z is extremely useful for the determination of molecules that compose a sample. Molecule fragmentation can be employed to gain

additional knowledge about the molecule's structure, making mass spectrometry an information rich analysis method for not only compound identification but also for structure elucidation. The fragments produced will have distinct patterns based upon the molecule that is being analyzed. The bond energies can be overcome by inundating the molecule with energy. Once the energy being applied to the molecule becomes greater than the bond energy holding the molecule together, fragmentation will occur. In order for molecules to be able to be detected by a mass spectrometer, the molecule must have a charge. In order to ensure molecular charging a mass spectrometer is always paired with an ionization source. There are a variety of ionization sources available for mass spectrometers that have different benefits and disadvantages, depending upon the analysis objectives.

There are two different types of ionization techniques that are used for mass spectrometry introduction, either hard or soft ionization techniques.[3]

Hard ionization is a technique that fragments the sample as it is being ionized. This is due to the high amount of energy that is being applied to the molecule for ionization.[3] Electron impact ionization is a hard ionization technique that is ionizes the sample by bombardment with electrons.[3, 4] This technique is always conducted within a vacuum chamber that is sufficiently heated. The molecules must be in the gaseous state for proper ionization.[3] This technique can only be applied to molecules that are volatile and have a mass of less than ~1,000 amu, making it a perfect companion for gas chromatography, a separation technique that uses high temperature to convert liquid sample into the gas phase.[3, 4]

Soft ionization is a technique that sparingly transfers energy to the sample. Because there is not an excess of energy, the sample experiences little or even no fragmentation. Often times a spectra of the intact molecule is required for comprehensive analyte analysis. Electrospray and nanospray ionization (ESI and NanoESI) are two examples of a soft ionization techniques. Both are techniques that apply a voltage to sample as it is sprayed into a chamber where the charged molecule is then pulled into the mass spectrometer. The difference between ESI and NanoESI is the volume of sample that is used. ESI uses sample volume of milliliters while NanoESI uses much less sample in the nanoliters. With these methods the charged sample spray is nebulized into the sample chamber where it encounters a heated nitrogen drying gas. This gas evaporates the solvent from the sample droplet causing the droplet to shrink. As the droplet shrinks, the charge has less space and as the charges work to repel one another, the droplet reaches its limit and can no longer contain the charge and an explosion occurs, known as Coloumbic explosion. This Coloumbic explosion results in charged analytes that remain intact. Though the analyte isn't fragmented, a complicated mass spectrum can and usually does result due to multiple charging. This complexity of the spectra can be a significant deterrent. Another deterrent to ESI and NanoESI is the fact that the analyte must be soluble in a solvent system that is acceptable for the instrument's systems. Harsh solvents can degrade fittings and tubing. A sample solution that is basic or acidic can damage instrumentation along with solutions that have a significant salt component. Salts can come out of solution and clog various instrument components resulting in costly repairs.

Another ionization technique that has been recently developed is atmospheric pressure chemical ionization (APCI). It has been refered to as a hybrid technique due to the fact that it is a medium ionization technique, being somewhere between hard and soft ionization. As with electrospray or nanospray a charged sample is sprayed into a sample chamber, only instead of making its way directly to the mass spectrometer, a corona discharge intercepts the sample, ionizing neutral species. This technique gives the analyst a method of ionization that is more efficient than electrospray but the user will observe more fragmentation. The increased fragmentation will lead to spectra that are convoluted, the resulting spectra will not only have various fragments of molecules but will also contain multiply charged species. APCI as ESI and NanoESI, requires the analyte be dissolved into solution for analysis. The same problem with harsh solvents, acids, bases and salts exists with APCI.

Because of the sensitivity of the instruments to different solvents, pH and salts, extensive sample preparation must be executed before any analysis of sample, whether it be by ESI, NanoESI or APCI. Sample preparation, in some cases can be as simple as filtering a sample solution but in most cases, it is a multistep execution that involves the pH of solution being altered and a series of purification extractions. Solid phase extraction (SPE) is a sample preparation technique that is often employed before samples with a biological matrix can be studied. SPE separates components of a mixture based upon their chemical and physical properties. There are many different types of SPE columns available with different column packing that are designed for different analytes. In order for the SPE column to effectively

remove the unwanted components of a solution that can prevent efficient analysis of the sample it must have packing that will retain the desired analyte and allow the unwanted matrix to pass through. Great care needs to be taken to select the column that will correctly interact with the sample. SPE is a multistep process that involves passing solvents through a column, followed by the sample solution then various other washes to remove unwanted components and ultimately a wash to elute the analyte of interest. The first solvent that is passed through the column is required in order to 'charge' the column, prepare the column to bind to the analyte. This process is not only time consuming but it can be troublesome with the desired analyte eluting from the column prematurely or not at all.

Matrix assisted laser desorption/ionization (MALDI) offers a remedy for analytes that challenge other ionization techniques. MALDI is a soft ionization technique that produces singly charged analyte species with no fragmentation. This results in a straight – forward spectrum that can be rapidly processed. MALDI can be used to analyze a variety of analytes, in various states, liquid or solid without extensive sample preparation. This versatility is extremely useful enabling this technique to analyze samples that previously were thought to be impossible to analyze using mass spectrometry. MALDI is paired with time – of – flight mass spectrometry (ToF MS) giving a theoretically unlimited mass range that can be analyzed, allowing large proteins and synthetic polymers to be analyzed. The singly charged species of these large analytes allow for an intact spectrum to be collected, which elucidates the structure of the molecule. The versatility and extensive range of application made

MALDI an ideal choice for the analysis of the various samples that were characterized in the later chapters of this dissertation.

1.2 MALDI

1.2.1. Overview

MALDI is a two-step ionization process that produces a pulsed beam of ions that are focused and amplified in the time of flight mass spectrometer. The two steps in the

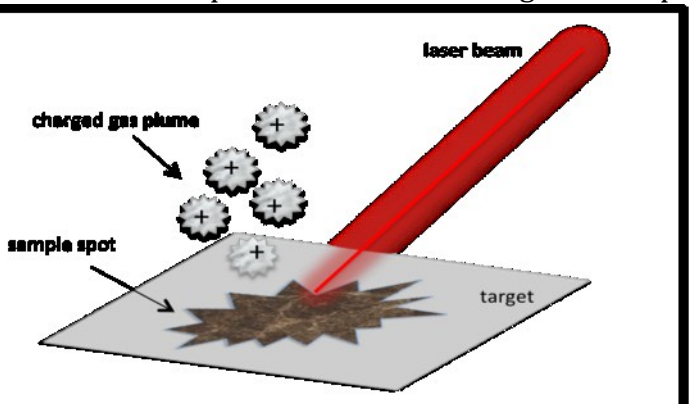

Figure 1.1. schematic drawing of MALDI ionization

ionization process are simply referred to as the primary and secondary ionizations. The primary ionization occurs when a laser beam strikes the MALDI target, resulting in an energy transfer from the laser beam to the matrix portion of the sample. Figure 1 is a schematic of this process. As illustrated in figure 1.1, as the laser beam strikes the sample spot, a charged gas plume is created. This creation of a gas plume is the subject of great debate, due to the fact that a process of ionization cannot be agreed upon.[5] This will be discussed in depth later. The resulting gas plume of both charged and neutral molecules interacts with itself resulting in many neutral molecules obtaining charge.[6] While there may not be a whole lot of controversy surrounding the secondary ionization reactions they are just as important as the

primary ionization step, as this step produces the ions that are detected and make up the produced mass spectrum.[6] This conglomerate of charged molecules is pulled into the various focusing lenses and ultimately into the flight tube where the ions are separated by mass. The microchannel plate then multiplies the signal and the multiplied signal is detected. The detected signal is then displayed as signal intensity as a function of mass to charge ratio (*m/z*).

1.2.2. Laser

Ablation is the term that is used to describe the process where a laser pulses at high irradiances that ejects a tremendous amount of material.[7] It has been realized that the parameters that surround the laser striking the sample can have profound effect upon the resulting reactions and ultimately observed spectra.[8] There have been different lasers that have been used for MALDI.[8-12] Some MALDI devices have a tunable laser that allows the analyst to select the wavelength to be used for ablation/desorption of sample.[10] There are three main types of radiation that is used for MALDI lasers: ultraviolet, visible and infrared light.[9] Table 1 shows different lasers and their wavelengths.[9]

Laser Type	**ArF**	**KrF**	**XeCl**	**Nd:YAG**	**Nd:YAG**	**Nd:YAG**	**N_2**	**ER:YAG**	**CO_2**
Frequency (nm)	**193**	**248**	**308**	**4xf 266**	**3xf 353**	**1xf 1,060**	**337**	**2,940**	**9100 – 1060**
Type of Light	**UV**	**UV**	**UV**	**IR**	**IR**	**IR**	**Vis**	**IR**	**IR**
Laser Description	**Excimer**	**Excimer**	**Excimer**	**Nd:YAG**	**Nd:YAG**	**Nd:YAG**	**N_2**	**OPO**	**OPO**

Table 1.1. Laser type, frequency and other description. Values from Hillencamp & Peter - Katalinić[9]

As indicated from table 1.1 there are quite a few lasers that have been used for MALDI analysis.[9] It should be noted that the different types of lasers that are currently and have been employed in the past were selected as an attempt to optimize conditions for the production of analyte ions. The most common type of laser paired with MALDI is the nitrogen laser due to its simplicity, small size and relatively low cost.[9] The main drawbacks to the nitrogen laser are the limited pulse frequency and the relatively low number of laser emissions, which is usually limited to $\leq 10^8$, which correlates with 0.5 – 2 years time frame before the laser cartridge needs replacement, of course depending upon instrument configuration and useage.[9] The Nd:YAG laser is used in conjunction with a frequency enhancers (denoted as 4fx, for frequency quadrupled, 3fx for frequency tripled etc.) which enables the Nd:YAG laser better suited for the needs of the MALDI.[9] The frequency 353 nm of Nd:YAG laser is the Nd:YAG laser that is most commonly found in conjunction with MALDI units.[9] The ER:YAG and CO_2 lasers appear less frequently, but are still worth mentioning, being labeled as OPO, or optical parametric ocillators which are usually tunable within a relatively narrow frequency range available.[9] The different lasers that have been used for MALDI have been used for multiple reasons, not just for the difference in frequency but also for the variability in emission pulse width, output energy per pulse, maximum pulse repetition frequency and the laser beam's shape characteristics also vary from one type of laser to another.[9] It is a combination of these parameters that make one laser favorable over another.[9]

1.2.3 Laser Ablation/Desorption

Both theories that are considered for the primary ionization contend that there is an ablation and desorption process that is responsible for ejection of material into the gas phase.[13] Ablation is, by definition, the removal of material from a surface by an erosive mechanism while desorption is characterized as the transition of material from the solid state into the gas phase.[13] Desorption is thought to occur as the laser strikes the sample desorption begins with the top layer of the solid sample smoothly transitioning into the gas phase as the energy from the laser is absorbed by the matrix and is converted into heat that spurs the disintegration.[13] Ablation encompasses multiple chemical and physical processes including photon absorption, energy redistribution, disintegration and ultimately molecular ejection and perhaps sublimation.[14] The ablation process is highly dependant upon the laser fluence, requiring a substantial amount of energy for the ejection of material.[8, 13, 14] At high fluences the sample becomes overheated and the substrate layer of the sample begins to nucleate resulting in an explosive boiling where chunks of the surface are ejected.[13] This phase explosion or sometimes referred to as explosive boiling, is home to thermal and mechanical contractions and rejections that are long in comparison to the duration of the laser pulse length causing the material to experience significant stress confinement till finally larger clump of material dislodges from the sample.[13, 14] Whether thermal or mechanical processes is the dominant or relatively more important mechanism that is occurring during the ablation event is dependent upon the ratio of duration of the laser pulse to the thermal and stress relaxation times.[7] This phase explosion has been shown to have

an exponential increase in the number of ejected molecules from the sample as a threshold of laser fluence is approached and crossed.[14] This ejection of material can be described by equation 1.1, the number of ejected molecules is directly related to the laser fluence and the laser penetration depth.[14]

$$N = n_m L_p \ln\left[\frac{F}{L_p\left(E_v^* - CT_0\right)}\right] \quad F \square F_{th'} \quad note: F_{th} = L_p\left(E_v^* - CT_0\right)$$

Equation 1.1. Number of molecules ejected per unit surface area during ablation

Where n_m is the molecular number density of the sample, L_p is the depth of laser penetration. F_{th} is the threshold of laser fluence that needs to be reached for the observation of the exponential release of molecules from the sample. E_v^* is the critical energy density of the surface layer, and CT represents the thermal energy density of the sample preceding laser irradiation.[14] For systems that do not reach the fluence threshold, it has been experimentally observed by Georgiu et al. that a bubbling of the different layers of sample does in fact still occur but falls short of the explosive boiling that displaces large chunks of material but this boiling has a great impact upon the morphology of the sample being that the bubbles ultimately collapses permanently altering the morphology of the sample.[7] The phase explosion is what is considered to enable fragile molecules to be ejected from the sample surface without fragmentation.[7] It is believed that the nonequilibrium phase transformation is a feature that is not only unique to phase explosion but is also the vehicle of intact molecular expulsion.[7] This process of laser ablation needs to be understood in order to understand the conditions under which the processes of

MALDI occur in able to accurately determine the mechanisms of the reactions. This understanding of the MALDI mechanisms will allow for an empirical knowledge of MALDI. It is this empirical knowledge that is key for better sample analysis and for the advancement of MALDI technology.

1.2.4 Cluster Model of Primary Ionization

The cluster model of primary ionization for MALDI processes is one theory that is employed to explain the mechanisms of ionization.[5] Of the two processes that are considered for primary ionization have great differences in reaction mechanism and role of the matrix for the creation of ions within the sample.[8, 13-15] The cluster theory of primary ionization was first proposed by the Karas group, University of Frankfort.[13] This theory maintains that the ions that are observed in the mass spectrum are preformed in solution before the analyte/matrix solution is deposited onto the MALDI target.[13] It is then postulated that within the gas plume the preformed ions then can interact with neutral molecules but the reaction does not complete to equilibrium, leaving the ions which are then observed in the mass spectrum.[13] This neutralization is said to occur within the clusters of the sample that are ablated off the target at high laser fluence.[13] The preformed ion within the solid sample is thought to occur similarly to the way a salt will form crystals of ionic materials.[13] It is known that the analytes often become charged within the sample solution during sample preparation.[13] It is then thought that these charged analytes become encased within the matrix crystal as the sample dries.[13] There is some evidence of the preformed ion creation that lasts through sample evaporation by employing the use of pH sensor dyes.[13] MALDI samples were made by Krüger et al.

and pH dyes were incorporated within the mixtures. The samples were then treated to alter the pH of the resulting sample solutions, and as expected the pH sensor dyes demonstrated the proper color to correspond with the varying pH. These portions of the different solutions were allowed to dry, the way a MALDI sample is normally allowed to dry under ambient conditions. It was observed that when dried and crystallized that the pH sensors retained the color that was observed within the liquid samples. This indicated that the de/protonation state of the solid sample was the same state of de/protonation that was in the liquid form of the sample.[13] While this study indicates that in fact charges that were obtained in solution are able to last through the drying of the sample into solid form, the mere presence of a charge does not indicate that this charge will be able to survive laser ablation, gas plume mechanisms or gain entry into the mass spectrometer. It has been pointed out by those skeptical of the cluster model that while there may be a charged molecule in the solid sample that they could be closely associated with the counterions within the solid state.[13] Another aspect of the cluster theory for primary ionization is that there would be an excess of electrons throughout the solid sample that is spurred by photoionization of the sample via the laser followed by loss of electrons from the sample to give the gas plume within the sample chamber a net positive charge.[13] Despite this electron loss theory, another theory is emerging from the cluster model of primary ionization namely the thought that an excess of electrons is irrelevant and the ablation and subsequent release of pieces of the solid sample is where the pivotal step of cluster ionization occurs.[13] This mechanism approach to the cluster theory has gained significant momentum with several groups embarking in

computer modeling and experimental endeavors.[7, 8, 13-17] The prevailing theory is that the preformed ions within the solid sample are released as relatively large pieces which are vaporized through a desolvation process as the gas plume expands.[13] The desolvation is what is needed to separate the various preformed ions that are within the ejected material.[13] This is described as the critical threshold where the density of excitational energy density within the matrix of the sample and an explosive cluster emission and subsequent ionization occurs.[15] It is believed that evaporation of the charged analyte molecule is attainable without abolition of the ionization is due to gas phase attachment of codesorbed alkali cations to analyte neutrals.[15] This cation addition mechanism requires that the matrix has a less prominent role within the ionization process, instead of providing electrons to the gas plume this mechanism requires that the matrix to simply transfer absorbed energy to the analyte molecule.[15] However it can be hypothesized that while the matrix's main function is to transfer energy to allow for the release of the preformed analyte ion, there remains the possibility that the matrix could be useful in the neutralization of counterions.[15] The neutralization of counterions becomes an essential reaction for the success of analysis, without the neutralization of counterions, there is a very good possibility that the MADLI reaction would not yield analyte ions which would render the entire analysis void.[15] There needs to be an effective charge separation. The efficiency of the separation can be predicted by assessing the acid – base properties, solvation and incorporation behavior of the analyte, matrix and any additives to the sample.[15] While there may be several factors that profoundly effect the primary ionization of the analyte the variable that

seems to have the most conspicuous impact is the pH – related condition of the analyte within the starting solution.[15] The foundation of the cluster theory of primary ionization is the creation and subsequent preservation of the preformed analyte ion.[13-15]

1.2.5. Pooling /Photoexcitation Model of Primary Ionization

The alternative theory of primary ionization for MALDI is known as the pooling or photoexcitation model.[13] This model for ionization describes a phenomena where the electronic excitation energy of two nearby molecules is redistributed.[13] The reasoning behind the proposed pooling mechanism is based upon close proximity and an overlap of wave function, which could potentially transfer energy.[13] Molecular wave function in its most basic form is the mathematical description of the wave – like behavior of an electron in a molecule and is used to calculate the physical properties of the molecule eg. the probability of finding an electron in a specific region of the molecule.[18] It is thought that neighboring molecules that have been raised to the first excited (S_1) singlet state by photoexcitation could distribute this excitation energy throughout the sample given that they have significant wave function overlap, which would provide a pathway for smooth energy sharing and transfer.[13] For example considering the nominal 1 quantum/molecule (S_1:S_1) an isoenergetic state formally consists of 2 quanta residing upon one molecule and 0 quanta residing upon the other (S_n:S_0) and given a non-negligible plausibility high energy processes become reasonable via pooling.[13] This process evolves to something more likely when it is considered that excitations could move freely within the matrix, which expels the stipulation of high intensity energy laser

dominance.[13] The energy that is believed to penetrate through the solid structure of the sample is known as excitons.[13] Excitons have been describes as pseudo-particles that are mobile excitations that can transport its way through the solid crystal structures of molecules usually with the aid of chromophores (conjugated pi systems and metal complexes).[13, 19] The presence of chromophores would not be unusual within a MALDI sample due to two important common components of samples; matrix and metal salts to aid in ionization. The matrixes that are used in MALDI are always highly conjugated, and for the analysis of certain analytes, a metal salt is added to enhance ionization. The benefit of adding a metal salt could possibly be attributed to excitons. It is imperative for a successful transfer of excitons for there to be close proximity of the molecules to each other for overlap of wave function which allows for this energy transfer to transpire.[13] Pooling has been studied and demonstrated in 2,5-dihydroxybenzoic acid (DHB) when Ehring and Sundqvist established that with pooling can be observed with DHB with fluorescence quenching but the veracity of the study was questioned because of the short time frame that was studied resulted in critics suggesting that it was not unequivocal evidence of pooling but merely a brief phenomenon.[13] A more extensive study was then produced Setz and Knochenmuss that demonstrated that pooling was discontinued at low laser fluence and time – resolved trapping by dopants were employed to establish that S_1 excitons are in fact mobile and encounter pooling extinguishment reactions within the DHB matrix.[13, 20] Setz et al. was able to quantify the amount of time required for an exciton to hop – occurring in only 50 picoseconds, which indicates that within the 0.5 – 1.5 nanosecond exciton

existence significant transference can occur.[13, 20] It was also demonstrated that analytes, with excitation energies that were significantly lower than the matrix, tend to collect or trap the excitons, which can reduce the efficiency of the ion signal when compared to solely matrix samples indicating that the exciton is essential for the transfer of energy for the ionization of the analyte molecule.[13, 20] Further evidence of the pooling model can be deduced from the acknowledgement of the fact that the photon transfer from the laser are not capable to free matrix molecules from the solid sample; there is simply just not enough energy for a direct photonionization, indicating that there must be some type of collection of energy that occurs in order to ionize free molecules of matrix.[13] Pooling of an S_1 state molecule with a S_n molecule has been established as providing an excitation energy that is sufficient for ionization.[13] The quantitive nature of the pooling model for primary reaction allows for a direct comparison with experimentally obtained data.[13] There has been a lot of investigation to define the parameters of this pooling method of primary ionization and it has been determined that the most critical parameter for the ionization is laser fluence.[13] It has been determined that the act of desorption/ablation efficieny (based on laser fluence) is essential to raise the temperature of the sample that enables the temperature of the sample to efficiently ionize the sample.[13]

While both of the primary ionization methods presented are still topics of great debate, a knowledge of both of the highest regarded theories it can enable scientist to attempt to alter samples and sample preparation method to attempt to enhance the ionization of the desired analyte. This knowledge can aid in the assistance of efficient ionization that will in turn provide experimental evidence to help

deconvolute which ionization method is indeed taking place or maybe a combination of the methods.

1.2.6. Gas Plume: Home of Secondary Ionization Process

The gas plume is formed as a result of the laser beam striking the sample, this much about MALDI ionization processes can be agreed upon.[5, 7, 8, 14, 15] The formation of the expanding gas plume is a result of the primary ionization step in the two step process that composes the MALDI ionization reaction.[21] The gas plume that occurs is home to the secondary ionization processes, where there are believed to be countless collisions between charged and neutral molecular species which in turn, increases the number of charged molecules that then are able to enter into the mass spectrometer.[13] Without the secondary ionization process within the gas plume, which leads to multiplication of ions, MALDI ionization would not be a viable method of analysis.[8] It is the reactions within the expanding gas plume that results in enough ions to be detected.[6] It has been confirmed by a variety of experiments that analyte ions are formed predominately within the gas plume via secondary reactions with matrix or metal ions.[22] Not only do the reactions within the gas plume explain the spectra that are produced by MALDI but can also explain different phenomena that are observed such as matrix suppression effect and analyte – analyte suppression effects.[6, 22]

In order to fully understand and appreciate the mechanisms of ionization that occur within the gas plume, understanding the physical conditions is essential. The condition of the plume will to a great extent influence the way molecules will

interact with each other to produce analyte ions.[23] Studies using UV laser and the matrix 2,5-dihydroxybenzoic acid (DHB) provide a view into the state within the gas plume. It was recorded that the internal temperature was about 500 K, plume velocities of about 500 – 1000 m/s resulting in a high collision rate of ions and molecules since the mean free path is equal to about only a few molecular diameters.[23] These conditions of high energy in a condensed space not only gives an idea of why there are so many significant collisions within the gas plume but also gives clues to the types of reactions that are occurring.[23] It is thought that there are four specific types of secondary reactions that occur within the plume, being proton transfer, cation transfer, electron transfer and finally electron capture reactions.[22-24] One thing that seems to be constant in the secondary plume reactions is that the predominate neutral partner is the matrix due to the overconcentration present in MALDI samples.[21]

Proton transfer reactions have been deemed probably the 'most important' of the reactions that occur within the plume.[21] This designation has been appointed to this type of reaction due to the fact that most of the analyte classes which are examined by MALDI are detected in the protonated form.[21, 24] The high rate of protonation of analyte molecules can be attributed to the fact that most analytes have a proton affinity of at least 900 kJ/mol which is much higher than the proton affinites of common matrixes which is around 850 – 900 kJ/mol.[21] The protonation reaction has been one that has been extensively studied. Kinsel et al. have studied this topic rigorously by employing a series of experiments that involve the grinding of amino acids having increasing gas – phase basicities with conventional MALDI matrixes.

This fine powder was then affixed by adhesive onto a metal target and MALDI analysis was performed at 337 nm and data was acquired under continuous extraction conditions.[21] The data was evaluated comparably to the methodology for analysis of kinetic determination of gas – phase thermodynamic properties which indicated that equilibrium is achieved therefore no kinetic barrier exists within the reaction.[21] This suggests that the simple reaction demonstrated in equation 1.2 holds true.

$$MH^+ + A \rightarrow M + AH^+$$

Equation 1.2. Analyte ionization; proton transfer rxn.

Where MH^+ is the protonated matrix, A is uncharged analyte, M is the neutral matrix and AH^+ is the protonated analyte.[21] While this is a simplistic equation it accurately describes the protonation of the analyte the above mentioned experiment conducted by Kinsel et al.. This experiment also furthered the notion that gas – phase basicities of the matrix donor plays less of a role in the protonation reaction and indicates that the internal energy of the analyte that is dependent on the exothermicity of the proton transfer reaction.[21] A drawback to this experiment is that the results obtained as far as the temperature where the proton transfer reaction is most effective which measured in at about 1733 K, which is significantly higher than the observations/predictions of other works that estimate the temperature range within the plume to be closer to 600 – 800 K. This discrepancy was addressed and shown to be a result of an odd ratio of matrix to analyte molar ratio 1:4, instead of the more commonly used 15:1. When the experiment was altered to be within the normal molar ratio range, the temperature that was

observed dropped to a more expected 600 – 800 K range.[21] The experimental data in this specific instance and other studies (not specifically mentioned) have been able to rule out other contributors to analyte activation including matrix sublimation and preformed analyte protonation but a couple factors that cannot seemed to be effectively ruled out are extensive plume reactions and gas plume equilibrium.[21] At this point it is also important that the case of analytes that have low proton affinity will still have analyte – charge reaction. In these cases two remedies can be applied for effective ionization and therefore good MALDI spectra, the first of these being that the analyte can have functional groups attached to encourage protonation or the use of a basic matrix and measure the creation of negative ions.[21]

Another experiment to explore the proton transfer reaction was conducted by Breuker et al. This experiment set is important because it utilizes the thermochemical data that has become available over the past several years on common matrixes and analytes that are used readily in MALDI analysis.[24] These experiments were conducted using the Gibbs free energies of matrix – matrix and matrix – analyte reactions allowing the authors to experimentally test the hypothesis that it is thermochemistry that determines the final distribution of ions as a result of efficient secondary reactions that occur within the gas plume.[24] The experiments were carried out using a matrix analyte ratio of 1:1 in order to ensure that the experiments would not be hindered by the quantities of reactants. The experiment in addition to studying the in plume reactions of matrix and analyte molecules but also examined the effect that laser fluence has by altering the laser

fluence settings at different points in the experiment expecting the plume density and therefore plume collisions would increase as the laser fluence.[24] The matrix that was examined was, 2,4,6-trihydroxyacetophenone (THAP) and the tripeptide glycyl – glycyl – histidine (GGH) was used for the analyte.[24] FT-ICR mass spectrometer and Odyssey data acquisition system were used along with a vacuum system that held the operating pressure of 10^{-8} mbar equipped with a Nd:YAG laser operated at 355 nm was used.[24] The experiment was able to demonstrate that in the positive mode, the reactions varied at different laser fluences such that as the laser fluence increased and plume density then increased, there was indeed an increased number of collisions between the protonated matrix and the neutral analyte which resulted in the secondary proton transfer via equation 1.3, and ion – molecule equilibrium was established.[24]

$$GGH + [THAP{+}H]^{+} \xrightarrow{\Delta G} [GGH{+}H]^{+} + THAP \qquad \Delta G = -130\,kJ/mol$$

Equation 1.3. secondary ion formation proton transfer reaction

When this experiment was repeated in negative mode, only matrix ions were detected despite the increasing of laser fluence indicating that the proton transfer reaction likely occurred by means of equation 1.4.[24]

$$[THAP - H]^{-} + GGH \xrightarrow{\Delta G} THAP + [GGH - H]^{-} \qquad \Delta G\ endoergic < +75\,kJ/mol$$

Equation 1.4. secondary ion formation proton transfer reaction

The negative mode results indicated that equation 3 was occurring where is would be thermochemically unfavorable for negative analyte ions to be produced.[24] It was then concluded that in – plume collisions allow ion – molecule thermodynamical equilibrium to be approached when laser fluence high and when the laser fluence is

low that the ion distributions are kinetically limited.[24] This experiment was not only useful for explaining the proton transfer reaction within the expanding gas plume but was also able to show that laser fluence has a considerable influence upon the resulting ions in the mass spectrum.[25]

The next type of reaction that is suspected to occur within the expanding gas plume is cation transfer reaction.[23, 26] While frequently analytes are observed as protonated ions there are some analyte classes that are better analyzed with alkali metals or transition metal cations.[13] In order for proton transfer reactions to occur, analyte must compete with neutral matrix for available protons, but if the analyte has a low proton affinity there will not be enough energy to force the reaction towards analyte protonation.[23] Synthetic polymers are one class of analyte that preferentially binds with cations to obtain a charge.[13] In this case, synthetic polymers usually have a poor affinity for protonation being that they usually have proton affinities that are much lower than commonly matrixes.[13] It has been documented that Na^+ affinity for matrixes is in the range of 150 – 170 kJ/mol and K^+ affinities measure even lower with an affinity on the order of 50 kJ/mol.[23] These low matrix cation affinities make the addition of cations favorable for the analysis of molecules that do not have polar groups to attract a proton, such is often the case with synthetic polymers. An example of a cation transfer reaction is the interaction between divalent copper and styrene pentamers. The resulting spectra showed that equation 1.5 was the reaction that had occurred within the gas plume.[13]

$$Cu^{2+} + PS \rightarrow Cu^{+} + PS^{+}$$

Equation 1.5. The reaction between divalent copper and polystyrene pentamers

Where Cu^{+2} is the divalent metal used for the ionization of the polystyrene pentamers. The analyte in this case does not have the proton affinity to protonate, therefore for successful analysis the sample must be doped with a metal salt.[13]

The energy barrier for the transfer of a cation, such as sodium has been found to be on average below 10 kJ/mol which is on the same magnitude of the thermal energy that is available within the warm gas plume which leads to the knowledge that the cation transfer reaction is not kinetically limited.[23]

The next type of accepted secondary reaction is that of electron transfer.[13, 22, 23] This type of reaction is believed to occur within the expanding gas plume but only under certain circumstances.[13, 23] In order to have this reaction mechanism occur the ionization potentials of the matrix and analyte are the thermodynamic parameters that will determine whether an electron transfer does occur.[13] In order for the reaction the matrix must have ionization potential much higher than all of the analytes within the system but must not exceed about 1.5 eV or the analyte will not be ionized.[13, 23] This restriction makes choosing a matrix that would favor this reaction rather difficult and complex. It has been hypothesized that this reaction is similar kinetically to the Marcus inversion theory but since this reaction occurs within the gas phase, many questions about the reaction remain.[13] While the particulars of reaction is difficult to establish conclusively, it has been used as a mode of reaction to explain some spectral results.[23]

The final type of secondary reaction to be considered is the electron capture reaction (this secondary ionization reaction is also known as the “lucky survivor” reaction).[13, 22, 23, 27] This type of reaction seeks to further explain the plethora of +1

ions observed within MALDI spectra.[23] This reaction is believed to occur within the presence of an excessive amount of free electrons that occur within imbalance within the gas plume between negative and positive charges that originate from matrix photoionization.[27] This theory is based on the reasoning that because there would be such a great number of neutral molecules, ions should not survive.[27] Karas et al. contends that the gas plume is positively charged in excess and this phenomena is due to the rapid loss of electrons.[27] They also contend that this is the causation of lower ion signal within spectra that are obtained under negative polarity conditions.[27] This reaction is thought to be heavily dependant upon the primary reaction which remains a topic of great debate.[27]

1.2.7. Matrix

The matrix is essential to the successful MALDI analysis of an analyte.[8, 9, 15] The analyte is the part of the sample mixture that absorbs energy from the laser.[9, 15] The role of the matrix is essential and its importance is crucial to both the clustering and pooling theories of primary ionization.[8, 13, 15] There is not one MALDI matrix that is universally used for all analytes.[9] Due to the wide range of analyte types and different laser types that are used with MALDI, it follows that there would be an extensive collection of matrixes that are used for MALDI analysis. Table 1.2 shows the most popular matrixes that are used for MALDI analysis.[9] The matrix is essential to the successful MALDI analysis of an analyte.[8, 9, 15] The analyte is the part of the sample mixture that absorbs energy from the laser.[9, 15] The role of the matrix is essential and its importance is crucial to both the clustering and pooling theories of primary ionization.[8, 13, 15]

Matrix	Absorption Wavelength (nm)	Usual Application
Nicotinic Acid	UV 266	Proteins, peptides, adduct formation
2,5-Dihydroxybenzoic acid	UV 337, 353	Proteins, peptides, carbohydrates, synthetic polymers
Sinapinic Acid	UV 337, 353	Proteins, peptides
α -Cyano-4-hydroxycinnamic acid	UV 337, 353	Peptides, fragments
3-Hydroxypicolinic acid	UV 337, 353	Nucleic acids
6-Aza-2-thiothymine	UV 337, 353	Proteins, peptides, non-covalent complexes, near neutral pH
2',4',6' − Trihydroxyacetophenone monohydrate	UV 337, 353	Proteins, peptides, non-covalent complexes, near neutral pH
Succinic Acid	IR 2940, 2790	Proteins, peptides
Glycerol	IR 2940, 2790	Proteins, peptides

Table 1.2. Common matrixes, absorption wavelength and usual applications. Adapted from Hillencamp & Peter - Kataliníc[9]

It has been discovered that the properties of the matrix can influence the success of the analysis.[9] Some analytes are not compatible with certain matrixes due to the incompatible physical properties of the matrix and analyte.[9] This makes having multiple matrixes that can be used for analysis essential.[9, 15]

1.2.8. Time of Flight Mass Spectrometer

The 1980s brought to analytical chemistry the development of the orthogonal acceleration time-of-flight mass spectrometer.[28] Dawson and Guilhaus were one of the groups of scientists that developed this flight method for the analysis of ions. This design had several advantages over the classical linear time-of-flight mass spectrometers which were the only type that had existed up to this point. These advantages, include the capability of reducing the average initial velocity component

of the ions to zero and the ability to independently control the continuous ion beam and ion drift energy; making these times approximately equal to the time that is required for ion beam to fill the orthogonal accelerator, which is needed for the ions to get to the detector. The reducing of the average initial velocity component in turn reduces the spread in the velocity components in the TOF direction and increases the resolving power of the instrument. The advantage of making the time required to fill the accelerator and the drift time about the same provides the user an increase in detection sensitivity.[28]

The time-of-flight mass spectrometer basically collects ions and accelerates them through a flight tube and into a detector.[1] While this may seem like a straightforward, uncomplicated moving of ions, it is actually a synchronized ballet of pulsing voltages, reflections, deflections and drifting.[2] The TOF-MS ultimately separates ions that have the same kinetic energy but different mass to charge ratios.[2] MALDI is often paired with a time-of-flight mass spectrometer due to its ability to create a pulsed ion beam.[28]

1.3 Applications of MALDI-TOF-MS

Since its introduction in 1980s MALDI has caught the attention of scientists wishing to analyze large molecules.[29] MALDI is usually applied to four main areas of research: biochemistry, polymer chemistry, organic chemistry and microbiology.[30-34] These areas of research have a similar need which is to comprehensively analyze large molecules without extensive fragmentation. This objective can be applied by MALDI analysis.

Biochemistry relies upon MALDI analysis for proteomic studies.[35] MALDI can accurately depict in-tact proteins. For the identification of proteins and polypeptides MALDI has proven to be an important analysis method, being able to produce singly charged species, giving the user a spectrum that is not convoluted by multiply charged species.[33] Multiply charged proteins and peptides are commonly produced by other soft ionization techniques such as ESI and NanoESI which results in spectra that are complicated and difficult to decipher. Microbiologist have also found that MALDI can be extremely accurate in the identification of different bacterial and fungal colonies.[36] MALDI represents a method that can be applied to the microbiological identification of multiple biological systems that provides comprehensive analysis in the timeframe that is usually required for simple screening causing the interest in this technique to increase among microbiologists.[32, 36, 37]

MALDI analysis is often applied for the analysis of synthetic polymers.[38, 39] Though there are other methods that have been used in the characterization of synthetic polymers, in order to get all the required information about the polymer's composition and structure, multiple methods need to be applied.[40, 41] MALDI can provide the information about a polymer's composition and structure in a single analysis saving great amounts of time and in many cases providing information that is superior to the combined efforts of other analysis types.[42-45]

1.4 Sample Preparation for MALDI Analysis

While sample preparation for MALDI is relatively simple, not requiring extensive sample manipulation, the way the sample dries upon the MALDI target has crucial effect upon the quality of signal obtained.[46-48] At its basics, for effective sample analysis, the sample needs to be mixed with a matrix and spotted onto a target for MALDI analysis.[49] It has quickly become clear that MALDI sample preparation needs to be conducted carefully in order to obtain crystals that are a homogeneous mixture of both the sample and the matrix.[50, 51] Not only is an integration of sample and matrix needed for successful analysis but it has also been determined that crystal size can also have a great impact on the produced sample signal.[52-54] Due to the fact that sample preparation/sample deposition can have such dramatic influence upon the resulting spectra, optimization of these parameters is crucially important.

1.5 Included work

In this work the various applications of MALDI and the caveats of sample preparation will be explored. Chapter 2 will delve into the complexities that exist within the sample preparation and the effect that the seemingly simple act of depositing the sample onto the target can have upon the quality of spectra that are obtained. The different methods that have been developed will be compared by evaluating signal intensity, quantitation error and crystal morphology. The results from these three categories will provide enough information to make sound

conclusions about the different techniques that are commonly used in sample preparation.

Following the trend of evaluating how sample preparation can influence results, chapter 3 will investigate the effect that amounts of sample, matrix and cationizing agent have upon the collected signal. Different ratios will be exploited to determine the effect upon the analysis of synthetic polymers. It has been established that the 'recipe' or amounts of sample, matrix and cationizing agent that is used can have significant impact on the intensity of the polymer's signal in the mass spectrum.[55] This will be investigated to determine how varying these sample components will influence the produced spectrum.

In chapters 4 – 6 MALDI is employed for the analysis of various analytes. Chapter 4 uses MALDI to analyze in-tact carpet fibers for their additives. This analysis has the potential to provide forensic scientists another tool for the identification and classification of important evidence. Fiber evidence can place an individual at a certain place which can be extremely useful within the investigation of a crime. Chapter 5 will use MALDI for the analysis of glutathione, an important biomolecule. Glutathione is a biomolecule that has recently been found to have great importance in the detoxification of the body.[56, 57] Levels of glutathione within the body are being investigated to determine the implications of different levels of the two different forms of glutathione that are found within the human body, oxidized and reduced.[58] There have been connections drawn between glutathione and neurological disorders/neurotoxicity, cancers, tumors, liver disease, cardiovascular disease, chronic toxicity and autism among other ailments.[56, 57, 59, 60] Because this molecule

is so important to the body, it has been selected to be one of the analytes to be studied for this dissertation.

The last application of MALDI analysis will be to cell wall extracts from the bacteria *Staphylococcus Epidermidis*. This bacteria has been found to form a biofilm upon devices such as catheters and orthopedic implants causing severe infection.[61] The biofilm that has been formed by the bacteria makes antibiotic treatment only marginally effective and usually results in the removal of the implanted device.[62] Because the biofilm forming bacteria results in severe infection that is resistant to antibiotics the way it adheres and forms biofilm is an area of interest, which is why it is analyzed in chapter 6.

References:

1. Skoog, D. H., F. James; Crouch, Stanley R., *Principles of Instrumental Analysis Sixth Edition*. 6 ed.; Thomson Brooks/Cole Thompson Corporation: Belmont, CA, 2007; p 1039.
2. Harris, D., *Quantitative Chemical Analysis*. Sixth ed.; W.H. Freeman and Company: 2003; p 739.
3. Harvey, D. J.; Editors-in-Chief:¬†¬† Paul, W.; Alan, T.; Colin, P., MASS SPECTROMETRY | Ionization Methods Overview. In *Encyclopedia of Analytical Science (Second Edition)*, Elsevier: Oxford, 2005; pp 350-359.
4. Eljarrat, E.; Barcel√≥, D.; Editors-in-Chief:¬†¬† Paul, W.; Alan, T.; Colin, P., MASS SPECTROMETRY | Electron Impact and Chemical Ionization. In *Encyclopedia of Analytical Science (Second Edition)*, Elsevier: Oxford, 2005; pp 359-366.
5. Georgiou, S.; Hillenkamp, F., Introduction: Laser Ablation of Molecular Substrates. *Chemical Reviews* **2003,** *103* (2), 317-320.
6. Knochenmuss, R.; Vertes, A., Time-delayed 2-Pulse Studies of MALDI Matrix Ionization Mechanisms. *Journal of Physical Chemistry* **2000,** *104* (23), 5406-5410.
7. Georgiou, S.; Koubenakis, A., Laser-Induced Material Ejection from Model Molecular Solids and Liquids:¸Äâ Mechanisms, Implications, and Applications. *Chemical Reviews* **2003,** *103* (2), 349-394.
8. Dreisewerd, K., The Desorption Process in MALDI. *Chemical Reviews* **2003,** *103* (2), 395-426.
9. Hillenkamp, F. P.-K., Jasna, *MALDI MS A Practical Guide to Instrumentation, Methods and Applications*. 1st Reprint ed.; Wiley- VCH Federal Republic of Germany, 2009; Vol. 1st Reprint, p 339.
10. Boesl, U.; Weinkauf, R.; Weickhardt, C.; Schlag, E. W., Laser ion sources for time-of-flight mass spectrometry. *International Journal of Mass Spectrometry and Ion Processes* **1994,** *131* (0), 87-124.
11. Knochenmuss, R., A Quantitative Model of Ultraviolet Matrix-Assisted Laser Desorption/Ionization Including Analyte Ion Generation. *Analytical Chemistry* **2003,** *75* (10), 2199-2207.
12. Knochenmuss, R., A quantitative model of ultraviolet matrix-assisted laser desorption/ionization. *Journal of Mass Spectrometry* **2002,** *37* (8), 867-877.
13. Knochenmuss, R., Ion formation mechanisms in UV-MALDI. *Analyst* **2006,** *131* (9), 966-986.
14. Zhigilei, L. V.; Leveugle, E.; Garrison, B. J.; Yingling, Y. G.; Zeifman, M. I., Computer Simulations of Laser Ablation of Molecular Substrates. *Chemical Reviews* **2003,** *103* (2), 321-348.
15. Karas, M.; Kruger, R., Ion Formation in MALDI: The Cluster Ionization Mechanism. *Chemical Reviews* **2003,** *103* (2), 427-440.
16. Knochenmuss, R.; Zhigilei, L. V., Molecular dynamics simulations of MALDI: laser fluence and pulse width dependence of plume characteristics and consequences for matrix and analyte ionization. *Journal of Mass Spectrometry* **2010,** *45* (4), 333-346.
17. Vogel, A.; Venugopalan, V., Mechanisms of Pulsed Laser Ablation of Biological Tissues. *Chemical Reviews* **2003,** *103* (2), 577-644.

18. Silberg, M. S., Chemistry: The Molecular Nature of Matter and Change. In *Chemistry: The Molecular Nature of Matter and Change*, Fifth Edition ed.; Good - Hodge, T., Ed. McGraw - Hill Higher Education: New York, New York, 2009; pp 268 - 297.
19. Mukamel, S.; Abramavicius, D., Many-Body Approaches for Simulating Coherent Nonlinear Spectroscopies of Electronic and Vibrational Excitons. *ChemInform* **2004,** *35* (24), 2073-2098.
20. Setz, P. D.; Knochenmuss, R., Exciton Mobility and Trapping in a MALDI Matrix. *The Journal of Physical Chemistry A* **2005,** *109* (18), 4030-4037.
21. Knochenmuss, R.; Zenobi, R., MALDI Ionization: The Role of In-Plume Processes. *Chemical Reviews* **2002,** *103* (2), 441-452.
22. Knochenmuss, R. S., A.; Breuker, K.; Zenobi, R., Secondary ion-molecule reactions in matrix-assisted laser desorption/ionization. *Journal of Mass Spectrometry* **2000,** *35* (11), 1237-1245.
23. Knochenmuss, R.; Zenobi, R., MALDI Ionization: The Role of In-Plume Processes. *Chemical Reviews* **2002,** *103* (2), 441-452.
24. Breuker, K.; Knochenmuss, R.; Zhang, J.; Stortelder, A.; Zenobi, R., Thermodynamic control of final ion distributions in MALDI: in-plume proton transfer reactions. *International Journal of Mass Spectrometry* **2003,** *226* (1), 211-222.
25. Knochenmuss, R., Positive/Negative Ion Ratios and In-Plume Reaction Equilibria in MALDI. *International Journal of Mass Spectrometry In Press, Accepted Manuscript*.
26. Zhang, J.; Ha, T. K.; Knochenmuss, R.; Zenobi, R., Theoretical Calculation of Gas-Phase Sodium Binding Energies of Common MALDI Matrices. *Journal of Physical Chemistry* **2002,** *106* (28), 6610-6617.
27. Karas, M.; Glückmann, M.; Schäfer, J., Ionization in matrix-assisted laser desorption/ionization: singly charged molecular ions are the lucky survivors. *Journal of Mass Spectrometry* **2000,** *35* (1), 1-12.
28. M. Guilhaus, D. S. V. M., Orthogonal acceleration time-of-flight mass spectrometry. *Mass Spectrom. Rev.* **2000,** *19* (2), 65-107.
29. Karas M; Hillenkamp, F., Laser Desorption Ionization of Proteins with Molecular Masses Exceeding 10,000 Daltons. *Anal. Chem.* **1988,** *60* (20), 2299-301.
30. KARAS, M. B., U., Laser desorption ionization mass spectrometry of large biomolecules. *Trends Anal. Chem.* **1990,** *9*, 5.
31. McEwen, C. N.; Jackson, C.; Larsen, B. S., Instrumental effects in the analysis of polymers of wide polydispersity by MALDI mass spectrometry. *International Journal of Mass Spectrometry and Ion Processes*
In Honour of Fred McLafferty **1997,** *160* (1-3), 387-394.
32. Stahl, B.; Linos, A.; Karas, M.; Hillenkamp, F.; Steup, M., Analysis of Fructans from Higher Plants by Matrix-Assisted Laser Desorption/Ionization Mass Spectrometry. *Analytical Biochemistry* **1997,** *246* (2), 195-204.
33. Tanaka, K. W., Hiroaki; Ido, Yutaka; Akita, Satoshi; Yoshida, Yoshikazu; Yoshida, Tamio; Matsuo,T., Protein and polymer analyses up to m/z 100 000 by laser ionization time-of-flight mass spectrometry. *Anal. Chem.* **1988,** *2* (8), 151-153.
34. Todd, P. J.; Schaaff, T. G.; Chaurand, P.; Caprioli, R. M., Organic Ion Imaging of Biological Tissue with MALDI and SIMS. *J. Mass Spectrom.* **2001,** *36* (null), 355.

35. Zhou, J.; Ens, W.; Standing, K. G.; Verentchikov, A., High-resolution laser desorption mass spectrometry of peptides and small proteins. *Rapid Commun. Mass Spectrom.* **1992,** *6* (null), 671.
36. Seng, P.; Drancourt, M.; Gouriet, F. d. r.; La Scola, B.; Fournier, P.-E.; Rolain, J. M.; Raoult, D., Ongoing Revolution in Bacteriology: Routine Identification of Bacteria by Matrix-Assisted Laser Desorption Ionization Time-of-Flight Mass Spectrometry. *Clinical Infectious Diseases* **2009,** *49* (4), 543-551.
37. Tan, P. V.; Taranenko, N. I.; Laiko, V. V.; Yakshin, M. A.; Prasad, C. R.; Doroshenko, V. M., Mass spectrometry of N-linked oligosaccharides using atmospheric pressure infrared laser ionization from solution. *Journal of Mass Spectrometry* **2004,** *39* (8), 913-921.
38. Schriemer, D. C.; Li, L., Mass Discrimination in the Analysis of Polydisperse Polymers by MALDI Time-of-Flight Mass Spectrometry. 2. Instrumental Issues. *Anal. Chem.* **1997,** *69* (20), 4176-4183.
39. Royo, E.; Brintzinger, H.-H., Mass spectrometry of polystyrene and polypropene ruthenium complexes. A new tool for polymer characterization. *Journal of Organometallic Chemistry*
Special Issue dedication to Professor Pascual Royo **2002,** *663* (1-2), 213-220.
40. Provder, T. E., *Chromatography of Polymers Characterization by SEC and FFF*. American Chemical Society: New York, 1993; p 337.
41. Gaborieau, M. G., Robert G.; Gray-Weale, Angus; Hernandez, Javier M.; Castignolles, Patrice Theory of Multiple-Detection Size-Exclusion Chromatography of Complex Branched Polymers. *Journal of Mass Spectrometry* **2007,** *16* (1), 13-28.
42. Chen, H.; He, M.; Pei, J.; He, H., Quantitative Analysis of Synthetic Polymers Using Matrix-Assisted Laser Desorption/Ionization Time-of-Flight Mass Spectrometry. *Anal. Chem.* **2003,** *75* (23), 6531-6535.
43. Cox, F. J.; Johnston, M. V.; Dasgupta, A., Characterization and relative ionization efficiencies of end-functionalized polystyrenes by matrix-assisted laser desorption/ionization mass spectrometry. *Journal of the American Society for Mass Spectrometry* **2003,** *14* (6), 648-657.
44. Wetzel, S. J.; Guttman, C. M.; Flynn, K. M.; Filliben, J. J., Significant Parameters in the Optimization of MALDI-TOF-MS for Synthetic Polymers+. *Journal of the American Society for Mass Spectrometry* **2006,** *17* (2), 246-252.
45. Wetzel, S. J.; Guttman, C. M.; Girard, J. E., The influence of matrix and laser energy on the molecular mass distribution of synthetic polymers obtained by MALDI-TOF-MS. *International Journal of Mass Spectrometry*
Polymer Characterisation by means of Mass Spectrometry: A Snapshot **2004,** *238* (3), 215-225.
46. Wetzel, S. J., Guttman, Charles M., Flynn, Kathleen M., The Influence of Electrospray Deposition in Matrix - Assisted Laser Desorption/Ionization Mass Spectrometry Sample Preparation for Synthetic Polymers. *Rapid Communications in Mass Spectrometry* **2004,** *18*, 1139 - 1146.
47. Hensel, R. R.; King, R. C.; Owens, K. G., Electrospray sample preparation for improved quantitation in matrix-assisted laser desorption/ionization time-of-flight mass spectrometry. *Rapid Communications in Mass Spectrometry* **1997,** *11* (16), 1785-1793.

48. Hilker, B.; Clifford, K. J.; Sauter Jr, A. D.; Sauter 3rd, A. D.; Harmon, J. P., The Measurement of Charge for Induction-Based Fluidic MALDI Dispense Event and Nanoliter Volume Verification in Real Time. *Journal of the American Society for Mass Spectrometry* **2009,** *20* (6), 1064-1067.
49. Hoteling, A. J.; Erb, W. J.; Tyson, R. J.; Owens, K. G., Exploring the Importance of the Relative Solubility of Matrix and Analyte in MALDI Sample Preparation Using HPLC. *Analytical Chemistry* **2004,** *76* (17), 5157-5164.
50. Axelsson, J. H., Anne-Mette; Waterson, Carl; Myatt, Paul; Shield, Gary L.; Varney, Julie; Haddleton, David M.; Derrick, Peter J. , Improved Reproducibility and Increased Signal Intensity in Matrix-assisted Laser Desorption/Ionization as a Result of Electrospray Sample Preparation. *Rapid Communications in Mass Spectrometry* **1997,** *11* (2), 209-213.
51. Tu, T.; Sauter Jr, A. D.; Sauter 3rd, A. D.; Gross, M. L., Improving the Signal Intensity and Sensitivity of MALDI Mass Spectrometry by Using Nanoliter Spots Deposited by Induction-Based Fluidics. *Journal of the American Society for Mass Spectrometry* **2008,** *19* (8), 1086-1090.
52. Vorm, O.; Roepstorff, P.; Mann, M., Improved Resolution and Very High Sensitivity in MALDI TOF of Matrix Surfaces Made by Fast Evaporation. *Analytical Chemistry* **1994,** *66* (19), 3281-3287.
53. Schriemer, D. C.; Li, L., Mass Discrimination in the Analysis of Polydisperse Polymers by MALDI Time-of-Flight Mass Spectrometry. 1. Sample Preparation and Desorption/Ionization Issues. *Analytical Chemistry* **1997,** *69* (20), 4169-4175.
54. Erb, W. J. O., Kevin G. , Development of a dual-spray electrospray deposition system for matrix-assisted laser desorption/ionization time-of-flight mass spectrometry. *Rapid Communications in Mass Spectrometry* **2008,** *22* (8), 1168-1174.
55. Macha, S. F.; Limbach, P. A.; Hanton, S. D.; Owens, K. G., Silver cluster interferences in matrix-assisted laser desorption/ionization (MALDI) mass spectrometry of nonpolar polymers. *Journal of the American Society for Mass Spectrometry* **2001,** *12* (6), 732-743.
56. Obolenskaya, M. Y.; Teplyuk, N. M.; Divi, R. L.; Poirier, M. C.; Filimonova, N. B.; Zadrozna, M.; Pasanen, M. J., Human placental glutathione S-transferase activity and polycyclic aromatic hydrocarbon DNA adducts as biomarkers for environmental oxidative stress in placentas from pregnant women living in radioactivity- and chemically-polluted regions. *Toxicology Letters* **2010,** *196* (2), 80-86.
57. Yochum, C. L.; Bhattacharya, P.; Patti, L.; Mirochnitchenko, O.; Wagner, G. C., Animal model of autism using GSTM1 knockout mice and early post-natal sodium valproate treatment. *Behavioural Brain Research* **2010,** *210* (2), 202-210.
58. Sies, H., Glutathione and its role in cellular functions. *Free Radical Biology and Medicine* **1999,** *27* (9,Äì10), 916-921.
59. Pastore, A.; Federici, G.; Bertini, E.; Piemonte, F., Analysis of glutathione: implication in redox and detoxification. *Clinica Chimica Acta* **2003,** *333* (1), 19-39.
60. Dalton, T. P.; Chen, Y.; Schneider, S. N.; Nebert, D. W.; Shertzer, H. G., Genetically altered mice to evaluate glutathione homeostasis in health and disease. *Free Radical Biology and Medicine* **2004,** *37* (10), 1511-1526.
61. Gotz, F., Staphylococcus and biofilms. *Molecular Microbiology* **2002,** *43* (6), 1367-1378.

62. Theis, J.-C. G., Shanu; White, Jonathan FACTORS AFFECTING IMPLANT RETENTION IN INFECTED JOINT REPLACEMENTS. *ANZ Journal of Surgery* **2007,** *77* (10), 877-879.

Chapter 2

Sample Deposition's Effect on MALDI Quantitation

2.1 Introduction

Matrix assisted laser desorption ionization (MALDI) was introduced in 1988 by Karas and Hillenkamp.[1] Since its introduction MALDI analysis has been found to be useful for the analysis of proteins, synthetic polymers, DNA, enzymes and a variety of small molecules.[2-6] Due to the wide range of molecules that can be effectively analyzed MALDI remains a powerful tool for qualitative and quantitative analysis.

Since its introduction in the late 1980s, scientists have been striving to improve signal intensity and sensitivity of MALDI by altering the various parameters of sample preparation.[1, 6-9] It has been demonstrated that the various components of sample preparation, such as concentration, solvent, cationizing agent, target suface and type of matrix can all have a profound impact on the resulting spectra.[5, 6, 10-14]

MALDI sample preparation is a several step process; the last step being sample deposition, the way the sample solution is delivered onto the target. There have been quite a few sample deposition techniques such as dried droplet, electrospray, fast evaporation, refrigerated droplet, two-layer, thin layer, nano-volume and induction fluidics deposition methods have all been studied[8, 9, 11, 14-16] to improve signal intensity and sensitivity as well as reproducibility. While the goals of these different methods are the same, they each employ very different mechanisms for deposition and try to alter different variables within the sample spot. Some of these

methods try to create smaller, more uniform crystals within the sample spot,[5, 8, 17, 18] while others try to minimize sample heterogeneity by altering the sample spot's diameter to be the same as the laser's diameter[9] resulting in oblation of the entire spot simultaneously

The fact that sample deposition technique has an impact on the quality of spectra has been previously discussed in other papers.[3, 8, 9, 18-20] However, these papers focus on the improvement in signal, resolution and reproducibility of the sample deposition methods; not the potential affect on quantitation.

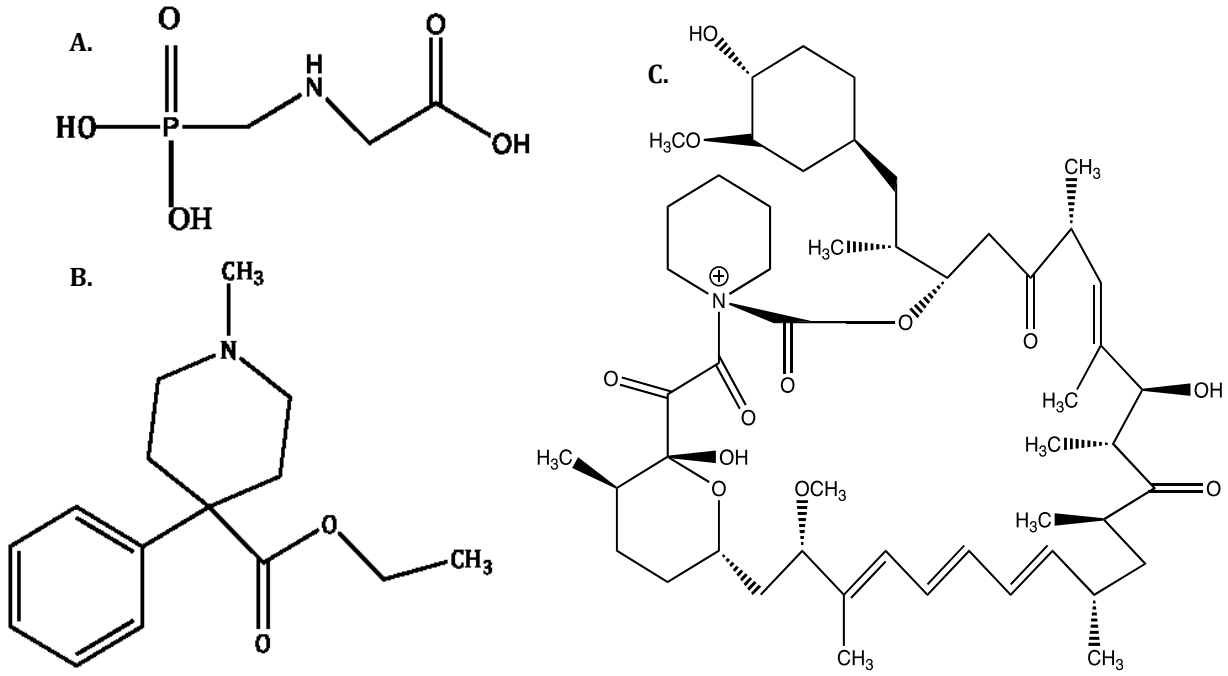

Figure 2.1. Chemical structures of analytes. **A.** glyphosate. **B.** meperidine. **C.** rapamycin

It would follow that if the sample deposition has such a profound affect on the quality of spectra produced that the quality of quantitation would vary with each of

the techniques. The simultaneous testing of these techniques and comparing the same analytes using each technique will provide for an objective evaluation.

Three analytes will be analyzed for this study. The analytes are glyphosate, an herbicide that is the active ingredient in Roundup, meperidine, the pain medicine commonly known as Demerol, and rapamycin, an immunosuppressant drug used in the course of organ transplantations. Figure 2.1 depicts the chemical structure of the selected analytes. These analytes were selected for their diversity in both physical properties and molecular mass. They were analyzed using atmospheric pressure matrix assisted laser desorption ionization time of flight mass spectrometry (AP – MALDI – TOF – MS). AP – MALDI is very similar to traditional MALDI. The difference between AP and conventional MALDI is the ionization process takes place under atmospheric pressure conditions instead of under vacuum.

This study focuses on three sample deposition techniques: electrospray, handspotting, and nanospotting. Electrospray deposition seeks to deposit a thin layer of the sample onto the MALDI target. It has been reasoned that the spray will quickly dry, resulting in homogeneous, small crystals. The oldest method for sample deposition is the hand spotting method. This method has a small amount of sample, $\sim$ 500 nL, onto the MALDI target. It is theorized that because such volatile solvents are used that the crystals will quickly form, resulting in a homogenous sample. The nanospotter is a variation of the hand spotting technique. The nanospotter deposits a small amount of sample > 300 nL onto a MALDI target. There are several ideas

that seek to explain the reported success of the nanospotter technique. One explanation is that the charge is inductively applied to the droplet resulting in the charge existing on the surface of the droplet, which gently pulls the sample to the target. This droplet creates a small spatially concentrated sample spot.[21, 22] Another theory is that because of the small spot produced that the laser will be able to ablate the entire spot at once producing a homogeneous sample spectrum or possibly that the concentrated spot contains ''sweet spots'' in close proximity that produces a high intensity spectrum that will enable high quality quantitation.[9, 21] These techniques will all be used to deposit three different analytes onto MALDI targets for quantitative analysis. Each technique will be evaluated using the calculated error associated with the molecule's quantitation.

2.2 Materials and Methods

2.2.1 Samples and reagents

AP – MADLI – TOF – MS analyses were performed using rapamycin (Cayman Chemicals, Ann Arbor, MI) and rapamycin – D4 (IsoScience, King of Prussia, PA), Meperidine and Meperidine – D4 standard (Cerilliant, Austin, TX) and Glyphosate (Sigma Life Science, St. Louis, MO) and Glyphosate C13 (Isotech Champaign Illinois). The matrix used to analyze each of the analytes was α – Cyano – 4 – hydroxycinnamic acid (CHCA) (Fluka, Lausanne, Switzerland) and used as received. The solvents used for the experiments were HPLC grade methanol and ethanol (EMD Chemicals Merk Rockland, MA).

2.2.2 Instrumentation

All experiments were performed on an updated Agilent (Santa Clara, CA) LC/MSD/TOF 6200 equipped with a MassTech (Columbia, MD) AP – MALDI source with a nitrogen laser operating at 337 nm with a spiraling raster motion. The Agilent TOF – MS is an orthogonal high-resolution mass spectrometer with pulsed dynamic focusing.

For analysis of the meperidine, the sample was analyzed in positive mode, the capillary voltage was set to 3200 volts, fragmentor voltage was kept at 100 volts, drying gas 5 L/min, temperature 350° C, skimmer 65 volts and laser attenuation was 6.

Sample analysis of rapamycin, used positive mode, the capillary voltage was set to 3200 volts, fragmentor voltage was kept at 325 volts, drying gas 5 L/min, temperature 350° C, skimmer 65 volts and laser attenuation was 7.

Glyphosate spectra were collected in negative mode with capillary voltage was set to 3200 volts, fragmentor voltage was kept at 100 volts, drying gas 5 L/min, temperature 350° C, skimmer 65 volts and laser attenuation was 6. A sample spectrum was collected over a minute and the laser was set to raster as to not burn through the sample spot for the ESD and handspotted samples. For nanospotter samples the laser was manually controlled so as not to move off of the small spot that was produced by the nanospotter. The described parameters for the analysis of each sample were optimized for quality data collection.

2.2.3 Sample Deposition

An electrospray sample deposition device was built using a Harvard Apparatus PHD 2000 infusion pump (Harvard Apparatus, Inc., Holliston, MA) and a high voltage

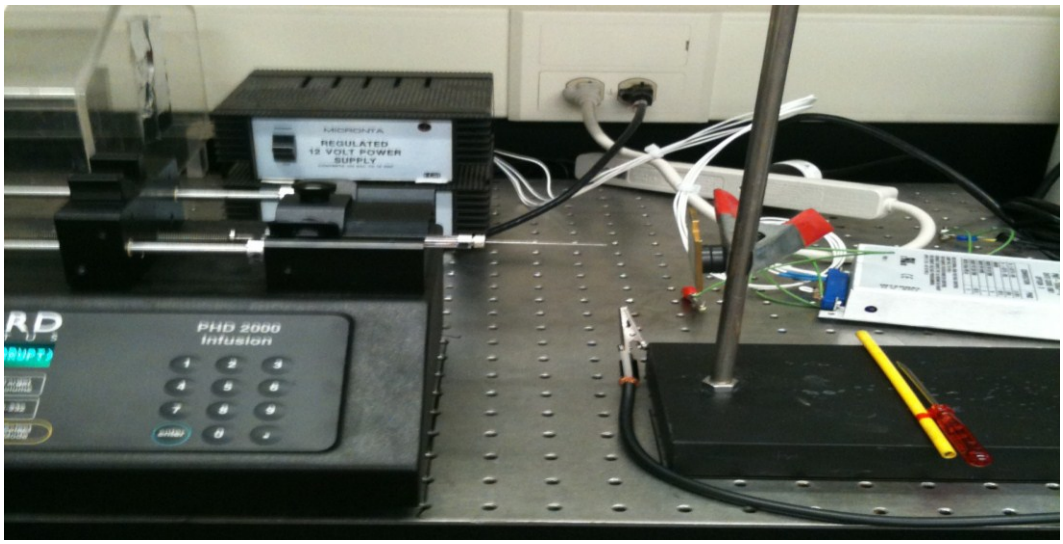

Figure 2.2. electrospray deposition device

power supply (Bertan, Inc.). The electrospray device was based upon others that have been described by Owens et al. [15, 19] Figure 2.2 is a photograph of the ESD device built in-house. Once the sample deposition device was built a series

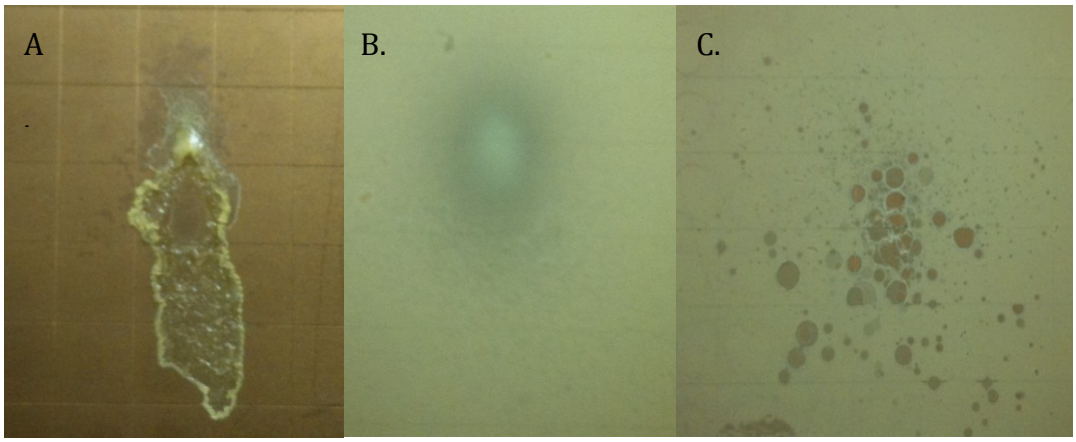

Figure 2.3. Picture of PEG 1430 sprayed at different voltages. **A.** 2 kV applied **B.** 3 kV applied **C.** 4 kV applied

of trials were performed to find the optimal settings for the device. The first parameter that was investigated was the flow rate. This was simply done by pushing a sample containing polyethylene glycol with average mass of 1430 da (PEG 1430) with retinoic acid (RA) matrix in tetrahydrofuran (THF), through the syringe while a voltage was being applied to visually inspect which flow rate produced the best spray to coat the grounded target. The flow rate had a significant effect upon the spray being produced, if the flow was too low the syringe would only drip and if it were too high, the produced spray was too wide resulting in sample spraying outside the target. The optimal flow was determined to be 10 μL/min. The next parameter that was explored was the applied voltage for the spray. Once again PEG 1430 was used for this optimization. The sample was then sprayed at three different voltages, 2, 3 and 4 kV respectively. As figure 2.3 indicates, there were visual differences produced by the altering voltages. When the samples were run on

the AP-MALDI – TOF-MS, it became apparent the voltage also affected the signal intensity, with the 3 kV spray producing the most intense sample signal. The differences in the sample intensity with different applied voltages was statistically analyzed using analysis of variance (ANOVA) to 95%. While this optimization was completed using THF as a solvent it is noteworthy that the optimization was repeated whenever the sample solvent was altered. The optimal voltage will vary based upon the solvent used due to differences in dielectric constants among different organic solvents. The next parameter of the ESD device

that was explored for optimization was the duration of the spray time or the amount of sample sprayed upon the target. This was achieved by spraying PEG 1430 onto a target for different amounts of time. The samples were analyzed with

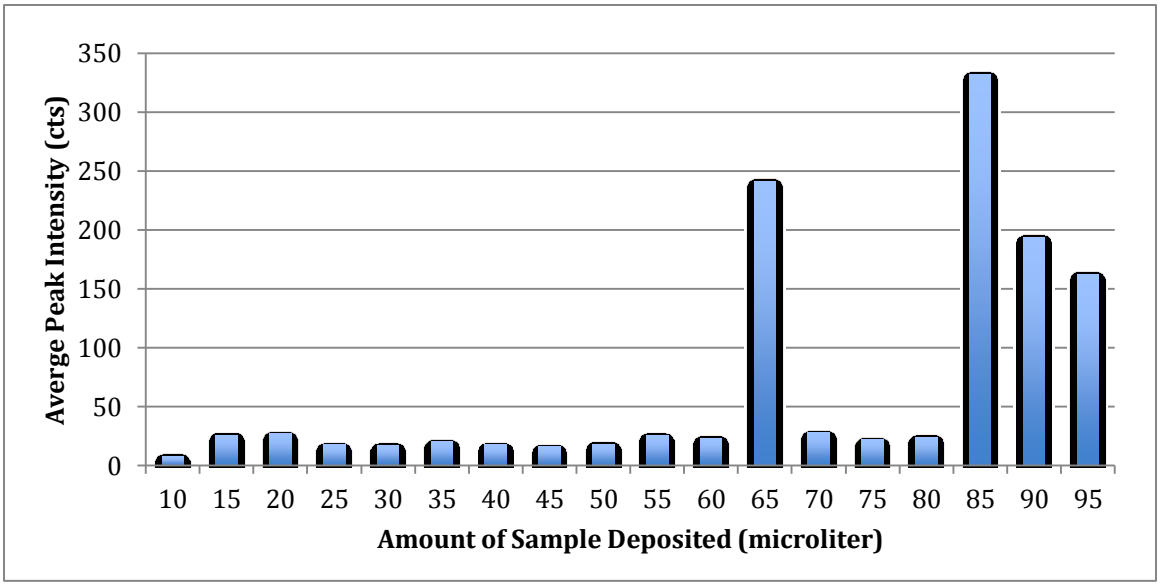

Figure 2.4. Average intensity of produced spectral signal vs. amount of sample deposited onto target in µL

the AP – MALDI-TOF-MS and the signal for the different targets was compared. For some of the targets with a less amount of sample solution the laser quickly burned

through the sample resulting in signal that only lasted briefly, while other targets produced seemingly suppressed signal. Figure 2.4 is a chart depicting the trials completed for the different amounts of time/amount of sample deposited. The signal intensities were compared using ANOVA and it was determined that a spray time of 8.5 min or 85 μL of sample being deposited onto the target.

The three samples for the quantitative sample deposition study were sprayed onto grounded MALDI targets at 10 μL/min with a voltage of 6 kV being applied in either methanol or methanol/ethanol mixture. The targets were sprayed for 8.5 min each, resulting in 85 μL of sample being deposited upon the target. The sample spray was allowed to coat the entire target.

Nanoliter spots were deposited using a nanospotter purchased from Nanoliter LLC. The spotter was set up and used according to the manufacturer user manual. As per instructed in the manual, sample solution was drawn up into a 10 μL gas tight syringe. A narrow capillary was then joined to the syringe needle by a junction that was provided with the nanospotter device. The syringe was then placed into the holder, that not only inductively applies a charge to the syringe, but also attaches the syringe to the stepper motor and controller, which allows for the unit to dispense a precise amount of sample to the target. The target was grounded in order to attract the charged droplet to the surface of the target. While the nanospotter seemed as if it would be relatively simple to use, this was not found to be the case. There were a multitude of issues that surrounded the device. The dispenser that controlled the amount of sample that was to be deposited worked

slowly preventing deposition of volumes smaller than 200 μL. Whenever a volume smaller than 200 μL was attempted the sample would simply evaporate before the inductively applied voltage could pull it down to the target.

The current being applied to the solution also offered some trouble. At times, though the current switch would be in the on position it appeared that the current was not being correctly applied, resulting in a droplet that just hung off the end of the capillary tube or a droplet that would travel upwards along the outside of the capillary tube and syringe needle. Although the device was repeatedly inspected for missing contacts or perhaps an incorrectly grounded target, all was found to be correctly connected. Figure 2.5 is a photograph of the nanospotter device. For each sample included in the quantitative sample deposition study, 200 nL was deposited onto the target for analysis using the nanospotter device. Hand spot samples were created by depositing ~0.5 μL of the sample solution onto the target using a Nichiryo Model 5000DG digital micropipette (Tokyo, Japan). The spots were

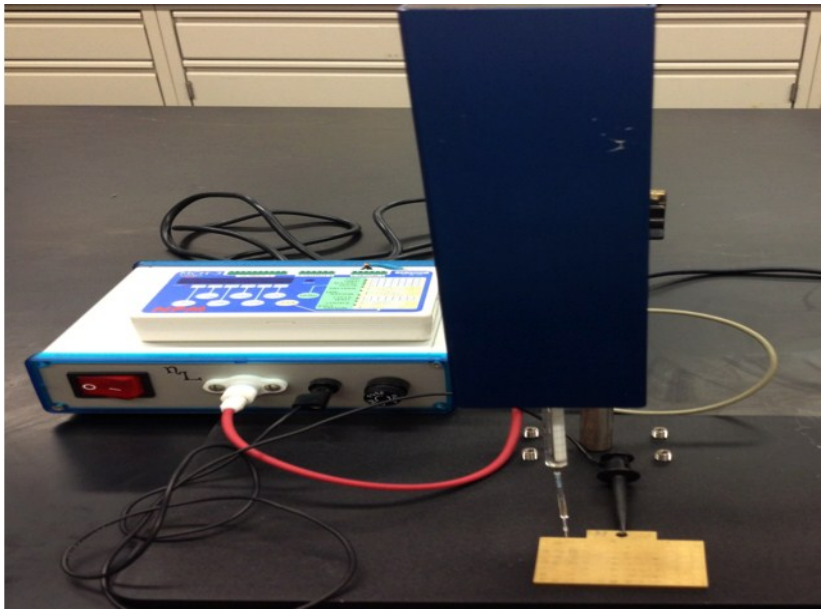

Figure2.5. Nanospotter device

allowed to dry under ambient atmospheric conditions. Figure 2.6 are screen shots of the Target 5 software that controls the sample stage and laser of the MALDI. The software automatically magnifies the image to a 10x magnification. As observed in figure 2.6, the spots that resulted from the sample deposition varied greatly among techniques.

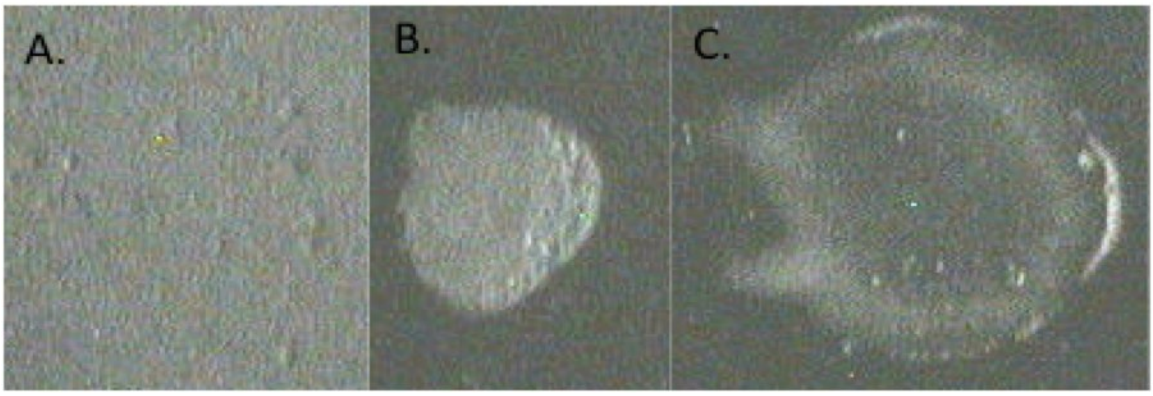

Figure 2.6. Sample spots, 10X magnification. **A.** ESD **B.** nanospot **C.** hand spot

The electrosprayed sample target (A) appeared to have a fine thick layer of crystals while the nanospotted (B) sample appeared to have variation in thickness with a thicker band on the one side of the spot and hand spotted (C) spots had some crystals that were larger than others and a ring of thicker sample around the spot. The resulting mass spectra of the different analytes also varied by deposition technique in intensity as expected from previous studies.[8, 15, 19]

2.2.4. Sample Preparation

Matrix solutions were prepared by mixing ~ 9.0 mg of α – Cyano – 4 – hydroxycinnamic acid with 250 µL of methanol. Sample solutions were prepared by dissolving 2 mg of sample into 250 µL of solvent for each analytical standard and

isotopically labeled standard. Methanol was the solvent for the dissolution of glyphosate and meperidine while ethanol was used to dissolve the rapamycin. Because the CHCA matrix would not dissolve into ethanol, the sample of rapamycin contained two solvents; the methanol that the CHCA was dissolved in and the ethanol that the rapamycin samples were dissolved into. Sample solutions were made by mixing 30 μL of natural sample, 30 μL of isotopically labeled standard and 60 μL of matrix. All samples were made using a 1:1 ratio of natural sample to isotopically labeled sample. The same sample was deposited using each of the three methods.

2.3. Results/Discussion

Each sample was able to produce spectra that had an acceptable signal to noise ratio. The spectra were then averaged and compared to indicate which sample deposition method produced the most intense signal. Once the signal intensity was judged, the samples were quantitated as planned. Figure 2.7 A – C are images obtained by utilizing scanning electron microscopy (SEM), to closely view the crystals resulting

from each sample deposition technique for the meperidine samples. The resulting images clearly demonstrate the impact that sample deposition has upon the manner of crystal formation within the sample spot. For good MALDI analysis it is desirable

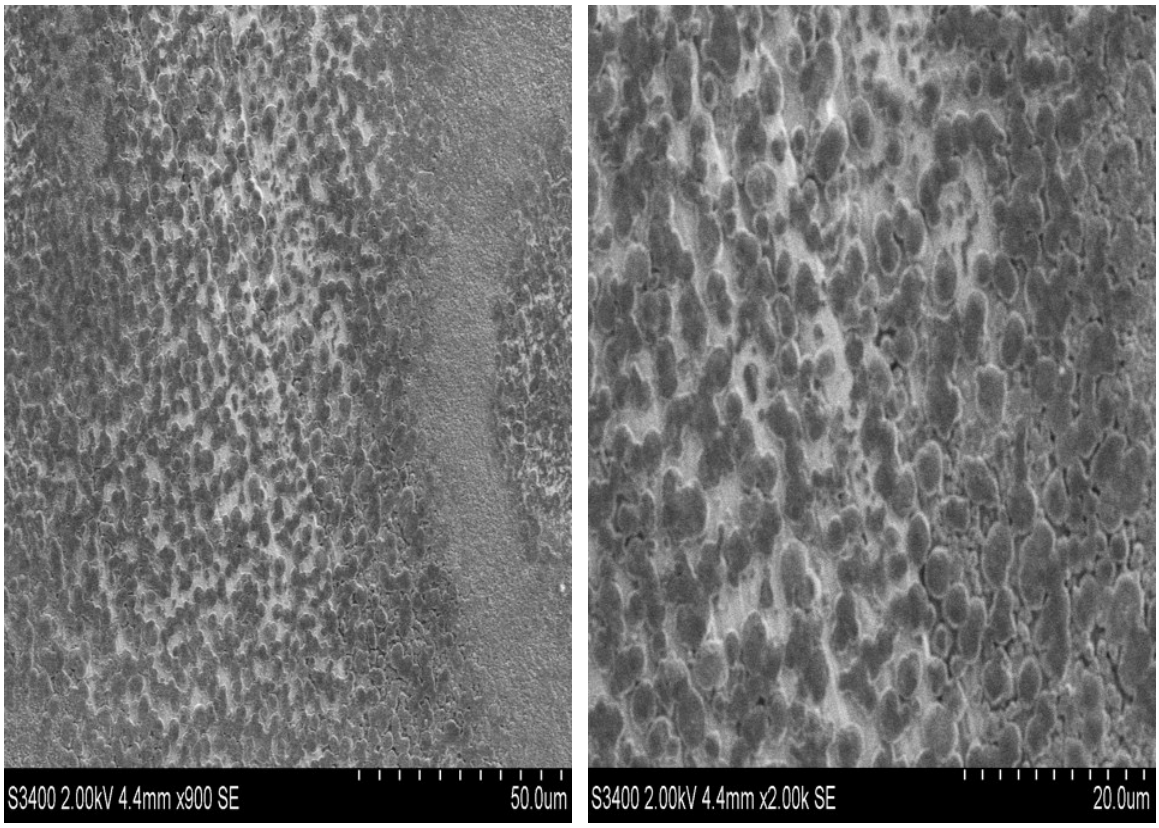

Figure 2.7.A. SEM images of ESD samples 900x and 2,000x magnification

to have uniform even sample film that incorporates the sample into the matrix crystals for signal intensity and reproducibility.[8] In figure 2.7.A., the ESD sample appears to the most uniform crystallization, having a diameter range of ~10 – 47 μm. While there does seem to be some degree of variation, this sample seems to have the best homogeneity overall. The nanospotter image, figure 2.7.B., produced crystals that were closer in morphology to the ESD crystals but these crystals had a diameter range of ~ 21.4 – 78.6 μm. While there was more variation among the sample spot, less uniform than the ESD but more uniform than the handspotting. With some

areas being thicker than others, it showed that the sample surface was less uniform than the ESD but more uniform than the handspotting. The image of the

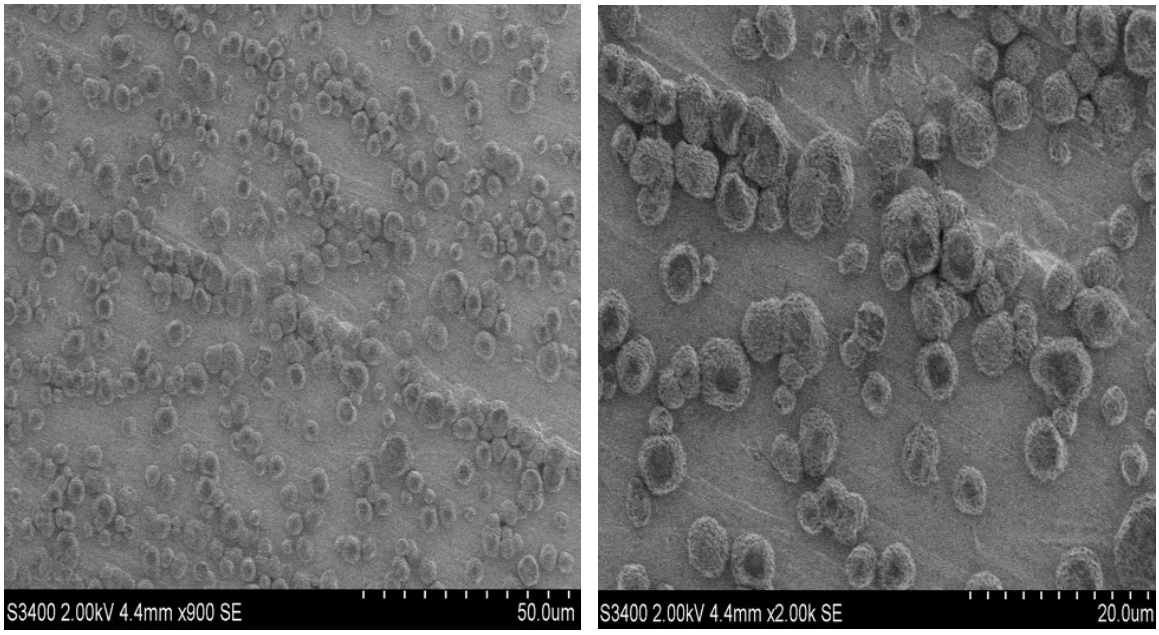

Figure 2.7.B. SEM images of nanospotter samples 900x and 2,000x magnification

handspotted sample, figure 2.7.C., clearly shows crystals of various shapes and sizes with a diameter range from ~ 30 – 392.9 μm. It is difficult to determine if the larger

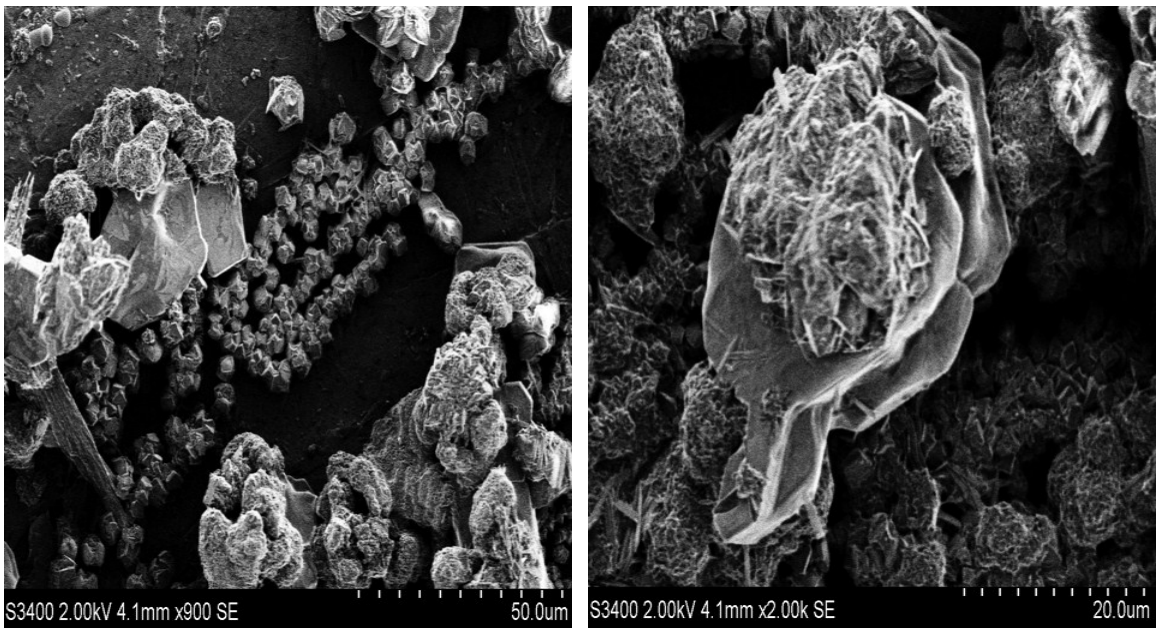

Figure 2.7.C. SEM images of hand spotted samples 900x and 2,000x magnification

crystals truly incorporate both the matrix and the sample analyte. The large crystals that are present would require more laser energy to overcome the lattice energy and ionize. The variation in crystal size could result in the laser energy being absorbed unevenly throughout the sample potentially causing a preferential ionization.

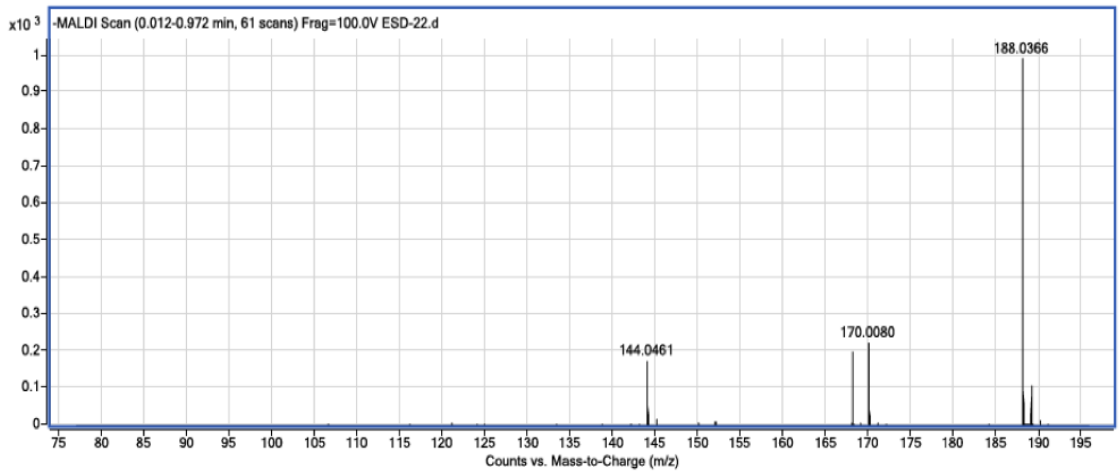

Figure 2.8. Raw data spectra of natural (168.9) and labeled (169.9) glyphosate.

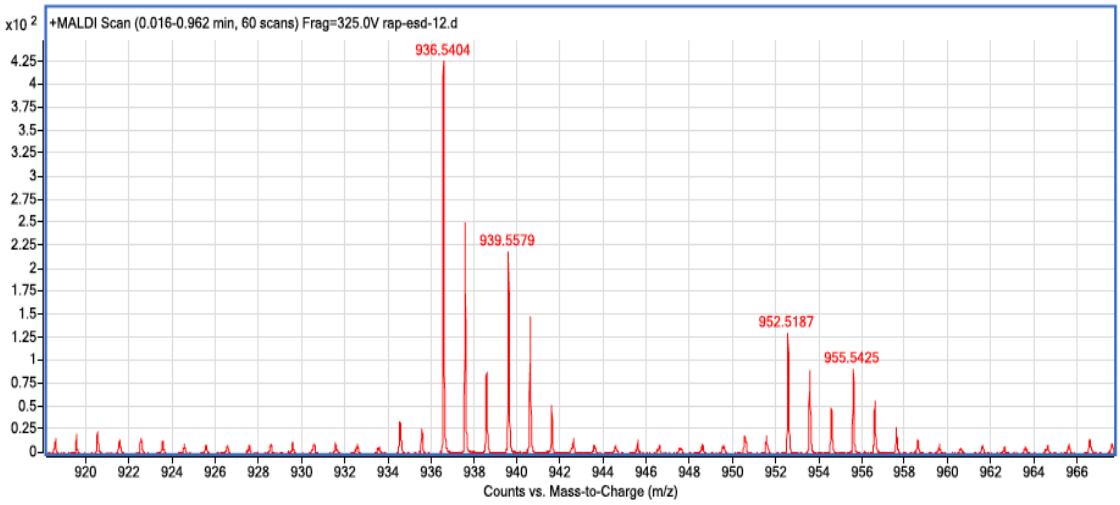

Figure 2.9. Spectra of natural (936.5) and labeled (939.5) rapamycin.

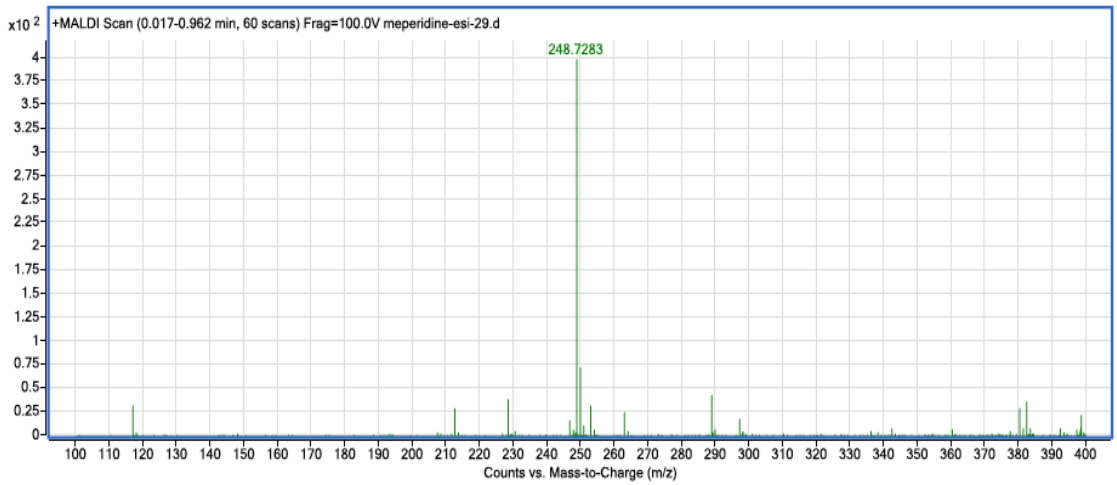

Figure 2.10. Raw data spectra of natural meperidine (248.7).

Figures 2.8 – 2.10 are the raw data spectra obtained by AP – MALDI – TOF – MS. The spectra are zoomed in where necessary to allow for the analyte peaks to be observed. Figure 2.8 is the spectrum of glyphosate. Within this spectrum the natural glyphosate is present at a *m/z* of 168.9 amu and the labeled form of glyphosate is found at 169.9 *m/z*. Both the natural and labeled glyphosate are protonated. Figure 2.9 is the mass spectrum of rapamycin. The natural rapamycin is located at *m/z* of 936.5 and 952.5. The isotopically labeled rapamycin is found at *m/z* 939.5 and 955.5. For both the natural and isotopically labeled species they are sodiated and potassiated, being ionized with a sodium and potassium respectively. Figure 2.10 is the spectra of natural meperidine. The sample peak is at *m/z* 248.7 which is the protonated ion species.

Figures 2.11 – 2.13 represent the average peak areas of the multiple spectra collected for each deposition method, n=32, and plotted in a graphing software. The different sample deposition techniques have lead to different intensities for

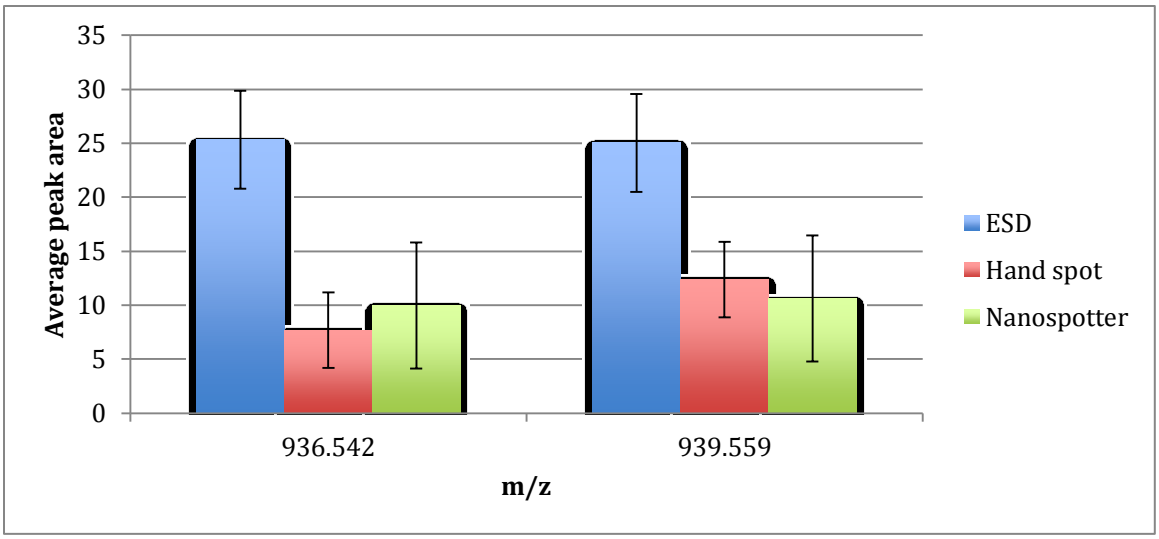

Figure 2.11. mass spectrum of rapamycin ESD produced the best signal

produced spectra. The mass spectra of rapamycin showed a greater intensity of signal for the ESD as is observed in figure 2.11 and handspotting yielded the greatest signal intensities in glyphosate and meperidine as observed in figures 2.12

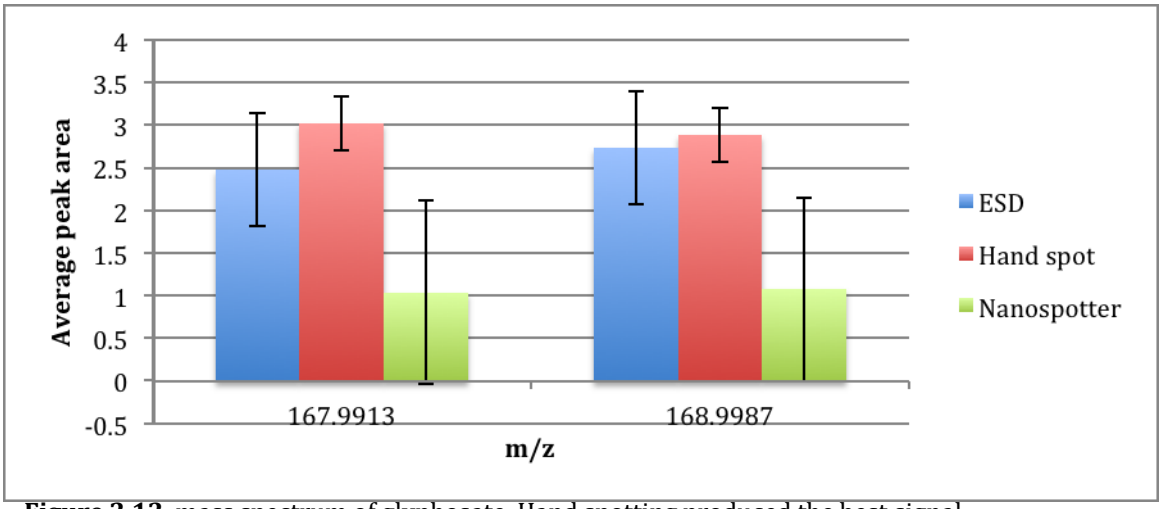

Figure 2.12. mass spectrum of glyphosate. Hand spotting produced the best signal

and 2.13. The spectrum for rapamycin shows sodiated ions of the natural and

labeled rapamycin samples. The natural abundance standard ion is located at *m/z* 936.5452 and the deuterated standard ion is located at 939.5604 and 955.5405 respectively as observed in figure 2.11 for rapamycin.

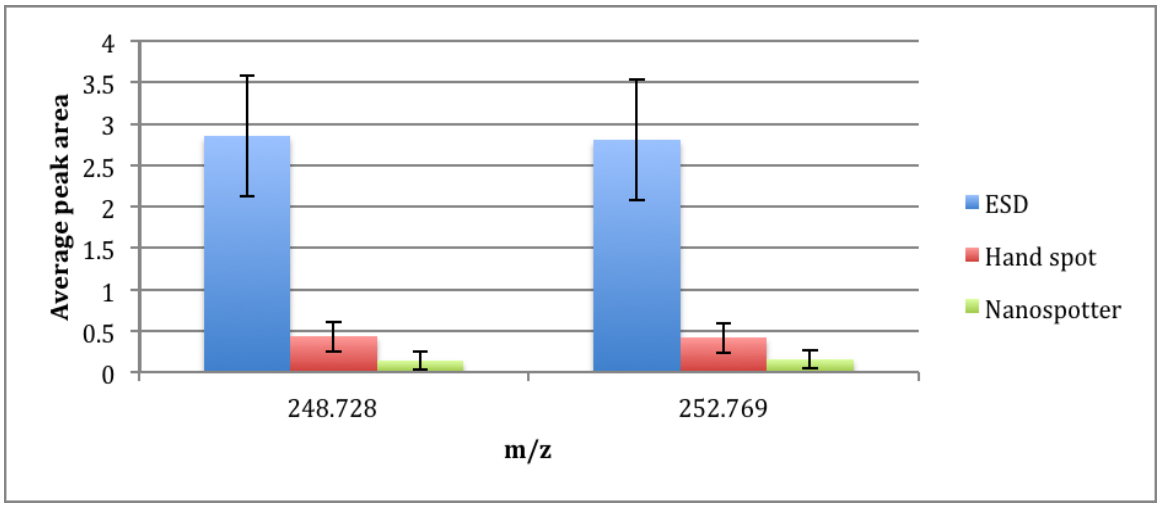

Figure 2.13. Mass spectrum of meperidine. Hand spotting produced the best signal intensity for this sample.

Figure 2.11 of glyphosate, shows the natural abundance standard deprotonated with a *m/z* of 167.9913 and the C13 standard deprotonated with a *m/z* of 168.9987. The meperidine and its deuterated standard, in figure 2.13, are protonated with *m/z* at 248.7281 and 252.7685 respectively. While the method of sample deposition producing the most intense signal intensity varied between ESD and handspotting methodology, the reproducibility of signal was found to be the best with the samples electrosprayed onto the target. When the peak areas of the different samples were compared using ANOVA, it was found that the difference in signal was statistically significant to a confidence of 95%.

2.3.1. Quantitation

Quantitation was done for each sample utilizing IDMS. IDMS is an internal standard method that includes an element's natural abundances to help further remove errors in the measurement.[23, 24]

$$\text{concentration,ug/g} = \frac{\left(\left(W_{sp} \cdot C\right)/W_s\right) \cdot \left(A_{sp} - \left(R \cdot B_{sp}\right)\right)}{\left(B \cdot R\right) - A} \quad \textbf{Equation 2.1.}$$

Equation 2.1 is the IDMS equation, which was used to calculate concentration. Within the equation W_{sp} is the mass of the labeled standard and C is the concentration of the labeled solution. This is then divided by W_s, the mass of the standard solution. R is experimentally measured ratio of sample to labeled standard, which is multiplied by B_{sp} the abundance of unlabeled element within the isotopically enriched standard. This product is subtracted from the purity of the isotopically enriched standard. B is the probability that the enriched isotope will naturally occur within the non-enriched sample (natural abundance) and A is the natural abundance of the unenriched element that is being used as the isotopic label, for example if C13 was the label, A would be the natural abundance of C12.[23-25] IDMS was used for quantitation of each analyte. The IDMS equation seeks to elucidate the exact concentration of the analyte by comparing the peak areas of the natural standard and the isotopically enriched standard. The equation uses the weight of the isotopically labeled solution (W_{sp}) (aka spike solution) and the concentration of this solution (C). The atomic fraction of isotope A in the natural standard (A_{sp}) and the atomic fraction of B in isotopically labeled standard (B_{sp}) are also considered to further reduce error. The other coefficients that are used in the

equation are the atomic weight of the analyte (M), the weight of the sample (W_s) and the experimentally measured isotopic ratio of A/B (R) using peak area of each. This quantitation method seeks to reduce error by taking into account that the natural labeled standard will have some enriched elements that occur naturally. The same holds true for the isotopically labeled standard due to the fact that it is not 100% pure, there will be some naturally occurring elements that have not been enriched. These 'impurities' within the standards will introduce error into the measurement if they are not addressed. For example, the meperidine standard and isotopically labeled standard have purity of 99.9% and 98.9% respectively. This indicates that there is a 0.1% possibility that the natural standard could contain an isotope that would change its location on the mass spectrum. While this 0.1% chance of an isotope being present in the natural sample is small, errors add together so eliminating as many errors as possible is desirable. The isotopically enriched standard of meperidine could contribute to error by having a purity of 98.9% meaning that there is 1.1% chance that unlabeled or natural meperidine is within this sample. Again, while this is not a dramatic amount of 'impurity' this can contribute to the overall error in the quantitation.

Analyte	**ESD (µg/g)**	**Hand spot (µg/g)**	**Nanospotter (µg/g)**
Meperidine	$7.71E^{-5}$ (-3.8% ± 10.1)	$7.63E^{-5}$ (-4.7% ±20.8)	$1.07E^{-4}$ (33.6% ±37.1)
Glyphosate	9463.5769 (-6.4% ±15.5)	11142.2001 (39.1% ±18.9)	10416.2027 (30.1% ±26.3)
Rapamycin	197.24 (-1.5% ±6.9)	196.72 (-1.8% ±4.9)	204.97 (2.4% ±15.5)

Table 2.1. Average measured sample concentration (µg/g) and percent error of the quantitation of different analytes deposited onto MALDI targets using different methods

The quantification results demonstrated a clear trend. Table 2.1 shows the average calculated concentration of each analyte (μg/g) and the average percent error in quantitation for the 3 different sample deposition methods. The ESD method of sample deposition produced mass spectra that were more accurate and precise for quantitation. The other two methods produced mass spectra that demonstrated larger errors and therefore less accurate quantitation results. The sample deposition method is the only variable within the group of samples that is being analyzed; therefore it is what is influencing the quantitation error.

The glyphosate sample that was analyzed produced errors that were significantly higher than the other samples. This is believed to due to possible reactions between the glyphosate sample and the matrix. Though there seemed to be reactions that occurred between the analyte and the matrix, the CHCA matrix was found to have less reaction with the sample than other available matrixes.

This methodology of analysis has demonstrated that AP – MALDI-TOF-MS is able to be a quantitative method of analysis. The errors that were reported for the meperidine and the rapamycin for all of the sample deposition techniques is an improvement over other studies that performed quantitative MALDI analysis[26,27]. The referenced studies produced average errors that ranged from 5.2 % – 78%.[26,27]

2.4. Conclusion

It was found that the sample deposition method used not only significantly influences the intensity and reproducibility of the signal produced, but also influences the outcome of analyte quantitation. In all of the three analytes used it was found that ESD was superior for accurate and precise quantitation. In two samples, the meperidine and the rapamycin it was discovered that the hand spotting method produced more accurate results than the nanospotter method but in the case of the glyphosate the nanospotter was found to produce more accurate results than the hand spotting. This would also explain the error within the quantitation of the samples because good signal intensity is essential for an accurate sample quantitation and the standard deviation for the samples demonstrates the spot to spot variability. The data is clear that the ESD method is the superior method of the three methods tested for accurate and precise quantitation of these analytes. ESD with IDMS was also found to consistently produce quantitation errors that were significantly lower than other previously published studies.[26,27]

References:

1. Karas, M.; Hillenkamp, F., Laser desorption ionization of proteins with molecular masses exceeding 10,000 daltons. *Analytical Chemistry* **1988,** *60* (20), 2299-2301.
2. Horak, J.; Werther, W.; Schmid, E. R., Optimisation of the quantitative determination of chlormequat by matrix-assisted laser desorption/ionisation mass spectrometry. *Rapid Communications in Mass Spectrometry* **2001,** *15* (4), 241-248.
3. Wetzel, S. J., Guttman, Charles M., Flynn, Kathleen M., The Influence of Electrospray Deposition in Matrix - Assisted Laser Desorption/Ionization Mass Spectrometry Sample Preparation for Synthetic Polymers. *Rapid Communications in Mass Spectrometry* **2004,** *18*, 1139 - 114.
4. Bucknall, M.; Fung, K. Y. C.; Duncan, M. W., Practical quantitative biomedical applications of MALDI-TOF mass spectrometry. *Journal of the American Society for Mass Spectrometry* **2002,** *13* (9), 1015-1027.
5. Kang, M.-J.; Tholey, A.; Heinzle, E., Application of automated matrix-assisted laser desorption/ionization time-of-flight mass spectrometry for the measurement of enzyme activities. *Rapid Communications in Mass Spectrometry* **2001,** *15* (15), 1327-1333.
6. Gobey, J.; Cole, M.; Janiszewski, J.; Covey, T.; Chau, T.; Kovarik, P.; Corr, J., Characterization and Performance of MALDI on a Triple Quadrupole Mass Spectrometer for Analysis and Quantification of Small Molecules. *Analytical Chemistry* **2005,** *77* (17), 5643-5654.
7. Tanaka, K., Protein and polymer analyses up to m/z 100000 by laser ionization time-of-flight mass spectrometry. *Rapid Commun Mass Spectrom* **1988,** *2*, 151-153.
8. Axelsson, J. H., Anne-Mette; Waterson, Carl; Myatt, Paul; Shield, Gary L.; Varney, Julie; Haddleton, David M.; Derrick, Peter J. , Improved Reproducibility and Increased Signal Intensity in Matrix-assisted Laser Desorption/Ionization as a Result of Electrospray Sample Preparation. *Rapid Communications in Mass Spectrometry* **1997,** *11* (2), 209-213.
9. Tu, T.; Sauter Jr, A. D.; Sauter 3rd, A. D.; Gross, M. L., Improving the Signal Intensity and Sensitivity of MALDI Mass Spectrometry by Using Nanoliter Spots Deposited by Induction-Based Fluidics. *Journal of the American Society for Mass Spectrometry* **2008,** *19* (8), 1086-1090.
10. Wetzel, S. J., Guttman, Charles M., Girard, James E., The Influence of Matrix and Laser Energy on the Molecular Mass Distribution of Synthetic Polymers Obtained by MALDI-TOF-MS. *International Journal of Mass Spectrometry* **2004,** *238*, 215 - 225.
11. Montaudo, G.; Samperi, F.; Montaudo, M. S., Characterization of synthetic polymers by MALDI-MS. *Progress in Polymer Science* **2006,** *31* (3), 277-357.
12. Schriemer, D. C.; Li, L., Mass Discrimination in the Analysis of Polydisperse Polymers by MALDI Time-of-Flight Mass Spectrometry. 1. Sample Preparation and Desorption/Ionization Issues. *Analytical Chemistry* **1997,** *69* (20), 4169-4175.

13. Holcomb, A.; Owens, K. G., Optimization of a modified aerospray deposition device for the preparation of samples for quantitative analysis by MALDI-TOFMS. *Analytica Chimica Acta* **2010,** *658* (1), 49-55.
14. Ericson, C.; Phung, Q. T.; Horn, D. M.; Peters, E. C.; Fitchett, J. R.; Ficarro, S. B.; Salomon, A. R.; Brill, L. M.; Brock, A., An Automated Noncontact Deposition Interface for Liquid Chromatography Matrix-Assisted Laser Desorption/Ionization Mass Spectrometry. *Analytical Chemistry* **2003,** *75* (10), 2309-2315.
15. Erb, W. J. O., Kevin G. , Development of a dual-spray electrospray deposition system for matrix-assisted laser desorption/ionization time-of-flight mass spectrometry. *Rapid Communications in Mass Spectrometry* **2008,** *22* (8), 1168-1174.
16. Lin, Y.-S. Y., Chin-Hsiung ; Chen,Yu-Chie Glass-chip-based sample preparation and on-chip trypic digestion for matrix-assisted laser desorption/ionization mass spectrometric analysis using a sol-gel/2,5-dihydroxybenzoic acid hybrid matrix. *Rapid Communications in Mass Spectrometry* **2004,** *18* (3), 313-318.
17. Hanton, S. D.; Cornelio Clark, P. A.; Owens, K. G., Investigations of matrix-assisted laser desorption/ionization sample preparation by time-of-flight secondary ion mass spectrometry. *Journal of the American Society for Mass Spectrometry* **1999,** *10* (2), 104-111.
18. Vorm, O.; Roepstorff, P.; Mann, M., Improved Resolution and Very High Sensitivity in MALDI TOF of Matrix Surfaces Made by Fast Evaporation. *Analytical Chemistry* **1994,** *66* (19), 3281-3287.
19. Hanton, S. D.; Hyder, I. Z.; Stets, J. R.; Owens, K. G.; Blair, W. R.; Guttman, C. M.; Giuseppetti, A. A., Investigations of electrospray sample deposition for polymer MALDI mass spectrometry. *Journal of the American Society for Mass Spectrometry* **2004,** *15* (2), 168-179.
20. Xianwen Lou, J. L. J. v. D., Direct sample fraction deposition using electrospray in narrow-bore size-exclusion chromatography/matrix-assisted laser desorption/ionization time-of-flight mass spectrometry for polymer characterization. *Journal of Mass Spectrometry* **2000,** *35* (11), 1308-1312.
21. Hilker, B.; Clifford, K. J.; Sauter Jr, A. D.; Sauter Iii, A. D.; Gauthier, T.; Harmon, J. P., Electric field enhanced sample preparation for synthetic polymer MALDI-TOF mass spectrometry via Induction Based Fluidics (IBF). *Polymer* **2009,** *50* (4), 1015-1024.
22. Hilker, B.; Clifford, K. J.; Sauter Jr, A. D.; Sauter 3rd, A. D.; Harmon, J. P., The Measurement of Charge for Induction-Based Fluidic MALDI Dispense Event and Nanoliter Volume Verification in Real Time. *Journal of the American Society for Mass Spectrometry* **2009,** *20* (6), 1064-1067.
23. Henrion, A., Reduction of systematic errors in quantitative analysis by isotope dilution mass spectrometry (IDMS): an iterative method. *Fresenius' Journal of Analytical Chemistry* **1994,** *350* (12), 657-658.
24. U.S. EPA Method 6800 in Test Methods for Evaluative Solid Water, Physical/Chemical Methods SW846, Update IVA. P, U. S. E., Ed. Washington, DC, , 2008.
25. Meija, J.; Mester, Z. n., Paradigms in isotope dilution mass spectrometry for elemental speciation analysis. *Analytica Chimica Acta* **2008,** *607* (2), 115-125.
26. Sleno, L.; Volmer, D. A., Some fundamental and technical aspects of the

quantitative analysis of pharmaceutical drugs by matrix-assisted laser desorption/ionization mass spectrometry. *Rapid Communications in Mass Spectrometry* **2005,** *19* (14), 1928-1936.
27. Wu, H.-F.; Ku, H.-Y.; Yen, J.-H., Liquid-phase microextraction for rapid AP-MALDI and quantitation of nortriptyline in biological matrices. Journal of Separation Science 2008, 31 (12), 2288-2294.

Chapter 3

Synthetic Polymer Analysis

3.1 Conventional Analysis Methods

Many methods for synthetic polymer analysis have been developed.[1] As expected with the implementation of different methods, each has their pros and cons. This holds true with the methods developed for the analysis of synthetic polymers. Overall there are two types of analysis techniques: absolute and relative techniques.[2] Relative techniques for sample analysis requires a mass calibration for comparison with the polymer desired to be analyzed while absolute techniques can take measurements of a sample without any calibration from a similar sample.[2] Polymer sample analysis usually consists of a variety of relative and absolute methods that measure one specific physical property of the sample.[3] Size-exclusion chromatography (SEC) is a method that has been used for the determination of the molar mass distributions.[4, 5] SEC is commonly done in conjunction with nuclear magnetic resonance (NMR) to obtain information on molecular mass distribution and mass number.[6, 7] Light scattering methods accompanied by viscosity measurements are also used for the analysis of synthetic polymers.[8] This technique can only provide limited information such as the mass average of the synthetic polymer.[9] NMR and light scattering methods along with analytical ultracentrifugation are examples of absolute methods; methods that do not require calibration with a like polymer, but they only obtain a mass average of the polymer.[5,

[7] SEC, which obtains the entire molecular mass distribution (MMD), not just a mass average, is a relative method.[7]

3.2 MALDI Analysis of Synthetic Polymers

In recent years MALDI-TOF-MS analysis of synthetic polymers has gained interest as a complementary method to the classical methods of polymer analysis.[10] Mass spectrometry is an absolute method of analysis that determines the MMD and completely characterizes polymers including end group and branching information.[11] Another benefit of MALDI analysis is that it is a soft ionization method producing spectra of in-tact molecular chains giving a complete picture of the molecule being analyzed which will allow for complete structure elucidation.[12] It was soon discovered that using MALDI-TOF-MS was a great asset to the analytical chemists because of its ability to provide information on molecular mass moment, distribution end group information as well as branching information.[13, 14] Despite the wealth of information that MALDI analysis has the potential to provide, it was slow to be widely accepted due to the fact that MALDI does have some issues with consistently reproducible data and analysis problems with polymers of wide polydispersity.[15-17] Despite these issues, it has been shown that mass spectrometry provides exact, direct, fast and complete characterization of synthetic polymers.[18] The fact that MALDI-TOF-MS analysis provides superior information outweighs inconsistencies that can be made statistically less significant with multiple sample runs.[19, 20]

Two types of synthetic polymers were chosen for the study of the AP – MALDI-TOF-MS analysis of synthetic polymers and the effect that sample preparation has upon the resulting signal. The polymers selected for analysis were polyethylene glycol (PEG) and polystyrene (PS). These polymers were selected due to their prominence in the literature. There have been a number of papers published on the vacuum MALDI analysis of PEG and PS.[2, 3, 6, 17-19, 21-32] Figure 3.1 A. is the structure of PEG and 3.1.B. is the chemical structure of PS.

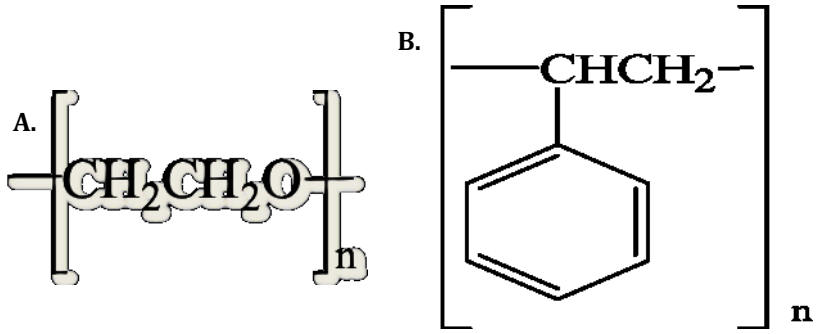

Figure 3.1. chemical structure of **A.** PEG and **B.** PS.

The reason for selecting polymers that have been discussed within the literature was to have an abundance of information to work from in the effort of finding an efficient way for the analysis of polymers using AP – MALDI-TOF-MS. There are only few molecules have been analyzed using AP – MALDI, usually being small molecules and not within the synthetic polymer category.

This experimentation was initiated to determine whether synthetic polymer analysis could be completed using AP – MALDI-TOF-MS analysis. Once it was determined that such analysis could in fact be accomplished, analysis was conducted to determine how sample preparation would affect the produced signal.

3.3 Materials and Methods

3.3.1 Reagents and Samples

Polymer samples of PEG and PS with differing mass moments (M_n) were gifted from NIST Polymers Division (Gaithersburg, MD). *All-trans*-retinoic acid (RA) was purchased from Sigma-Aldrich (St. Louis, MO, USA) and α-Cyano-4-hydroxycinnamic acid (CHCA) was purchased from Fluka (Lausanne, Switzerland). The solvent chosen was tetrahydrofuran (THF) also purchased from Sigma-Aldrich (St. Louis, MO, USA). This solvent was selected due to its ability to dissolve all of the components used and is quick drying. It is important for MALDI analysis that the solvent be quick drying to allow the formation of small matrix crystals and to prevent fractionation of the polymer. Previous work indicated that CHCA was the best matrix for the analysis of PS, figure 3.2. is the chemical structure of CHCA.

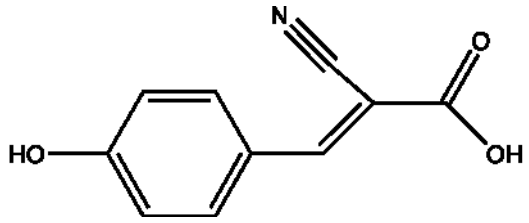

Figure 3.2. chemical structure of α-Cyano-4-hydroxycinnamic acid

Based on previous work and literature references it was determined that *all-trans*-Retinoic acid (RA) was a good matrix for the analysis of polyethylene glycol.[17] Figure 3.3. is the chemical structure of RA.

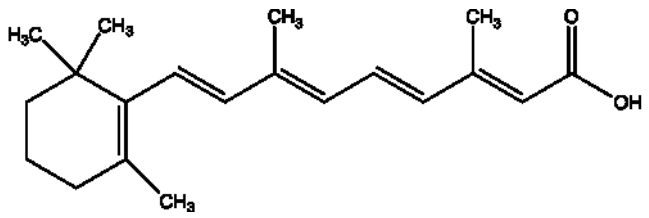

Figure 3.3. chemical structure of *all-trans*-Retinoic acid

Previous work also indicated that Trifluoroacetic acid sodium salt (NaTFA), purchased from Sigma-Aldrich (St. Louis, MO, USA), was the best cationizing agent available for the analysis of PEG.[31] For the analysis of PS, CHCA was used along with silver trifluoroacetic acid salt, gifted from NIST Polymers Division (Gaithersburg, MD) for the cationizing agent as it was used in the literature.[31]

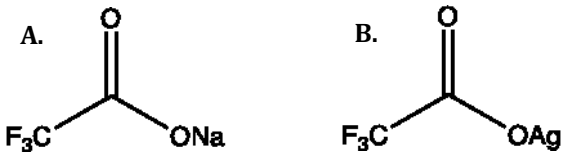

Figure 3.4. chemical structure of **A.** sodium TFA and **B.** silver TFA

While the literature was extremely helpful for determining the matrix and cationizing agent that should be used, special consideration was taken into account when a matrix was being selected due to the limitations of the instrument. The instrument does not have the capability to ionize all of the different matrixes that are available and have been used in literature, such as 2,5-Dihydroxybenzoic acid (DHB) due to the power of the nitrogen laser.[23]

3.3.2 Instrumentation

All experiments were performed on an updated Agilent (Santa Clara, CA)

LC/MSD/TOF 6200 equipped with a MassTech (Columbia, MD) AP – MALDI source with a nitrogen laser operating at 337 nm with a spiraling raster motion. The Agilent TOF – MS is an orthogonal high-resolution mass spectrometer with pulsed dynamic focusing.

Spectra were then collected of the different samples upon the Agilent 6200 series time of flight mass spectrometer with an atmospheric pressure MALDI unit from MassTech. For the analysis of the samples the AP – MALDI-TOF-MS used a laser attenuation setting ranging from 6 – 9. The capillary voltage was kept at 3200 volts while the fragmentor was set to 375 volts. The drying gas flowed at 5.0 L/min at a temperature of 350° C for all analyses. This method was optimized for the analysis of the synthetic polymers.

3.3.3 Experimental

Since the matrix and cationizing agent were decided upon, the focus then became the matrix to analyte to cationizing agent (MAC) ratio that would be used for analysis. It has been widely documented in the literature that by altering the MAC ratio the resulting signal can become more or less intense.[16, 17, 26, 32, 33] Table 3.1

µL matrix	µL analyte	µL cationizing agent
5	30	5
10	30	10
15	30	15
30	30	30
50	30	50
75	30	75
30	30	15
30	30	10
30	30	50
30	30	2.5
30	30	0
15	30	30
60	30	30

Table 3.1. MAC ratios used in the study

presents the different MAC ratios that were used for the study. To prepare the samples with differing ratios, solutions were made by combining 2.0 mg of PEG or PS sample with 250 µL of THF. The PEG samples that were used in this study had a M_n of 550, 1430 and 2064. The PS samples had M_n of 870, 1300 and 3900. The cationizing agent solutions were made similarly by combining 2.0 mg of NaTFA or AgTFA with 250 µL of THF. Matrix solutions were prepared by mixing 9.0 mg of

matrix, either RA or CHCA with 250 μL of THF. These solutions were subsequently used to create the sample solutions with varying component ratios. All samples were hand spotted onto a MALDI target using ~0.5 μL of the sample solution using a digital micropipette Nichiryo Model 5000DG (Tokyo, Japan).

3.4. Results

Spectra were collected to enable an accurate determination of the effectiveness of the sample preparation for effective sample ionization. The samples of varying MAC ratios were evaluated by collecting multiple spectra of each sample solution that was made. These spectra were subsequently collected and the three specific sample peaks were selected to get an accurate portrayal of the signal intensity from each sample. Due to the significant signal variation from one spot to another, a filtering of data is necessary. It is speculated that this variation is due to sample preparation and sample deposition methodology.[23] Filtering of data is a practice that is common to work involving MALDI.[34] There are commercially available software packages that will collect data only if it is within a certain intensity range.[34] Because our MALDI is not equipped with this type of software, the data was processed manually. When data that fell outside of 25% of the strongest intensity collected for a sample, it was disregarded. The included data was then further analyzed by using analysis of variance (ANOVA) to determine if there was significant variance between the intensities resulting from changing the MAC ratio. All data was analyzed to a 95% significance level.

3.4.1. MAC Ratio Results

The PEG and PS spectra that were collected did confirm the hypothesis that the intensity of the spectra would correlate with the variation of the ratio of sample components.

3.4.1.1 PEG 550 Results

For the analysis of PEG 550, there were several MAC ratios that did produce spectra with good intensity but some spectral signal intensity was better than others. Figure

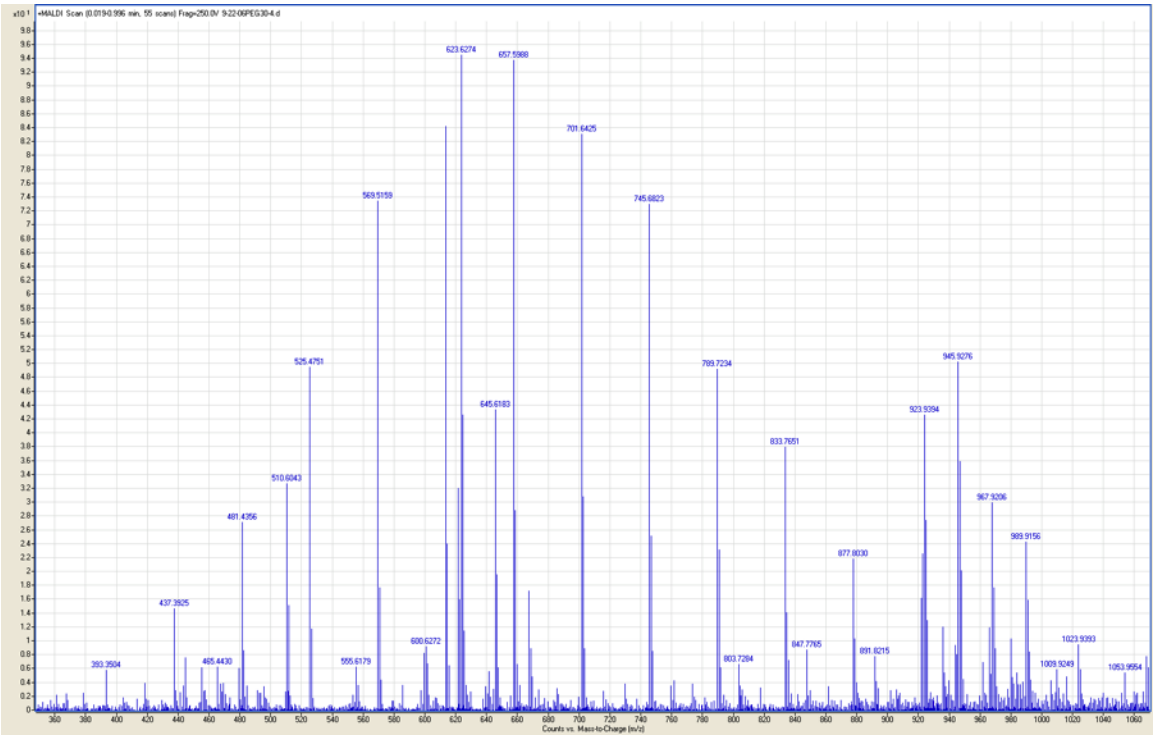

Figure 3.5. spectrum of PEG 550, 30:30:30 ratio used

3.5. is a spectrum of PEG 550 that was prepared with a MAC ratio of 30:30:30. Figure 3.5 shows the 30:30:30 ratio was favorable for the analysis. The polydispersity (PD) of the polymer is clearly visible and the peaks have an intensity that allows the ratio to be compared with spectra of the diverse MAC ratios. In this

mass spectrum the most abundant polymer chain is located at a mass to charge ratio (m/z) 657.6837 atomic mass units (amu). This depiction is indicative of what was observed in the other spectra collected of this PEG 550 with the same MAC ratio.

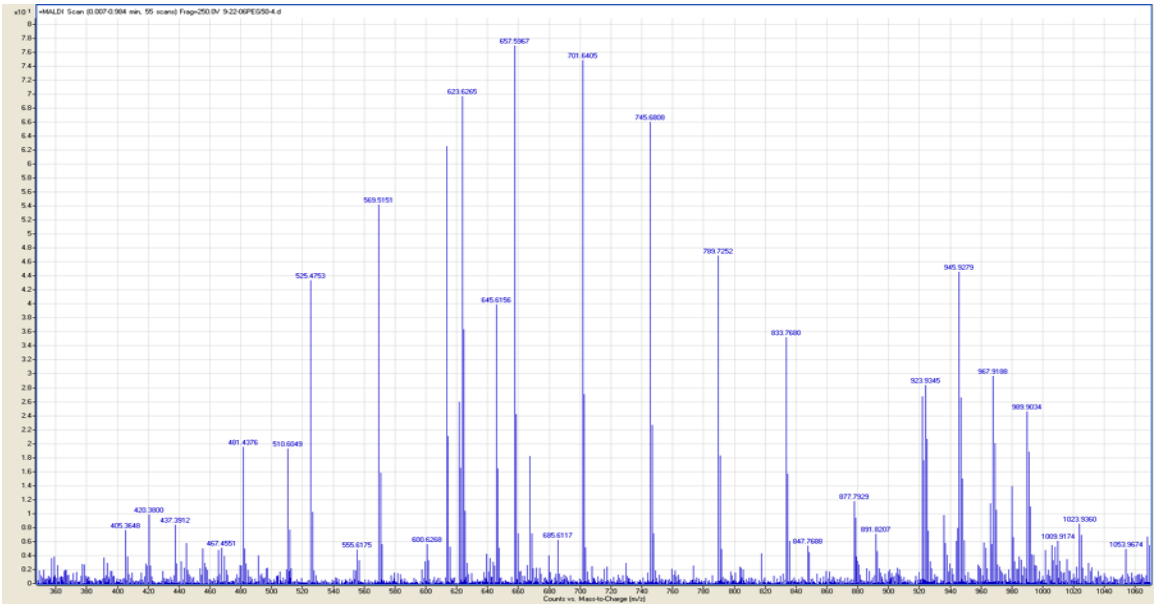

Figure 3.6. spectrum PEG 550, 50:30:50 ratio used

Figure 3.6 is once again PEG 550 but this sample has a MAC ratio of 50:30:50. This MAC ratio was determined to produce the best signal intensity for PEG 550 analysis.

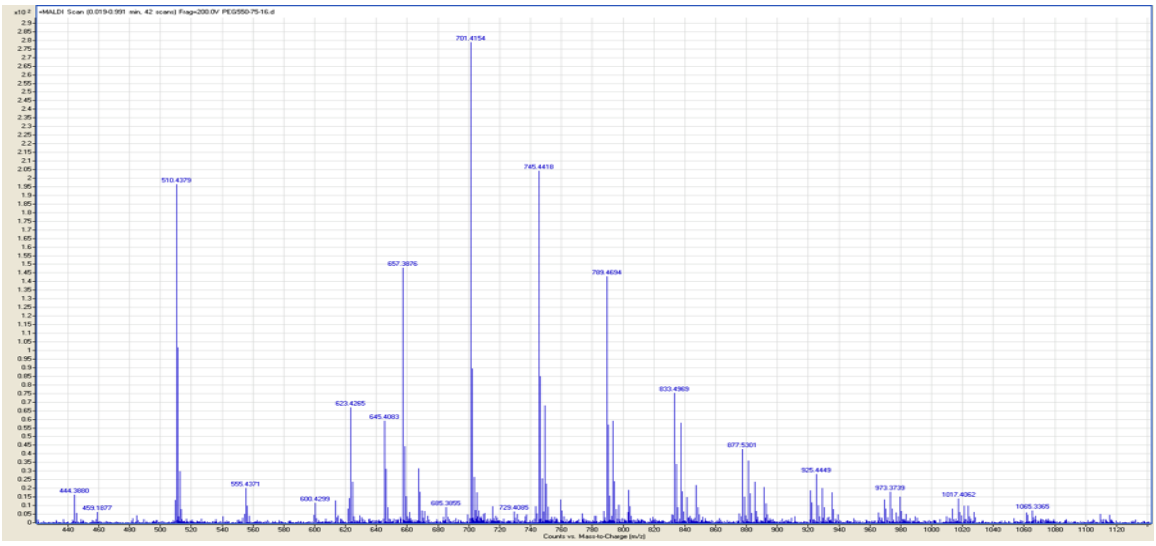

Figure 3.7. spectrum of PEG 500, 75:30:75 ratio used

The ratio that provided the weakest signal intensity was found to be a 75:30:75 ratio. Figure 3.7. is a representative spectrum for this MAC ratio.

It was determined that for PEG 550, several MAC ratios enabled collection of spectra that had good signal intensity but whenever there was comparison of peak intensity

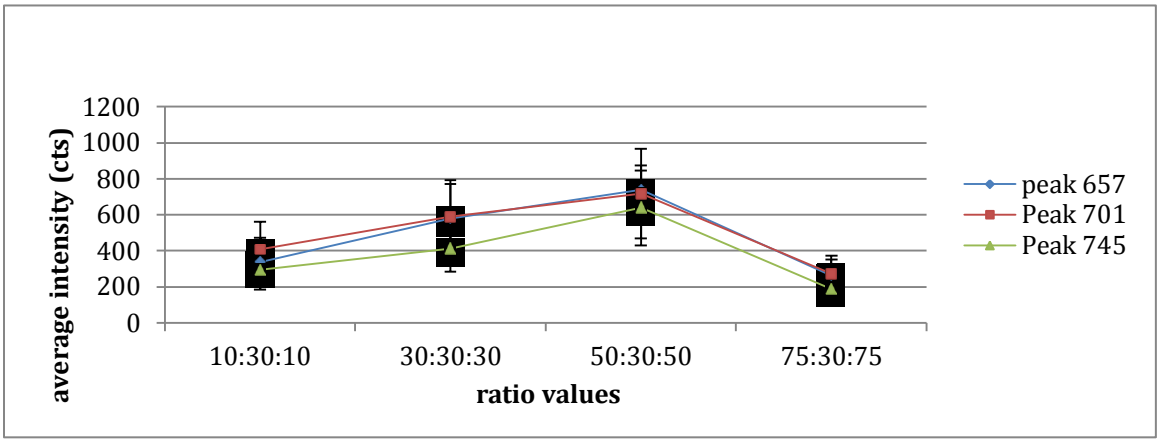

Figure 3.8. graph of the average peak intensity vs. ratio values of selected samples

among the different sample ratios it became clear that the 50:30:50 ratio consistently produced spectra with higher intensity while the 75:30:75 ratio produced the worst signal intensity with its most abundant peak having an intensity of ~ 30 counts. Figure 3.8. is a graph of the average peak areas vs. the MAC ratio used. (some data has been omitted for clarity) For the comparison, three peaks were selected and the peak intensity in counts was obtained and averaged. The peak area values were also analyzed with ANOVA to the 95% significance to determine if there was a statistical significance in the variation of peak areas by MAC ratio. It was shown that the observed differences were statistically significant for the PEG 550 sample.

3.4.1.2. PEG 1430 Results

The spectra obtained with PEG 1430 showed a trend similar to the PEG 550 with some MAC ratios producing spectra with good signal intensity. But as with the previous sample the intensity did vary as the ratio was adjusted. It was determined that for PEG 1430 the MAC ratio of 30:30:30 produced the greatest sample signal intensity. Figure 3.9. is a mass spectrum that is representative of the 30:30:30 ratio sample signal intensity.

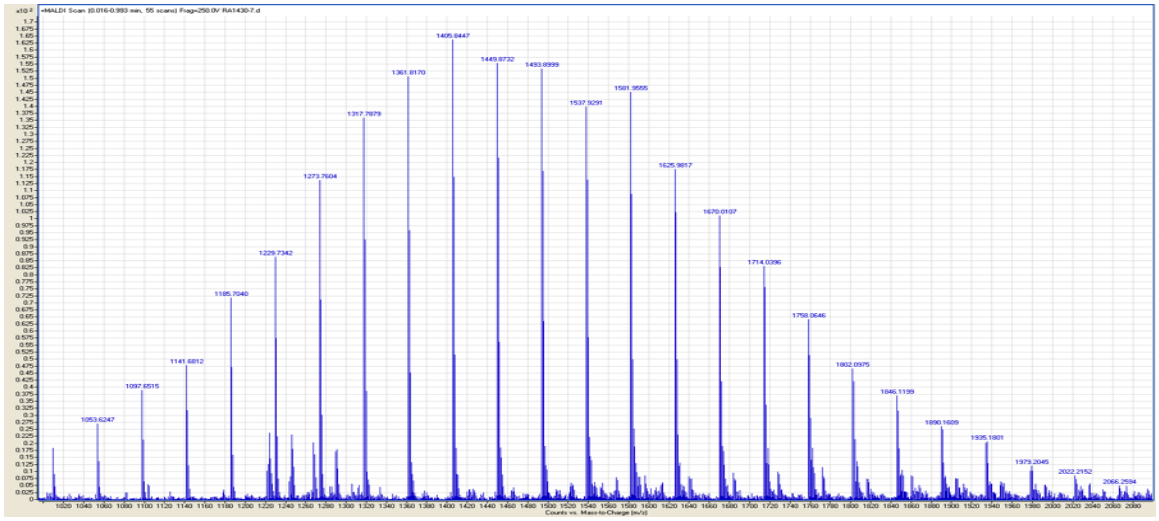

Figure 3.9. spectrum of PEG 1430, 30:30:30 ratio used

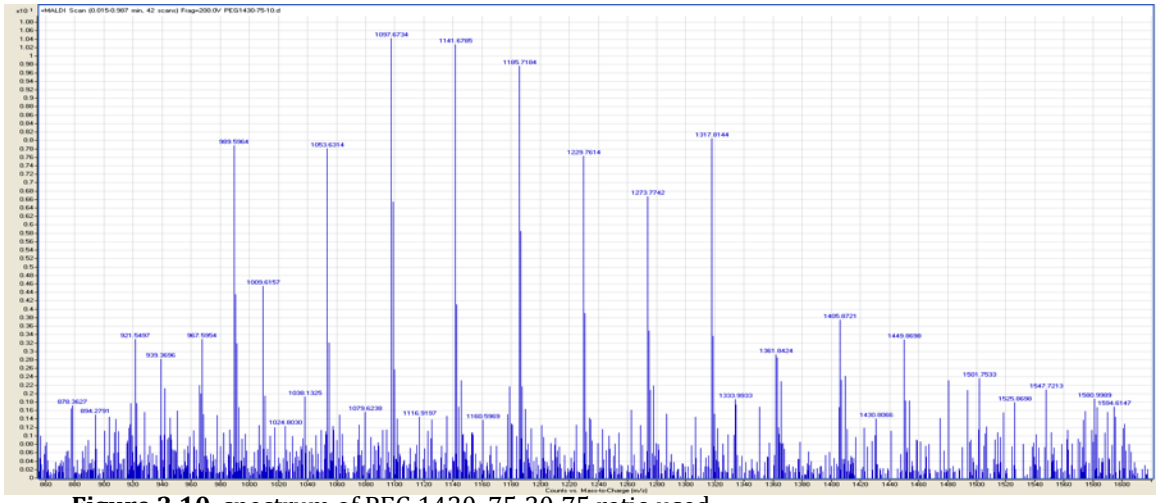

Figure 3.10. spectrum of PEG 1430, 75:30:75 ratio used

The ratio that produced the worst signal intensity was 75:30:75, as was the case with the PEG 550 samples. Figure 3.10. demonstrates the poor signal intensity that

this ratio produced. While there are sample peaks that are distinguishable from the

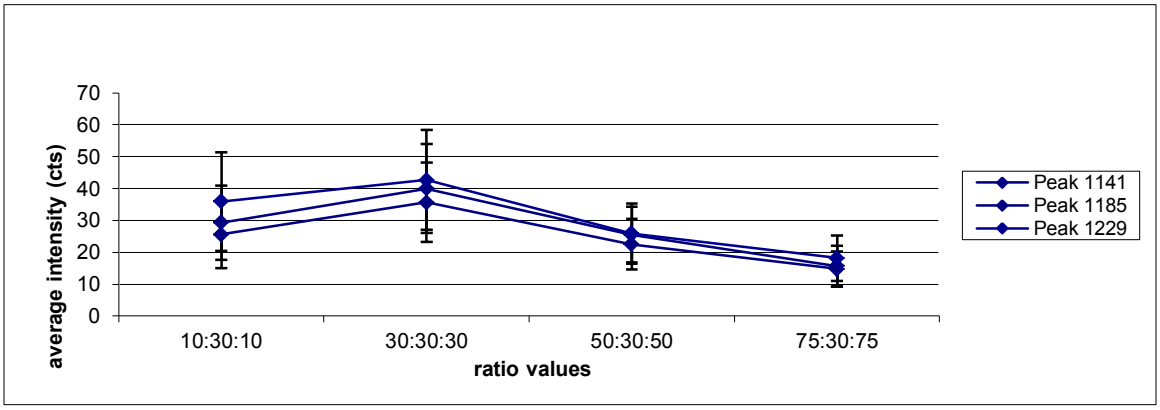

Figure 3.11. graph of the average peak intensity (cts) vs. MAC ratio

background noise, this ratio produced spectra with signal intensities that were considerably lower than other ratios tested. Figure 3.11. is a graph comparing the average peak intensities vs. different MAC ratios. (some data has been omitted for clarity) For the comparison, three peaks were selected and the peak intensity in counts was obtained and averaged. ANOVA analysis of the peak area values revealed that the observed differences due to changing MAC ratios were statistically significant for the PEG 1430 sample. It is clear that the signal intensity is dependent on the MAC ratio.

3.4.1.3 PEG 2064 Results

PEG 2064 was analyzed for optimal MAC ratios the same way the 2 other PEG samples were analyzed. As with PEG 550 and PEG 1430, there were multiple ratios that did produce spectrum with good intensity but as with the others, there was a significant difference among the samples. The best ratio for the best signal was the

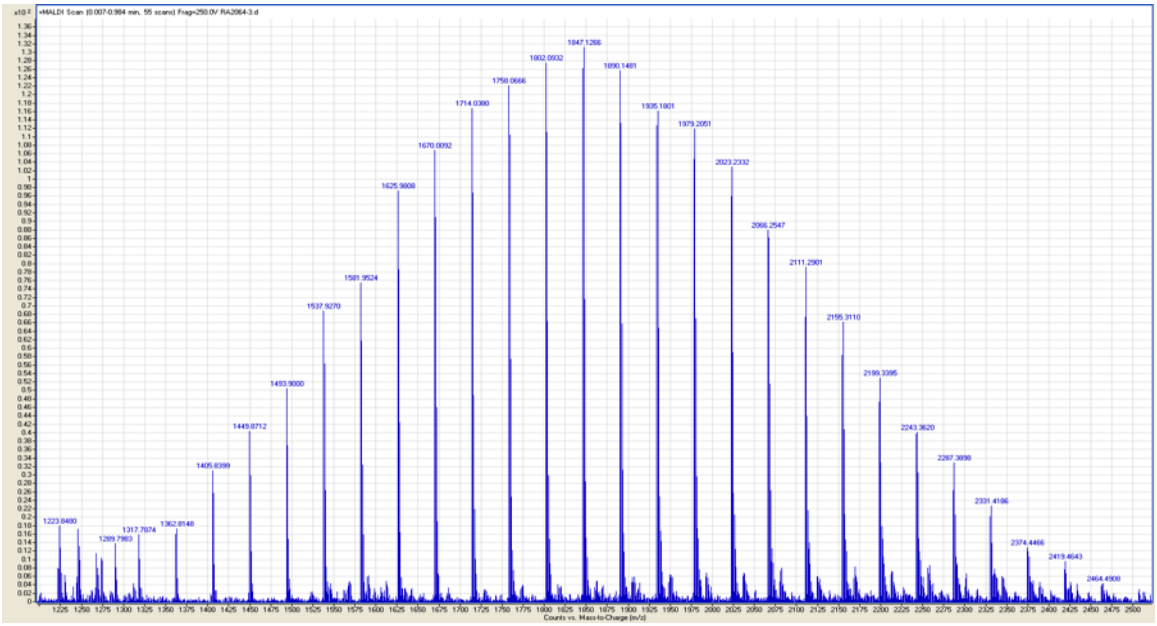

Figure 3.12. spectrum of PEG 2064, 30:30:30 ratio used

30:30:30 ratio. Figure 3.12. is a mass spectrum of PEG 2064 with the 30:30:30 ratio.

The ratio that produced spectrum with a significant decrease in signal was 75:30:75.

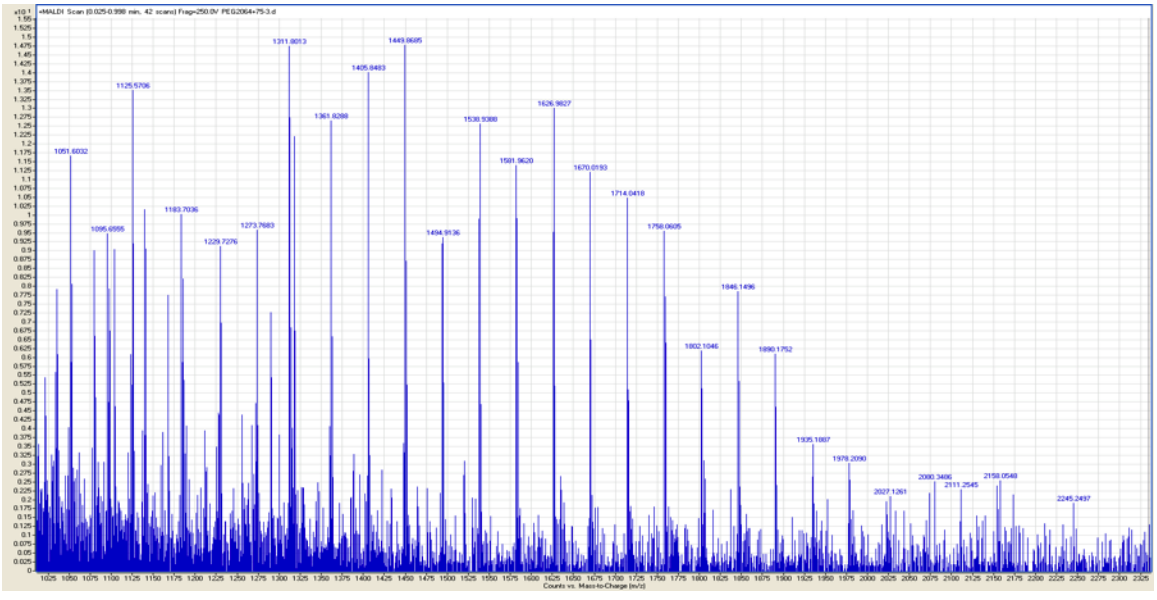

Figure 3.13. spectrum of PEG 2064, 75:30:75

Figure 3.13. is an example of the type of spectrum produced from the 75:30:75. The intensity that was observed with the 75:30:75 provided spectra with the lowest intensity. Figure 3.14 is a graph comparing the different peak intensities that were produced using the different ratios. (some data has been omitted for clarity)

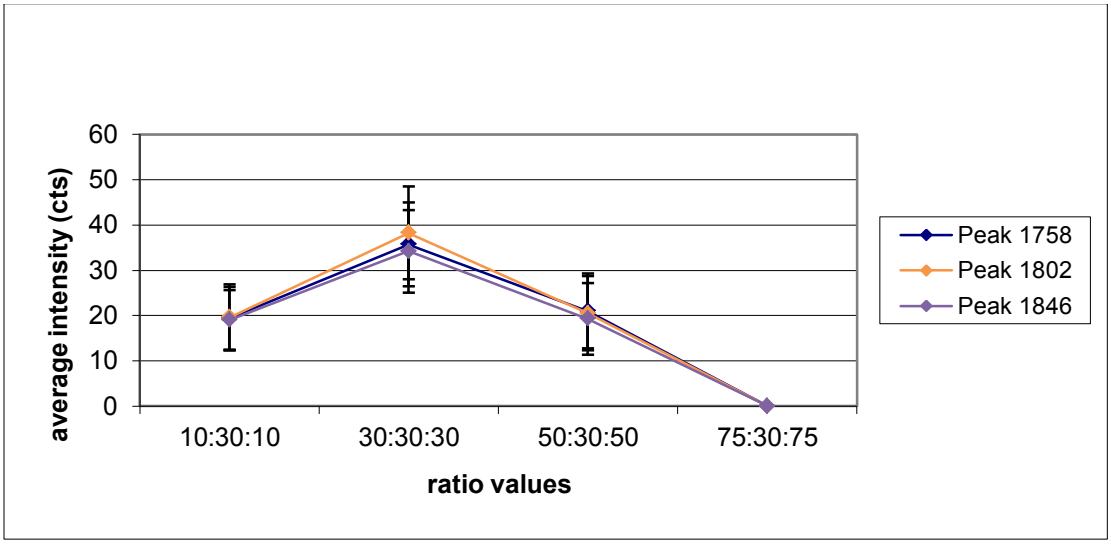

Figure 3.14. graph of the average peak intensity (cts) vs. MAC ratio

For the comparison, three peaks were selected and the peak intensity in counts was obtained and averaged. The peak area values were also analyzed with ANOVA to the 95% significance to determine if there was a statistical significance in the variation of peak areas by MAC ratio. It was shown that the observed differences were statistically significant for the PEG 2064 sample, and therefore the signal intensity does change with the MAC ratio.

The intensity observed in the MAC ratio for PEG 2064 was similar in intensity that was demonstrated with the PEG 1430 samples both samples having a preference for the 30:30:30 MAC ratio. All of the PEG samples produced spectra with poor intensity with the 75:30:75 ratio preparation.

3.4.1.4 PS 870 Results

The PS samples were analyzed as the PEG samples were to determine which MAC ratio would produce the best spectral results. Figure 3.15. is a spectrum of PS 870

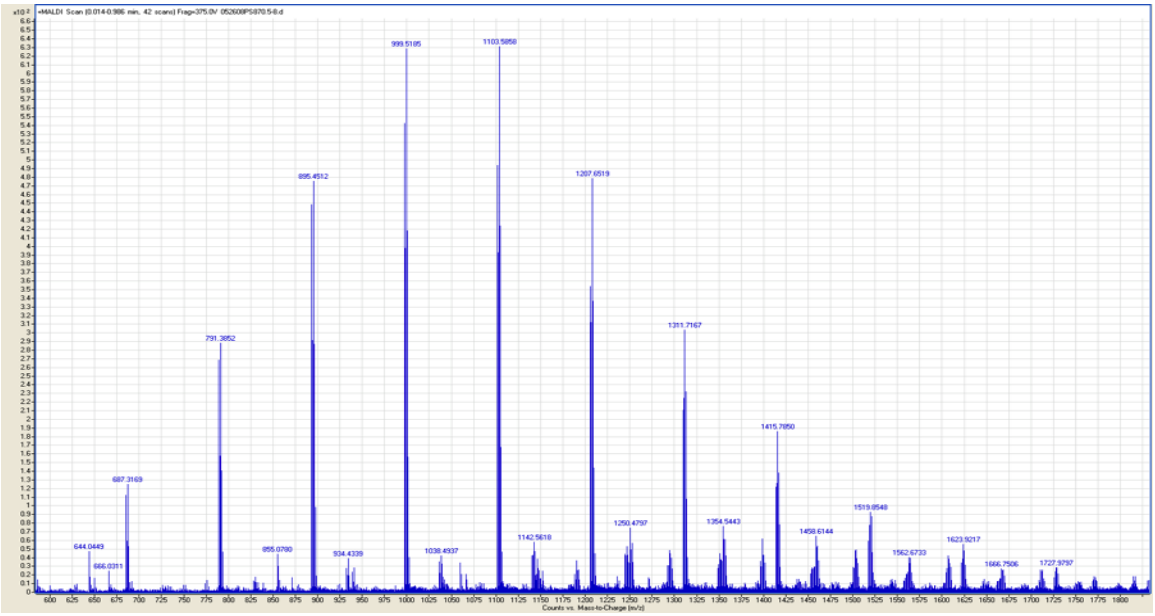

Figure 3.15. spectrum of PS 870, 30:30:5 ratio

with a ratio of 30:30:5 The ratio used in figure 3.15. produced a spectra with

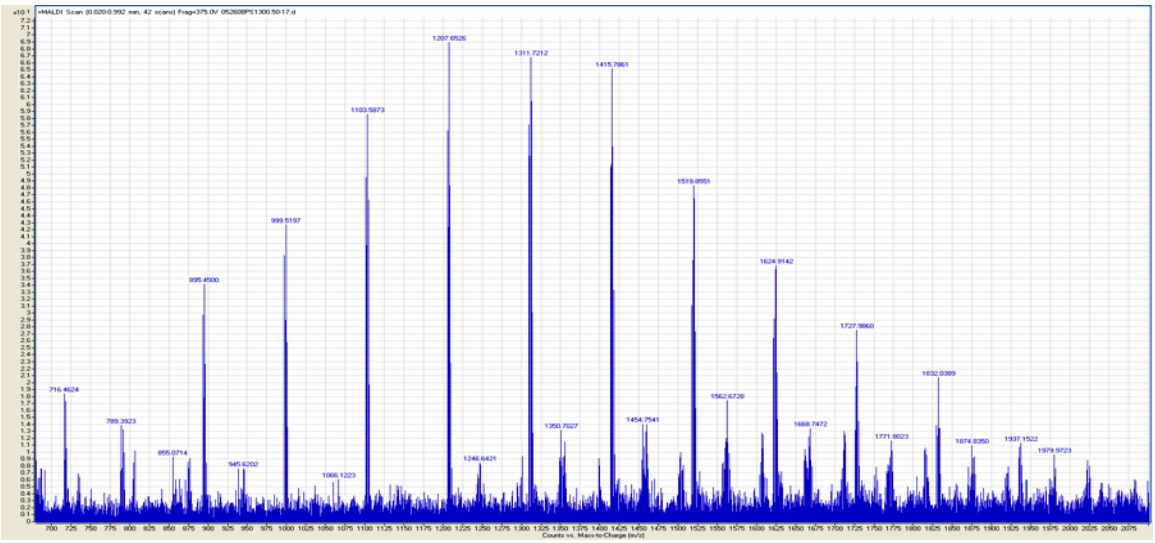

Figure 3.16. spectrum of PS 870 5:30:5 ratio

wonderful average intensity of the most abundant peak being about 650 counts. While this ratio was able to produce spectra with great signal intensity, the MAC ratio 5:30:5 produced spectra with relatively low sample signal intensity. Figure 3.16. is a representative of the type of spectra produced by this ratio.

It quickly becomes evident that the sample signal quality is not near the intensity produced by the 5:30:5 ratio samples. Figure 3.17. is a graph of PS 870 showing

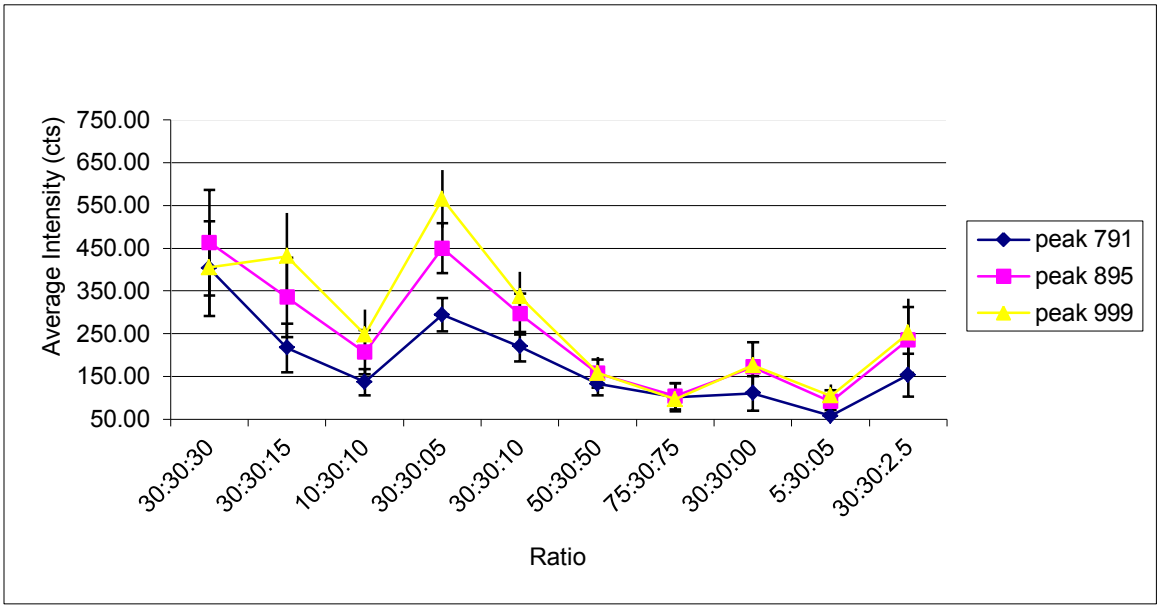

Figure 3.17. graph of average intensity (cts) vs. MAC ratio

average peak area (cts) vs. MAC ratio. (some data omitted for clarity) For the comparison, three peaks were selected and the peak intensity in counts was obtained and averaged. The ANOVA analysis of peak area values revealed a statistical significance in the variation of peak areas by MAC ratio for the PS 870 sample.

3.4.1.5. PS 1300 Results

PS 1300 was analyzed in the same manner the other samples were in order to determine which MAC ratio would produce the most intense sample signal intensity. Figure 3.18. is a spectrum that is indicative of the type of signal intensity that was obtained when samples utilizing a MAC ratio of 30:30:15.

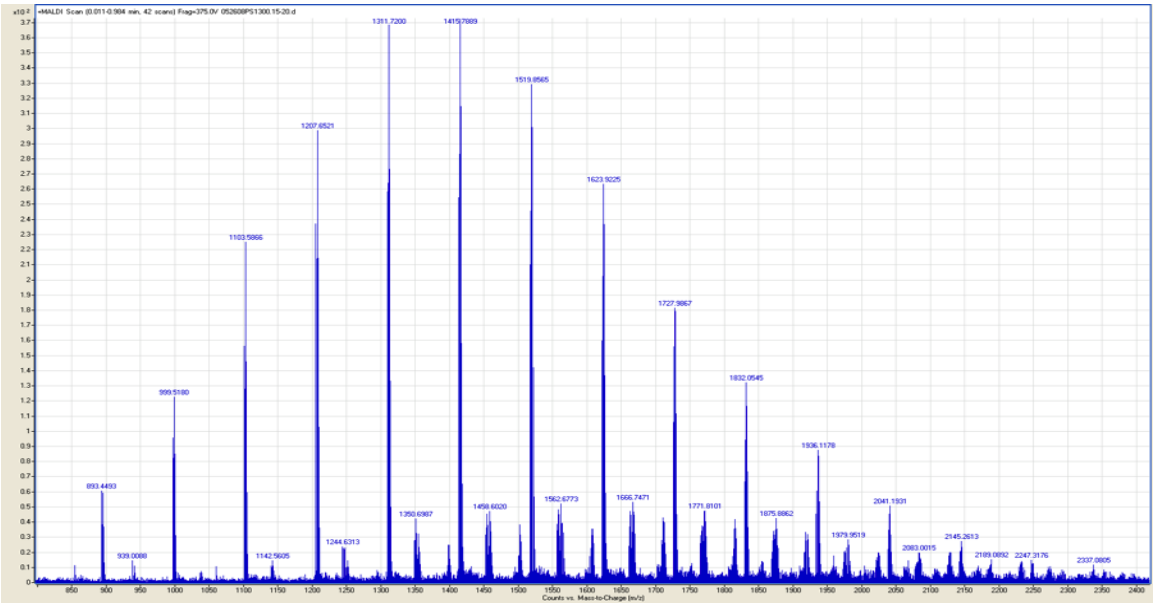

Figure 3.18. spectrum of PS 1300, 30:30:15 ratio

This MAC ratio produced spectra with consistent sample signal. The produced signal was the best signal produced among the MAC ratios. Figure 3.19. a representative of the signal produced by 50:30:50. The spectra produced using the 50:30:50 ratio were still able to show the different

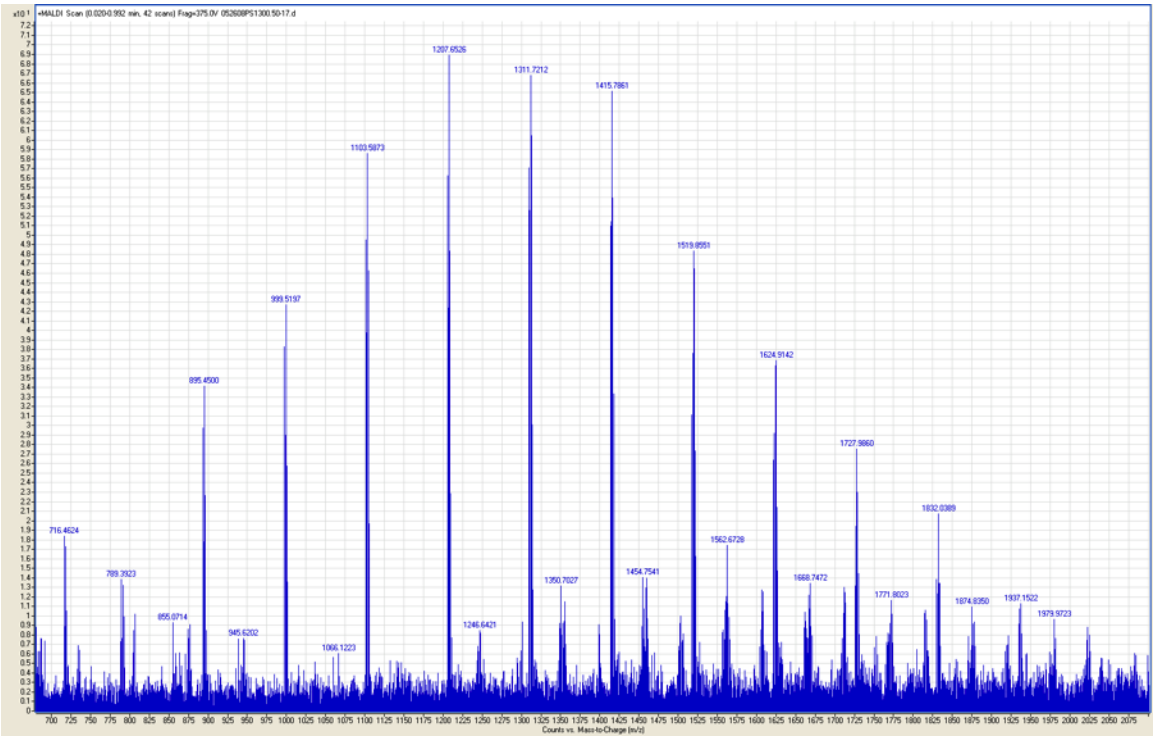

Figure 3.19. spectrum of PS 1300, 50:30:50 ratio

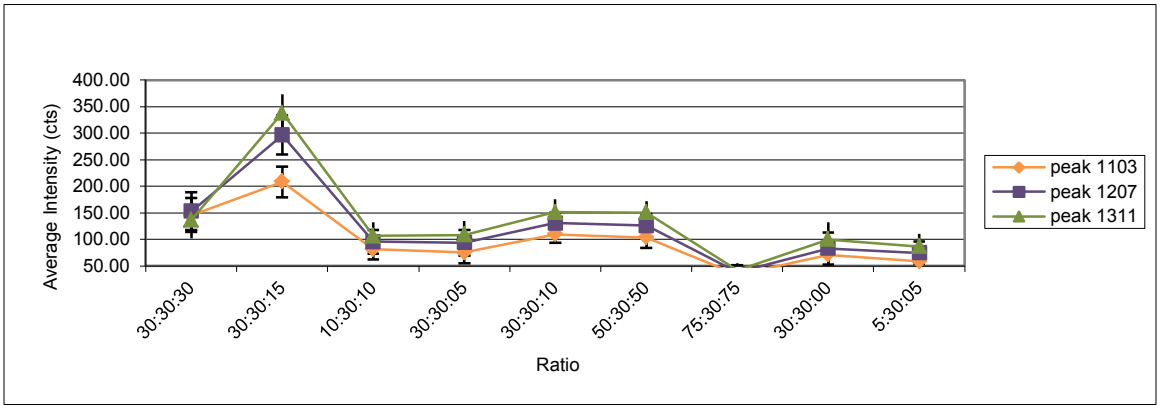

Figure 3.20. graph of average peak intensity (cts) vs. MAC ratio

polymer chains within the sample but whenever this ratio's intensity was compared with the data that the 30:30:15 ratio produced it was lacking in the signal intensity that not only the 50:30:50 ratio produced but also the signal produced by other ratios that were tested. Figure 3.20. is a graph of the average peak intensity (cts) vs. MAC ratio. (some data omitted for clarity) For the comparison, three peaks were

selected and the peak intensity in counts was obtained and averaged. The ANOVA to the 95% significance confirmed that the observed differences were statistically significant for the PS 1300 sample.

This research confirmed that the MAC ratio does in deed play a significant role in the ionization efficiency of the analyte. ANOVA analysis demonstrated that the variance among the ratios is significant to the 95% significance. This knowledge will make synthetic polymer analysis more effective.

Synthetic polymers are widely used in many different areas including materials science, industry and pharmaceutical sciences. Each of these fields utilizes synthetic polymers and because the physical properties are a result of their structure, it is crucial for these scientists to have all the information pertaining to their products. Because of the importance of synthetic polymers in a variety of fields, developing a way to improve signal intensity will greatly contribute to the analysis. Industry seeks a method that would comprehensively and quickly analyze many batches of synthetic polymers as they are produced for consistency.

3.4.2. Results Peak Shifting

While the study on the MAC ratio was being conducted, an unexpected trend became noticeable. It was observed that the most abundant peak within the polymer's distribution, which would indicate its M_n, would shift among sample peaks with different *m/z* ratios. This observation of the most abundant peak within a polymer's distribution is used to render conclusions about the polymer's physical properties. The shift that was observed within the sample polymer sample was concerning due

to the possibility of a shifted M_n resulting in incorrect assumptions in the material's physical properties which could in turn result in a material being employed for a specific task that the *actual* physical properties would deem inappropriate. MALDI-TOF-MS has become a popular choice for synthetic polymer analysis because it has the ability to provide information on multiple aspects of the physical characteristics of the synthetic polymer.[16, 35, 36] Information regarding the M_n, distribution, end group information as well as branching information.[18, 37] MALDI-TOF-MS provides exact, direct, fast and inexpensive characterization of synthetic polymers.[28] The sample preparation method and correct statistical analysis should be able to overcome the difficulties in peak intensities and peak shift with sample preparation. Knowing the issues that can afflict the analysis is important to determine methodology to reduce and even terminate the problems.

3.4.2.1. Peak Shifting in PEG

All of the PEG samples demonstrated a peak shift whenever the MAC ratio was altered. Figure 3.21.A. is a spectrum that is representative of the spectra that were collected using the 10:50:10 MAC ratio. Figure 3.21.A. shows that the most abundant peak is located at a *m/z* 569.5167 amu. The peak that is visable at a *m/z* 623.6270 is a matrix peak, a peak unrelated to the polymer sample. The polymer peaks range from a *m/z* of 437.3923 amu to 877.8522 amu. Figure 3.21.B. is a spectrum of PEG 550 that utilizes a MAC ratio of 75:30:75. While a reasonable

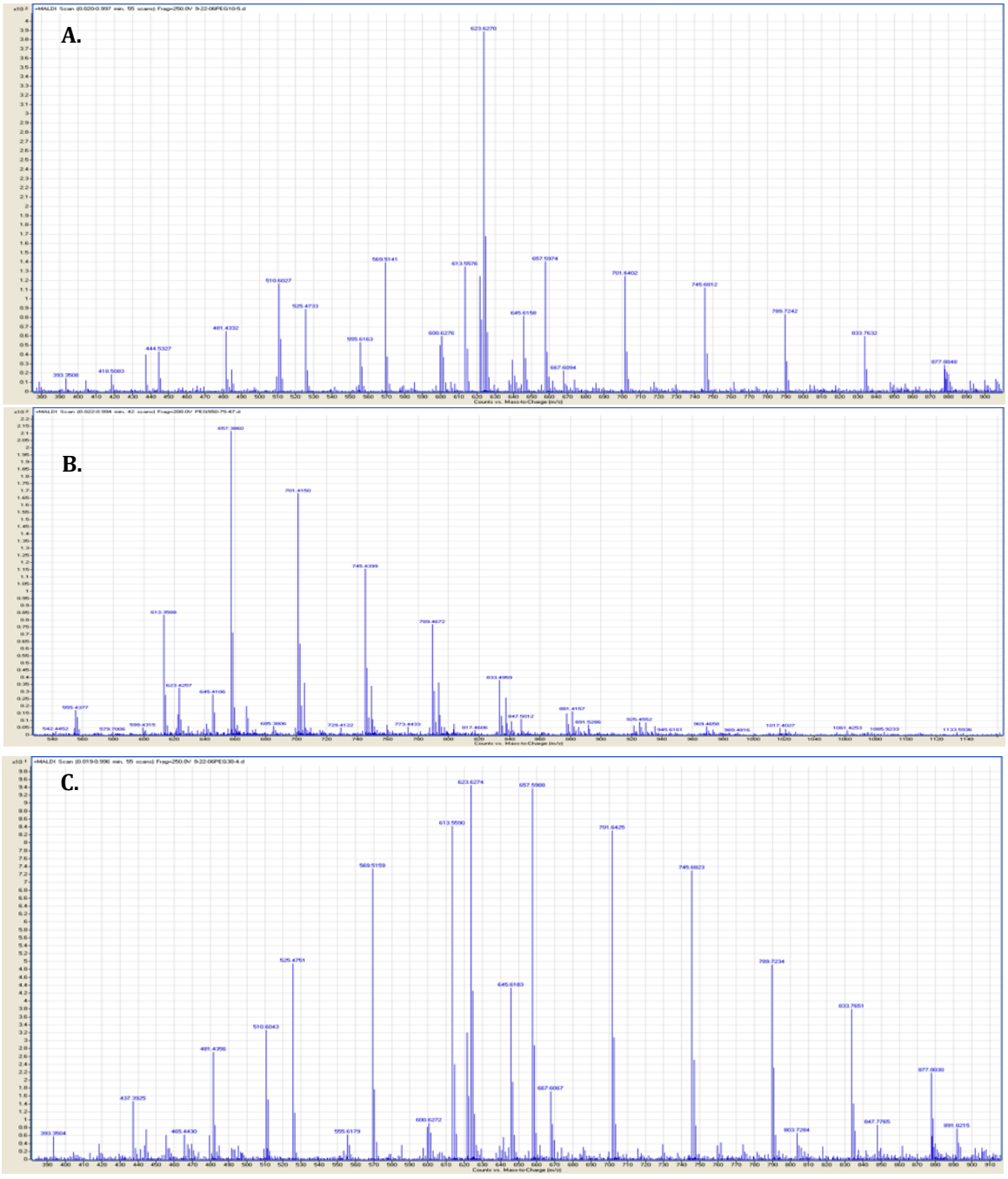

Figure 3.21. A. spectrum of PEG 550 sample peak *m/z* 569.5167 amu most abundant **B.** spectrum of PEG 550 sample peak 657.3927 **C.** spectrum of PEG 500 sample peak 745.6775 amu most abundant

assumption about this figure would be that it would differ from figure 3.21.A. with regards to intensity there is not only a difference in sample peak intensity but also a significant difference in the location of the peaks. The *m/z* range of polymer peaks for figure 3.21.B. is from 613 amu to 965 amu, with the most abundant sample peak

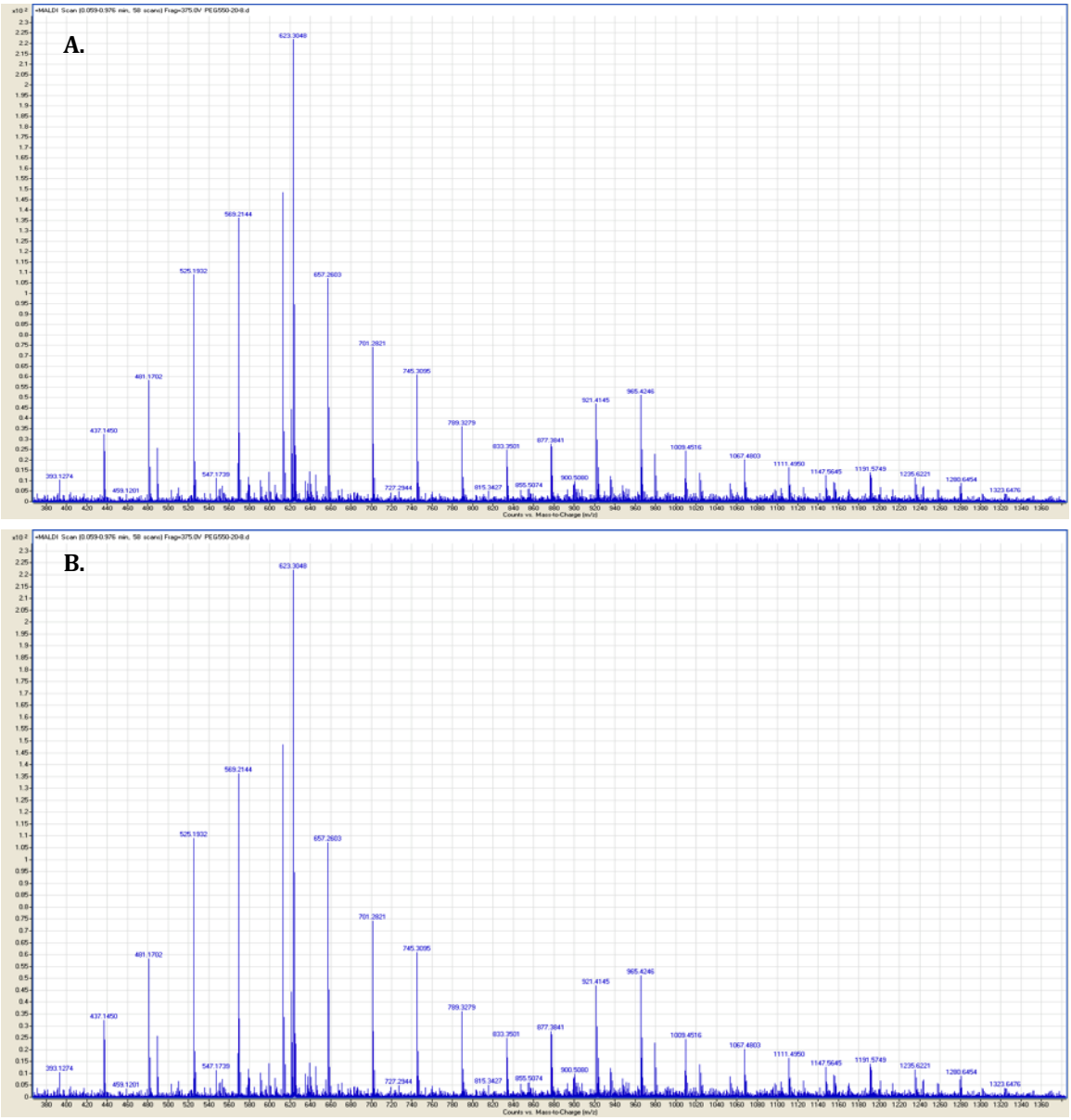

Figure 3.22. A. spectrum of PEG 550 sample peak 613.2453 amu most abundant **B.** spectrum of PEG 550 sample peak 613.2356 amu most abundant

occurring at a *m/z* of 657.3927. This range and peak with the most abundant sample peak occurring at *m/z* 657.3927. This range and peak with the most abundance is significantly different from the spectra produced using the 10:50:10 ratio. When observing spectra produced from MAC ratios 100:50:100 the trend continues. Figure 3.21.C. is a representative spectra of this ratio. This figure exhibits a mass range from 437 – 1009 amu with the strongest peak located at *m/z* 745 amu. This is once again quite a deviation from the other samples. Figure 3.22.A. is a spectrum where the amount of analyte and cationizing agent were both 30 μL and 15 μL of matrix was added. The spectra's most intense sample peak was found at the 613 *m/z* while the sample peaks covered a range of 393 – 1141 amu. To further explore what was most impacting this observed irregularity, a sample was then analyzed that again kept the analyte and cationizing agent at 30 μL but this time the amount of matrix was increased to 60 μL, doubling the previous amount. This spectrum, figure 3.22.C., displayed then most abundant peak to be the same as the previous ratio, located at *m/z* 613 but the range of sample peaks extended more than the previous figure's reaching a *m/z* of 1229 amu. This trend continued through the analysis of PEG 1430. Figure 3.26.A. is a spectrum of PEG 1430 with a MAC ratio of 30:30:30 and a most abundant sample peak at the 1405.8267 amu *m/z* mark. The range of sample peaks is from 1009 – 1978 amu. Whenever the MAC ratio is altered to 75:30:75, the most abundant sample peak takes a major shift downward landing at a *m/z* of only 1097.6729 amu. This is illustrated in figure 3.26.B. where the signal is not as strong as with the MAC ratio of 30:30:30 but the peaks are still distinguishable from the background noise. The mass range observed

in figure 3.26.B. is from a *m/z* of 921 – 1493 amu. Much better intensity is observed in figure 3.28.C. the spectrum utilizing 15 μL of matrix to 30 μL of analyte and cationinzing agent. The range of sample peaks for this sample

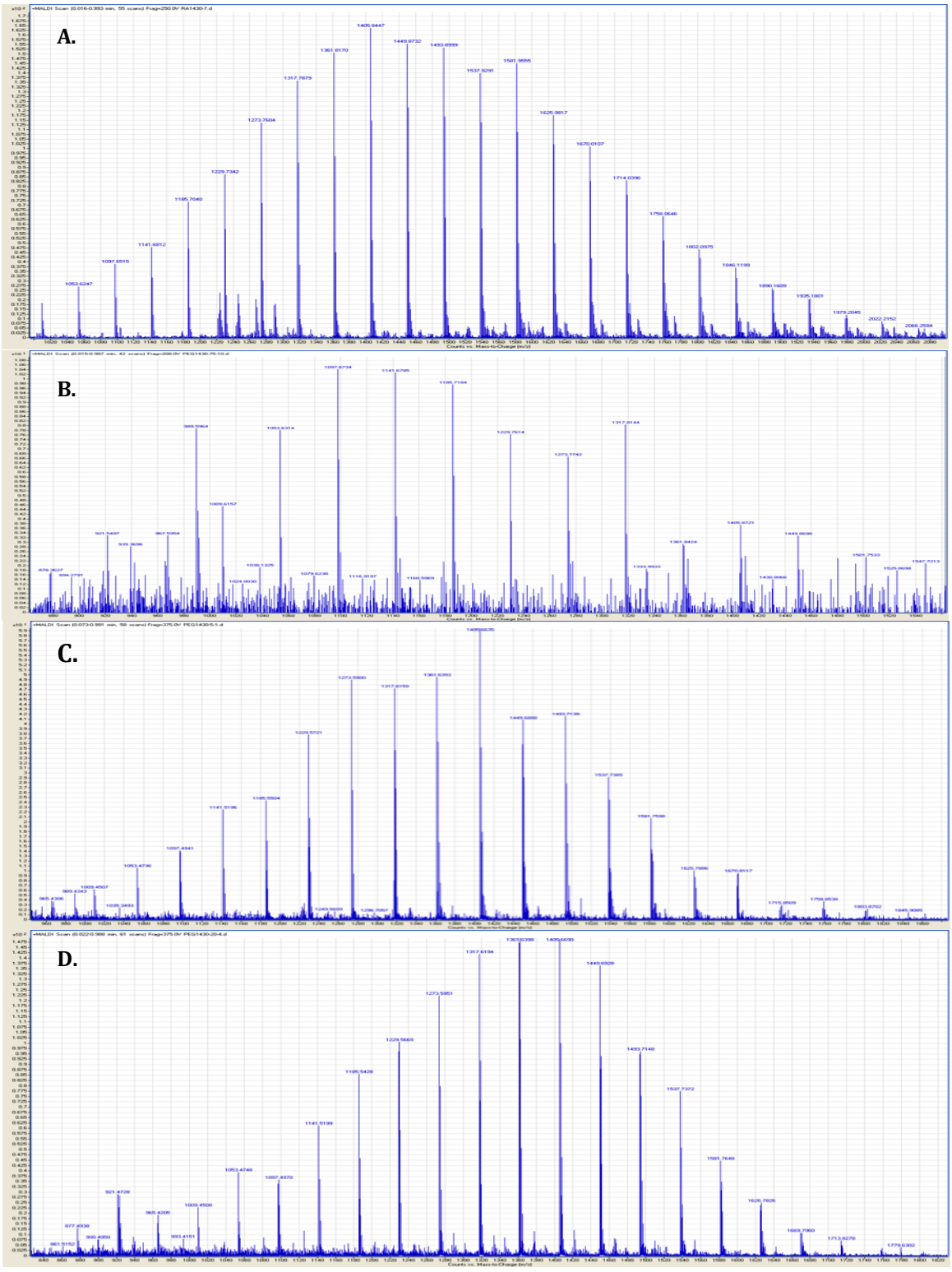

Figure 3.23. A. spectrum of PEG 1430 sample peak 1405.8267 amu most abundant **B.** spectrum of PEG 1430 sample peak 1097.6729 amu most abundant **C.** spectrum of PEG 1430 sample peak 1405.6635 amu most abundant **D.** spectrum of PEG 1430 sample peak 1361.6390 amu most abundant

preparation is 965 – 1845 amu. The most abundant sample peak within this sample occurs at *m/z* 1405.6635, a vast difference from the prominent peak within the previous sample. Figure 3.26.D. is another spectra of PEG 1430 but this figure depicts the sample with 60 µL of matrix being added to the analyte and cationizing agent both contributing 30 µL to the sample mixture. This sample has a most abundant peak of 1361.6390 amu with a sample peak range of 877 – 1757 amu.

The last PEG sample had a M_n of 2064. As with the previous two samples the same type of shifting of the prominent peak and the widening and narrowing of sample mass range was observed. Figure 3.27.A. is a spectrum of the PEG sample that was analyzed using a MAC ratio of 10:30:10. The prominent peak is located at a *m/z* of 1758.0634 amu. The range of the sample peaks is from 1261 – 2330 amu. Whenever the spectrum of PEG 2064 with a ratio of 75:30:75 is considered, the prominent peak in the spectrum has jumped to have a *m/z* of only 1405.8540. The sample peaks, as observed in figure 3.27.B., range from *m/z* 1053 – 2022 amu which greatly deviates from the previous sample. Figure 3.27.C. is the result of changing the ratio to 15:30:30 the peak of prominence has now shifted to a value of 1581.7616 amu with a range of sample peaks spreading from 1053 – 2217 amu. This range is ~ 200 amu wider than the range observed with figure 3.27.A. As shown in figure 3.27.C. the most abundant peak is 1581.7616 but the mass range of sample peaks has shifted to a mass range of 965 – 1934 amu whenever a ratio of 60:30:30 is utilized. The trend of the shifting peaks within the different PEG samples is an interesting one believed to be spurred by the matrix suppression affect.

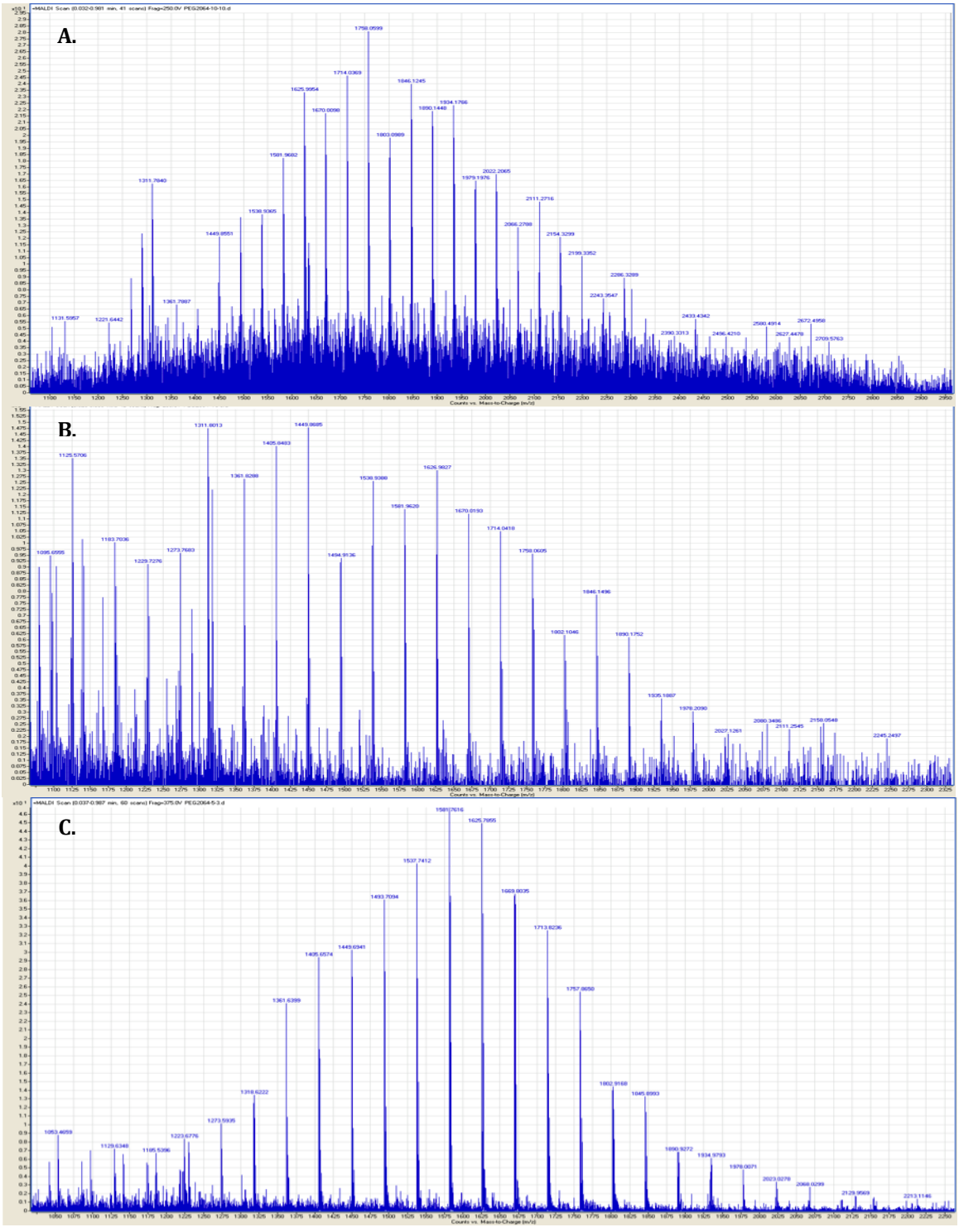

Figure 3.24. A. spectrum of PEG 2064 sample peak 1758.0634 most abundant **B.** spectrum of PEG 2064 peak 1405.8540 amu most abundant **C.** spectrum of 2064 peak 1581.7616 amu most abundant

This affect will be explained in more depth in the discussion section of this chapter. This surprising observation was not only observed among the PEG samples but was also seen within the PS samples.

3.4.2.2 Peak Shifting in PS

The observation of the most intensity abundant sample peak changing with MAC ratios in the PEG samples carried over into the analysis of the PS samples. All of the PS samples, the 870, 1300 and 2100, had the same trend emerge. In this section the data collected with regard to PS with a M_n will be shown. The other samples will be omitted. Good sample signal was obtained throughout the collection of PS 870 data. The trend of shifting intensity within sample peaks and sample peak mass range was observed. Figure 3.28.A. is a spectrum of PS 870 that represents the spectra collected with the prominent sample peak at *m/z* 997.5287. The MAC ratio used was 10:30:10. The range of sample peaks is from 581 – 1624 amu. Figure 3.28.B. illustrates how the spectra changed whenever the ratio was changed to 30:30:10. This spectrum has a sample range from 581 – 1831 amu and a prominent peak at *m/z* 1101.5937 amu, quite drastic from 997 amu as was the case with 10:30:10. Figure 3.28.C. is a spectrum of PS 870 that used a MAC ratio of 60:30:30 for analysis. This produced spectra that varied from the previous two samples. The last example of this phenomenon of different sample peaks despite having the same PS 870 sample is figure 3.28.D. which employed a ratio of 15:30:30 for analysis.

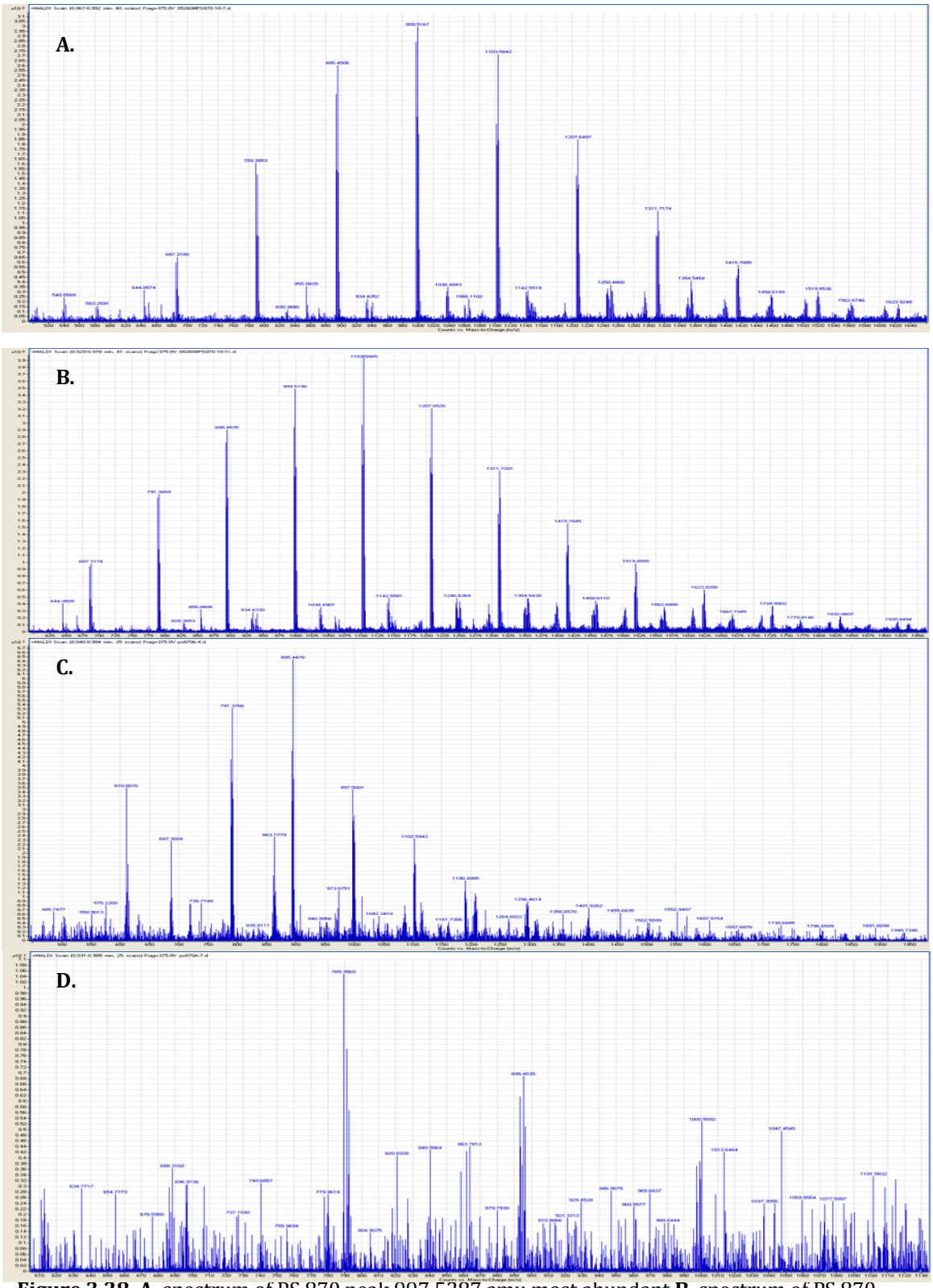

Figure 3.28. A. spectrum of PS 870 peak 997.5287 amu most abundant **B.** spectrum of PS 870 peak 1101.5937 amu most abundant **C.** spectrum of PS 870 peak 895.4478 amu most abundant **D.** spectrum of PS 870 peak 789.3569 amu most abundant

This sample ratio produced spectra with a sample peak range from 685 – 1104 amu and the promenant sample peak was located at *m/z* 789.3569 amu for this sample. As is shown throughout the figures in this section the changes that were observed within spectra that was simply due to altering the ratio of the sample components were quite drastic at times. This trend did continue throughout the samples of PS 1300 and PS 2100.

3.5. Discussion

The hypothesis that the MAC ratio used for the analysis of synthetic polymers would impact the produced sample signal intensity was confirmed. Over a range of MAC ratios it became clear that there was one ratio that was superior for the analysis of the synthetic polymer sample. The preferred ratio was also found to vary depending on the M_n of the polymer sample, which was not a surprise. The component ratio that is needed for the analysis of a synthetic polymer would be expected to change with the mass of the sample. In order for a successful analysis the charging of the sample with a cation must occur and as the sample mass changes the physical arrangement of the sample, matrix and cationizing agent would be altered. As the size of the polymer increases the probability that it would spatially be close to cationizing agent which would increase potential for cationizing agent interaction. Increasing or decreasing the different components poses the potential for a favorable configuration of the crystals allowing for better ionization of sample.

The surprising discovery that emerged from this study was whenever it was observed that the most abundant peak, which would indicate a change in M_n. While

this change could not occur by simply changing the amounts of matrix and cationizing agent used and a type of interference is being observed, the observed spectra could lead one to assume an incorrect value for the polymer's M_n and polydispersity index. If incorrect values are used for the characterization of the sample, this could result in a material being used for a purpose that it is not physically suited for. This phenomenon of seemingly changing M_n and PD is believed to occur due to matrix suppression effect (MSE). This observation does question the ability of MADLI to accurately portray the correct physical properties of synthetic polymers.

The MSE is a well known within the MALDI mass spectrometry community as an effect that can plague some analyses. This effect is usually observed whenever the concentration of matrix is too high resulting in the matrix peaks becoming very intense and prevents one of two things. Either the prevention of analyte ionization or the drowning out of sample signal due to being overshadowed by incredibly intense matrix peaks are the usual problems associated with MSE. The observed shifting of peaks is not a common effect of the MSE but within this sample study, it appears that the shifting of peaks are due to MSE. It was hypothesized that it would have to either be the matrix or the cationizing agent that was responsible for this peculiarity and further testing has provided evidence that indeed the matrix is responsible. Sets of samples were analyzed that only changed the amount of matrix. These spectra continued to shift around the mass range but whenever only the cationizing agent was altered there was very little to no change in mass range

produced. This has provided the needed evidence to confidently determine the matrix to be the culprit of this observation.

3.6. Conclusion

This study of synthetic polymers has provided a great deal of information about analyzing synthetic polymers using AP – MADLI-TOF-MS. It was determined that for the analysis of PEG 550 the MAC ratio that gives the best sample signal intensity is one that has a moderately higher matrix and cationizing agent concentration but the poorest intensity was observed whenever the ratio consisting of a matrix and cationizing agent concentration was much greater than the amount of analyte. PEG 1430 and 2064 both preferred a MAC ratio using equal amounts of matrix analyte and cationizing agent and performed poorly whenever a ratio that used a greater concentration of matrix and cationizing agent than analyte. The fact that both PEG 1430 and 2064 favored and hindered by the same ratios could be due to them having larger M_n's. The analysis of PS 870 showed a preference for a MAC ratio that kept the matrix and analyte at the same concentration but contained significantly less cationizing agent. Poor signal was obtained whenever a ratio with matrix and cationizing agent significantly lower than the analyte was used. PS 1300 had most intense signal with equal amounts of matrix and analyte with slightly lower cationizing agent added and the ratio that resulted in the weakest signal was a ratio that used equal amounts of matrix and analyte but had significantly lower volume of cationizing agent. The PS 2100 signal was best when equal amounts of matrix and analyte with significantly less cationizing agent was used, which was unique from

the other PS samples. PS 2100 had the lowest sample signal whenever a ratio was used that contained barely any of the cationizing agent. Among the PS samples, each M_n had different ratios that it found to produce the most intense and weakest signal. These results confirmed the suspicion that the ratio of matrix:analyte:cationizing agent would have significant impact upon the resulting signal intensity. Overall it seemed that both the PEG and the PS was best analyzed whenever the amount of matrix and analyte were combined close to the same values. The amount of cationizing agent that was added to the samples seemed to have a considerable impact upon the spectral intensity. The PEG required more of the cationizing agent, NaTFA, and the best spectra resulted whenever the amount of cationizing agent was approximately the same as the amounts of the matrix and analyte within the sample solution. The PS had a different trend from the PEG. The PS had better signal whenever the amount of the cationizing agent, AgTFA, was approximately half (or less) the amount of matrix and analyte that was added to the solution. The PS required the amount of matrix to be kept high, while the amounts of the cationizing agent had to be balanced at different amounts that were less than equal to the amounts of the other sample components, but greater than 0. The ratio of sample components must be carefully selected to achieve the desired signal intensity.

Peak shifting was also discovered to occur as the MAC ratio was changed. This alteration of spectra can be attributed to MSE. While MALDI MS provides invaluable information regarding the physical structure of synthetic polymers, this study highlights the importance of proper sample preparation in order to produce spectra

that not only elucidates structure but also accurately represents the synthetic polymer's physical properties.

More investigation is required to determine whether the trend seen here would still be present whenever the samples were analyzed by vacuum MALDI-TOF-MS. Another approach for further investigation could be to explore whether a matrix such as DHB would produce the same effects. While there are definitive conclusions that can be made about the research that has been done, there is always the potential to unlock more answers by following up this research project with another to fully analyze the trends and effects that are occurring.

References:

1. Philipsen, H. J. A., Determination of chemical composition distributions in synthetic polymers. *Journal of Chromatography A* **2004,** *1037* (1-2), 329-350.

2. Guttman, C. M.; Flynn, K. M.; Wallace, W. E.; Kearsley, A. J., Quantitative Mass Spectrometry and Polydisperse Materials: Creation of an Absolute Molecular Mass Distribution Polymer Standard. *Macromolecules* **2009,** *42* (5), 1695-1702.

3. Weidner, S. M.; Trimpin, S., Mass Spectrometry of Synthetic Polymers. *Anal. Chem.* **2008,** *80* (12), 4349-4361.

4. Marianne Gaborieau, R. G. G. A. G.-W. J. M. H. P. C., Theory of Multiple-Detection Size-Exclusion Chromatography of Complex Branched Polymers. 2007; Vol. 16, pp 13-28.

5. Pasch, H. S., W., *MALDI-TOF Mass Spectrometry of Synthetic Polymers*. Springer 2003; Vol. XVII, p 298.

6. Guttman, C. M.; Wetzel, S. J.; Blair, W. R.; Fanconi, B. M.; Girard, J. E.; Goldschmidt, R. J.; Wallace, W. E.; VanderHart, D. L., NIST-Sponsored Interlaboratory Comparison of Polystyrene Molecular Mass Distribution Obtained by Matrix-Assisted Laser Desorption/Ionization Time-of-Flight Mass Spectrometry: Statistical Analysis. *Anal. Chem.* **2001,** *73* (6), 1252-1262.

7. Campbell, D. W., J.R., *Polymer Characterization: Physical Techniques*. Chapman and Hall: London, UK, 1989.

8. Guttman, C. M.; Blair, W. R.; Maurey, J. R.; National Institute of Standards and, T., *Recertification of the SRM 706a, a polystyrene*. U.S. Dept. of Commerce, Technology Administration, National Institute of Standards and Technology: Gaithersburg, MD, 1998.

9. Guttman, C. M. W., S.J.; Blair, W.R.; Fanconi, B.M.; Goldschmidt, R.J.; Wallace, W.E.; VanderHart, D.L., Certification of SRM 2888, a Polystyrene. *NIST SPECIAL PUBLICATION 260-152* **2003**.

10. Tanaka, K. W., Hiroaki; Ido, Yutaka; Akita, Satoshi; Yoshida, Yoshikazu; Yoshida, Tamio; Matsuo,T., Protein and polymer analyses up to m/z 100 000 by laser ionization time-of-flight mass spectrometry. *Anal. Chem.* **1988,** *2* (8), 151-153.

11. Karas M; Hillenkamp, F., Laser Desorption Ionization of Proteins with Molecular Masses Exceeding 10,000 Daltons. *Anal. Chem.* **1988,** *60* (20), 2299-301.

12. Lehrle, R. S.; Sarson, D. S., Degradation and selective desorption of polymer can cause uncertainty in MALDI (matrix-assisted laser desorption ionisation) measurements. *Polymer Degradation and Stability* **1996,** *51* (2), 197-204.

13. M. Guilhaus, D. S. V. M., Orthogonal acceleration time-of-flight mass spectrometry. *Mass Spectrom. Rev.* **2000,** *19* (2), 65-107.

14. Skoog, D. H., F. James; Crouch, Stanley R., *Principles of Instrumental Analysis Sixth Edition*. 6 ed.; Thomson Brooks/Cole Thompson Corporation: Belmont, CA, 2007; p 1039.

15. Harris, D., *Quantitative Chemical Analysis*. Sixth ed.; W.H. Freeman and Company: 2003; p 739.

16. Montaudo, G.; Samperi, F.; Montaudo, M. S., Characterization of synthetic polymers by MALDI-MS. *Progress in Polymer Science* **2006,** *31* (3), 277-357.

17. Wetzel, S. J., Guttman, Charles M., Girard, James E., The Influence of Matrix and Laser Energy on the Molecular Mass Distribution of Synthetic Polymers Obtained by MALDI-TOF-MS. *International Journal of Mass Spectrometry* **2004,** *238*, 215 - 225.

18. Macha, S. F.; Limbach, P. A.; Savickas, P. J., Application of nonpolar matrices for the analysis of low molecular weight nonpolar synthetic polymers by matrix-assisted laser desorption/ionization time-of-flight mass spectrometry. *Journal of the American Society for Mass Spectrometry* **2000,** *11* (8), 731-737.

19. Nagahata, R.; Shimada, K.; Kishine, K.; Sato, H.; Matsuyama, S.; Togashi, H.; Kinugasa, S., Interlaboratory comparison of average molecular mass and molecular mass distribution of a polystyrene reference material determined by MALDI-TOF mass spectrometry. *International Journal of Mass Spectrometry* **2007,** *263* (2-3), 213-221.

20. Rashidzadeh, H.; Guo, B., Use of MALDI-TOF To Measure Molecular Weight Distributions of Polydisperse Poly(methyl methacrylate). *Anal. Chem.* **1998,** *70* (1), 131-135.

21. Cox, F. J.; Johnston, M. V.; Dasgupta, A., Characterization and relative ionization efficiencies of end-functionalized polystyrenes by matrix-assisted laser desorption/ionization mass spectrometry. *Journal of the American Society for Mass Spectrometry* **2003,** *14* (6), 648-657.

22. Zhu, H.; Yalcin, T.; Li, L., Analysis of the Accuracy of Determining Average Molecular Weights of Narrow Polydispersity Polymers by Matrix-Assisted Laser Desorption Ionization Time-of-Flight Mass Spectrometry. *Journal of the American Society for Mass Spectrometry* **1998,** *9* (4), 275-281.

23. Trimpin, S.; Keune, S.; Rader, H. J.; Mullen, K., Solvent-Free MALDI-MS: Developmental Improvements in the Reliability and the Potential of MALDI in the Analysis of Synthetic Polymers and Giant Organic Molecules. *Journal of the American Society for Mass Spectrometry* **2006,** *17* (5), 661-671.

24. Thomson, B.; Suddaby, K.; Rudin, A.; Lajoie, G., Characterisation of low molecular weight polymers using matrix assisted laser desorption time-of-flight mass spectrometry. *European Polymer Journal* **1996,** *32* (2), 239-256.

25. Schriemer, D. C.; Li, L., Mass Discrimination in the Analysis of Polydisperse Polymers by MALDI Time-of-Flight Mass Spectrometry. 2. Instrumental Issues. *Anal. Chem.* **1997,** *69* (20), 4176-4183.

26. Schriemer, D. C.; Li, L., Mass Discrimination in the Analysis of Polydisperse Polymers by MALDI Time-of-Flight Mass Spectrometry. 1. Sample Preparation and Desorption/Ionization Issues. *Anal. Chem.* **1997,** *69* (20), 4169-4175.

27. Saito, T.; Lusenkova, M. A.; Matsuyama, S.; Shimada, K.; Itakura, M.; Kishine, K.; Sato, K.; Kinugasa, S., Reliability of molecular weight determination methods for oligomers investigated using certified polystyrene reference materials. *Polymer* **2004,** *45* (25), 8355-8365.

28. Royo, E.; Brintzinger, H.-H., Mass spectrometry of polystyrene and polypropene ruthenium complexes. A new tool for polymer characterization. *Journal of Organometallic Chemistry*

Special Issue dedication to Professor Pascual Royo **2002,** *663* (1-2), 213-220.

29. Okamoto, K., MALDI mass spectrometry of synthetic polymers. *Toyota Chuo Kenkyusho R&D Rebyu* **2006,** *41* (3), 29-34.

30. Macha, S. F.; Limbach, P. A.; Hanton, S. D.; Owens, K. G., Silver cluster interferences in matrix-assisted laser desorption/ionization (MALDI) mass spectrometry of nonpolar polymers. *Journal of the American Society for Mass Spectrometry* **2001,** *12* (6), 732-743.

31. Hoteling, A. J.; Erb, W. J.; Tyson, R. J.; Owens, K. G., Exploring the Importance of the Relative Solubility of Matrix and Analyte in MALDI Sample Preparation Using HPLC. *Analytical Chemistry* **2004,** *76* (17), 5157-5164.

32. Chen, H.; He, M.; Pei, J.; He, H., Quantitative Analysis of Synthetic Polymers Using Matrix-Assisted Laser Desorption/Ionization Time-of-Flight Mass Spectrometry. *Anal. Chem.* **2003,** *75* (23), 6531-6535.

33. Knochenmuss, R.; Zhigilei, L. V., Molecular dynamics simulations of MALDI: laser fluence and pulse width dependence of plume characteristics and consequences for matrix and analyte ionization. *Journal of Mass Spectrometry* **2010,** *45* (4), 333-346.

34. Knochenmuss, R.; Vertes, A., Time-delayed 2-Pulse Studies of MALDI Matrix Ionization Mechanisms. *Journal of Physical Chemistry* **2000,** *104* (23), 5406-5410.

35. Wetzel, S. J.; Guttman, C. M.; Girard, J. E., The influence of matrix and laser energy on the molecular mass distribution of synthetic polymers obtained by MALDI-TOF-MS. *International Journal of Mass Spectrometry*

Polymer Characterisation by means of Mass Spectrometry: A Snapshot **2004,** *238* (3), 215-225.

36. Marie, A.; Fournier, F.; Tabet, J. C., Characterization of Synthetic Polymers by MALDI-TOF/MS: Investigation into New Methods of Sample Target Preparation and Consequence on Mass Spectrum Finger Print. *Anal. Chem.* **2000,** *72* (20), 5106-5114.

37. Wetzel, S. J., Guttman, Charles M., Flynn, Kathleen M., The Influence of Electrospray Deposition in Matrix - Assisted Laser Desorption/Ionization Mass Spectrometry Sample Preparation for Synthetic Polymers. *Rapid Communications in Mass Spectrometry* **2004,** *18*, 1139 - 1146.

Chapter 4.

Synthetic Fiber Additive Analysis

4.1 Introduction

The chemical additives to various synthetic fibers used for the composition of carpeting were comprehensively analyzed, highlighting the different additives that are unique to a specific company and time period. Additives are chemical components that are incorporated into a fiber to alter the properties of the fiber[1]. The additives generally provide the fiber with characteristics such as flame retardants, delusterants, antioxidants, optical brighteners and ultraviolent light absorbers[1]. Customarily pyrolysis gas chromatography mass spectrometry (PyGCMS) is used for the analysis of polymer additives[2]. Pyrolysis gas chromatography combines an extraction technique along with a separation technique. The extraction technique, pyrolysis forces the fiber apart by high temperature to allow for its components to be analyzed. Work that has been published in the literature demonstrates that polymer additives such as plasticizers[3], flame retardants[4], lubricants[5] and antioxidants[6] can be effectively analyzed with gas chromatography mass spectrometry (GCMS). Though the work with PyGCMS does provide forensic investigators with valuable evidence, the technique is destructive, destroying the fiber. Additives that are used in conjunction with synthetic polymers include plasticizers, flame-retardants, lubricants and antioxidants. A plasticizer is a material that is incorporated into the plastic to increase its flexibility, workability and extensibility[7]. The additives used in the

manufacturing of synthetic polymers are evolving as companies seek to make their products better. The fact that the additives change as research and development continues will give the forensic scientist another set of sample characteristics to observe. The different additives used in the manufacturing of carpets are proprietary information that is continually changing. Therefore, carpet fibers from different manufacturers or different time periods will contain unique additive signatures. This would enable the forensic scientist to conduct a fiber additive comparison in addition to the usual visual and spectroscopic analysis conducted for fiber comparison[4, 8].

The visual and spectroscopic methods that are commonly used for the analysis of fibers include microscopy, polarized light microscopy and Fourier transform infrared spectroscopy (FTIR).[8, 9] Microscopy is used to determine the color, size, shape, and cross section of the fiber.[9] Polarized light microscopy is used to determine if there is birefringence which is a change in the refractive index along the length of the fiber. FTIR can be used to determine the type of polymer material that the fiber is made of. While the FTIR can identify the type of polymer the fiber is, it cannot analyze the polymer additives. While these latter methods are nondestructive, they can only provide basic information that could imply many different types of fibers, leaving a need for more discriminating information.

When there is little evidence from a crime to begin with, destroying any part of the existing evidence is undesirable and an analysis method that could provide comprehensive evidence is quite desirable. This is where MALDI can be a wonderful asset for evidentiary analysis. Recent work with tissue samples has demonstrated

that a sample analyzed using MALDI will retain its structural integrity.[10] Tissue samples that were analyzed via MALDI could be removed from the target and undergo microscopic and histological analyses.[10] This could in turn be done with fibers. A carpet fiber could be analyzed using MALDI to analyze the additives, providing the same type of useful data as does PyGCMS but without destroying the sample.

4.2 Materials and Methods

4.2.1. Samples and Reagents

Two matrixes were chosen for the analysis of the in-tact carpet fibers; CHCA and (trans – 2 - [3 - (4 - tert-Butylphenyl) – 2 – methyl – 2 – propenylidene]malononitrile) (DCTB). Figure 4.1 is the chemical structure of DCTB and the chemical structure of CHCA was shown in figure 3.2.

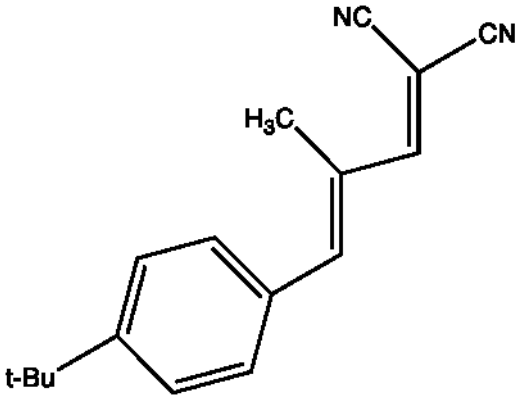

Figure 4.1 Structure of DCTB

The CHCA was purchased from Fluka (Lausanne, Switzerland). The DCTB was purchased from Sigma-Aldrich (St. Louis, MO, USA). The solvent chosen was

tetrahydrofuran (THF) and the cationizing agent was NaTFA, both purchased from Sigma-Aldrich (St. Louis, MO, USA).

The samples analyzed were from various carpet samples obtained from flooring stores; these samples are the rectangular pieces of different carpets used for customers to select carpet type and color. A variety of carpet type, color and manufacturers were obtained. The carpet types used for this study are in table 4.1.

Carpet Manufacturer	Color	Nylon Content	Type of Nylon
Masland Carpets	"Buttercream"	100%	DuPont Antron® Grand Luxuria nylon
Brahms Karastan's	"Sun Hue"	100%	Solutia Wear-Dated nylon
DuPont Stainmaster	"Lambskin"	100%	DuPont Continuous Filament Tactesse nylon
Stainmaster Masertlife Carpet	"Filber"	100%	Stainmaster Tactesse BCF nylon

Table 4.1. Carpet samples

4.2.2. Sample Preparation

Samples were prepared by first dissolving 9.0 mg of matrix into 250 µL THF. Similarly, 2.0 mg of the NaTFA was dissolved into 250 µL of THF. Single strands of the carpet fibers were removed from the carpet samples and placed onto the MALDI target. Approximately 5 – 15 µL of the NaTFA solution was pipetted on top of the fiber followed by ~ 5 – 15 µL of CHCA matrix solution. This preparation procedure was repeated for each of the four nylon carpet samples. Samples were also made using this same procedure but using DCTB as the matrix.

4.2.3. Instrumentation

AP – MALDI-TOF-MS was used for the analysis of the carpet fibers. The laser energy attenuation was set to 8. The capillary voltage was set to 3200 volts and the

fragmentor voltage was 400 volts. The drying gas was set to 9.9 L/min and the gas temperature was 325° C. The laser was manually directed to ensure the beam struck the fiber and sample signal was collected for 3 min. Spots of just matrix and NaTFA were collected so non-sample peaks could be excluded.

4.3. Results and Discussion

The samples were run to determine which matrix would provide the best spectra and if the additives to the fibers could be used to distinguish one brand of nylon

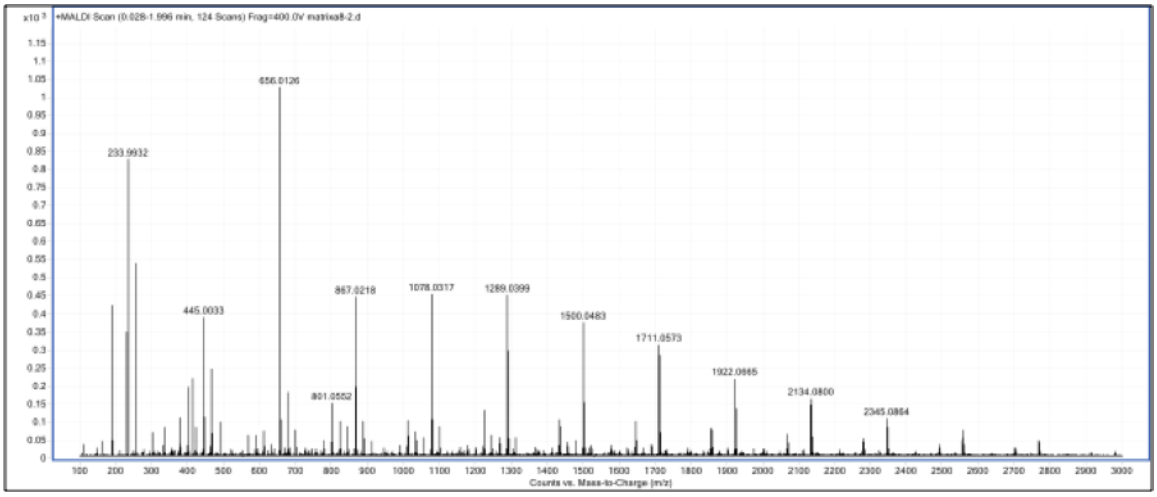

Figure 4.2. Mass spectrum of CHCA and cationizing agent (control) solution.

carpet from another. Figure 4.2. and figure 4.3. are spectra of the matrix/cationizing agent. Figure 4.2. depicts the matrix CHCA and figure 4.3. shows DCTB matrix.

The control spectra were important for this research because the peaks that were associated with the matrix and cationizing agent needed to be subtracted out of the sample spectra to be able to determine which peaks were originating from the carpet fiber. Figure 4.4. is the spectrum obtained from the analysis of the Masland

fiber sample. As is evident from the above figure, there are in fact a considerable amount of sample peaks that have been collected during the analysis. The bottom

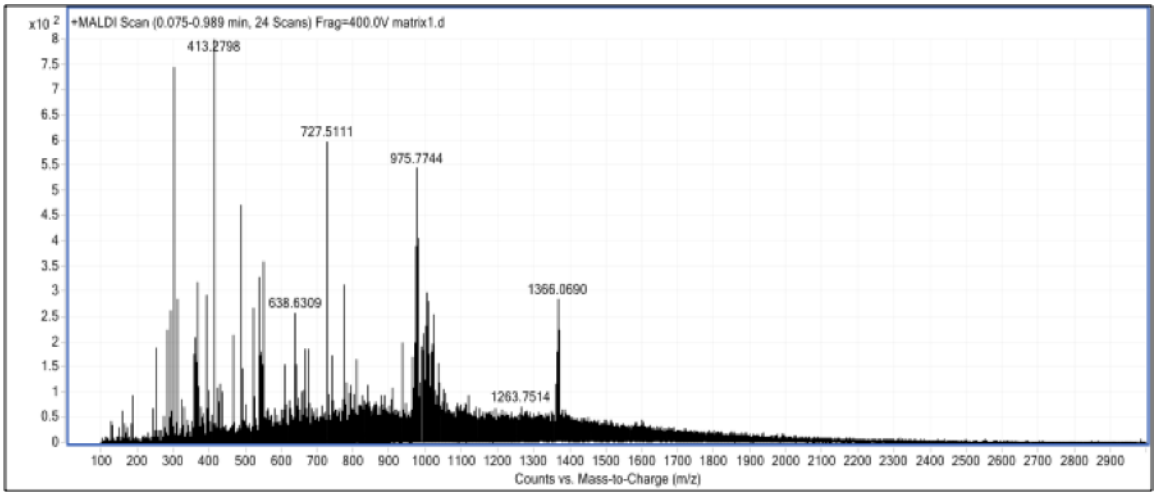

Figure 4.3. Mass spectrum of DCTB and cationizing agent (control) solution

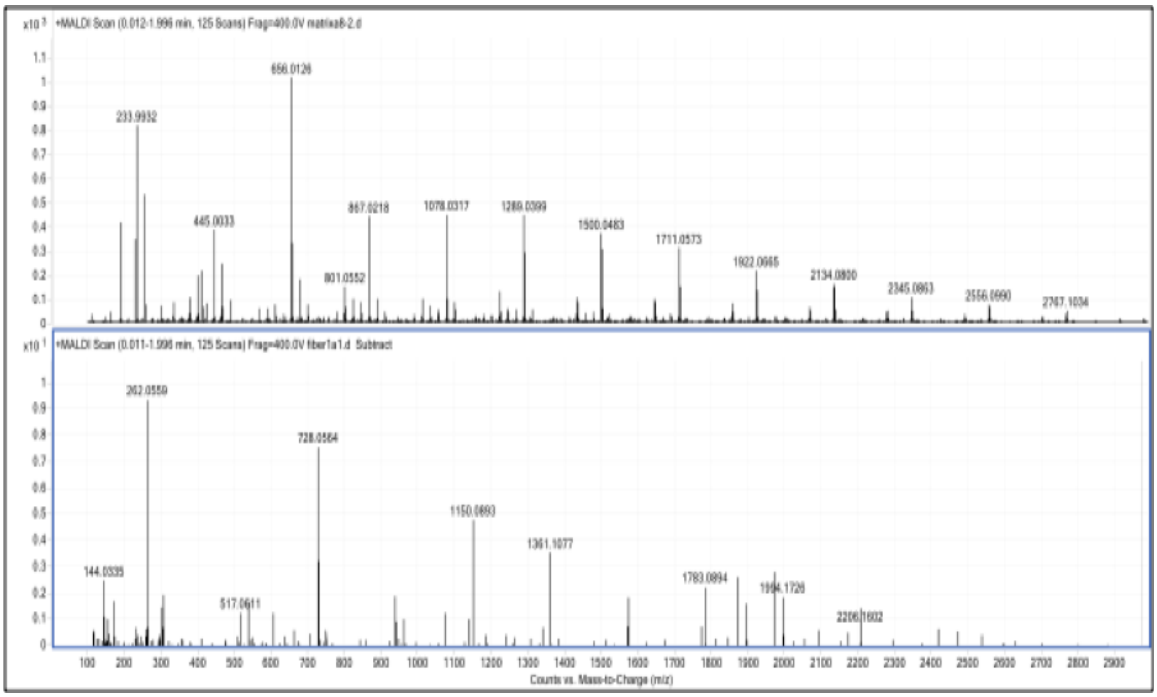

Figure 4.4. Mass spectra of CHCA (control- top) and Masland fiber sample (with matrix peaks subtracted –bottom)

spectrum of figure 4.4. has had the control matrix spectra subtracted, leaving only peaks that have originated from the carpet fiber. Figure 4.5. is spectra obtained from the Masland fiber sample using DCTB as the matrix. While it appears that with

this matrix not as many sample peaks have been produced, it should be noted that the peaks collected using this matrix differs from the CHCA matrix sample. This could be due to the ionization requirements of different molecules. As long as the differences within the spectra of the sample using different matrixes remain consistent through multiple collections of the sample type and matrix, the peaks

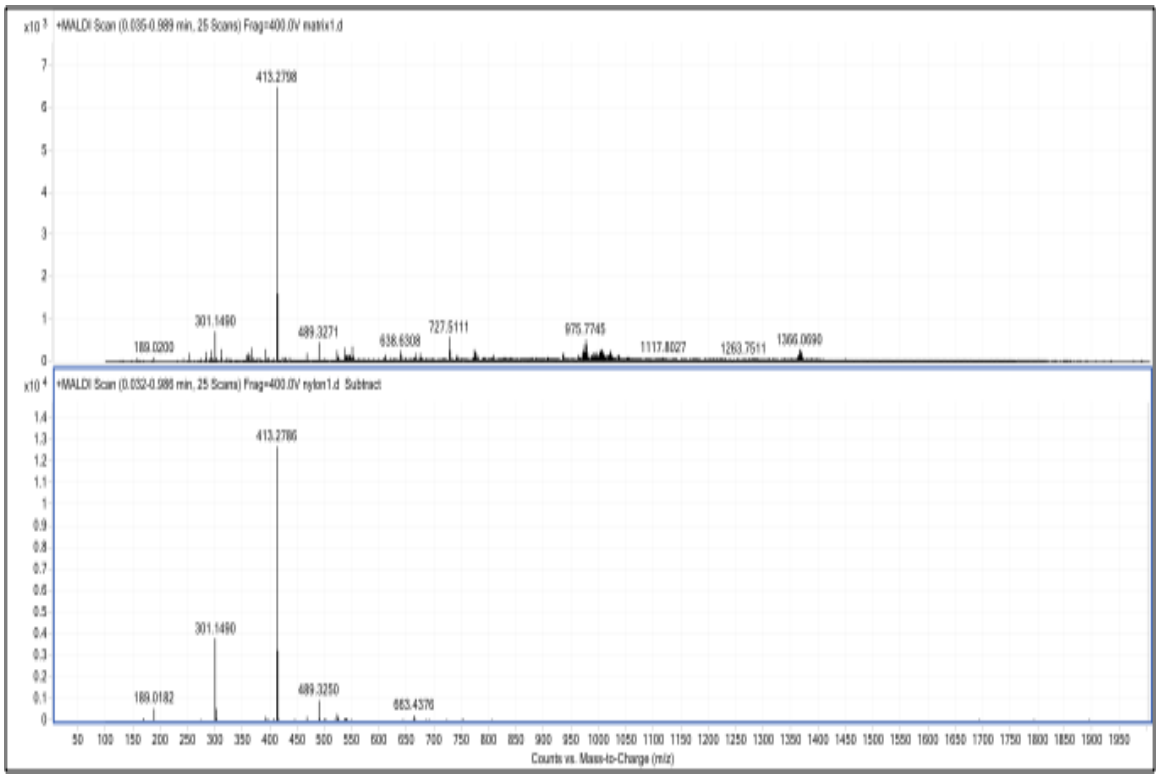

Figure 4.5. Mass spectra of DCTB (control- top) and Masland fiber sample (with matrix peaks subtracted –bottom)

can all be used and contributed to the different fiber additives.

The next analyzed carpet fiber was the Brahms fiber sample. Figure 4.6. is the mass spectra produced by the carpet sample using CHCA as the matrix. Figure 4.7. is the mass spectra produced using the sample carpet sample but employing DCTB as the matrix. As was observed with the Masland carpet fibers there are differences

between the Brahms fiber sample that used CHCA and DCTB. These differences provide more information for the comparison among the different nylon carpet fibers. The differences were consistently observed indicating that they are most

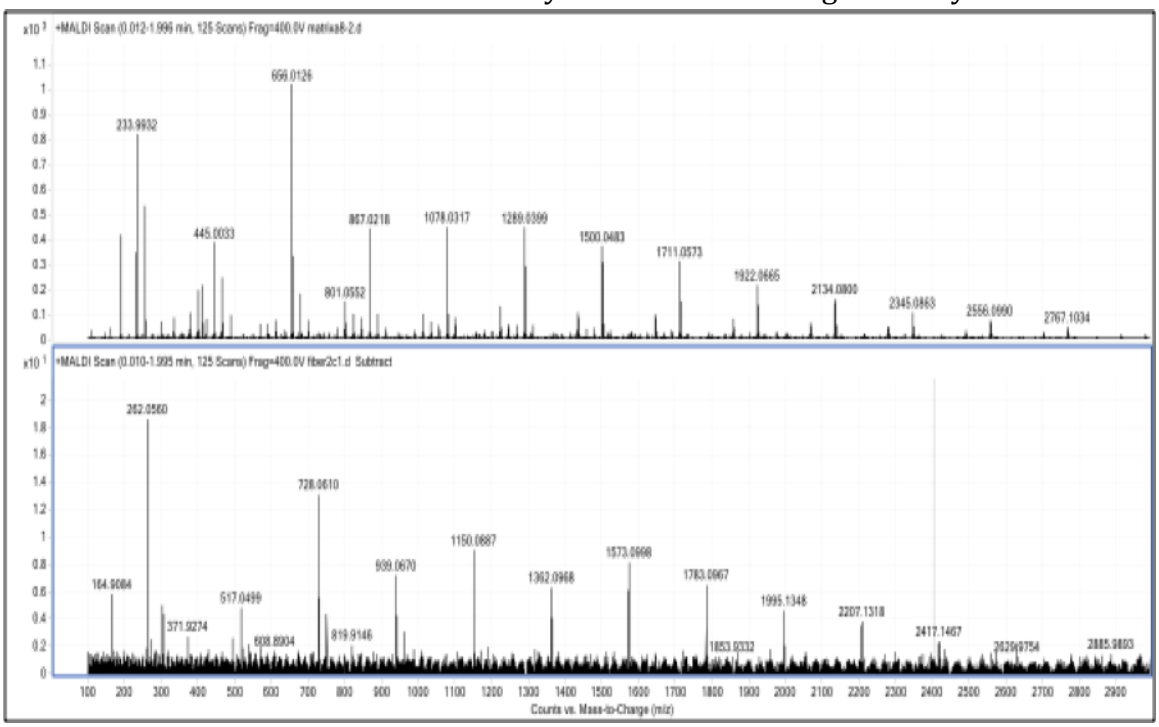

Figure 4.6. Mass spectra of CHCA (control – top) and Brahms fiber sample (with matrix peaks subtracted – bottom)

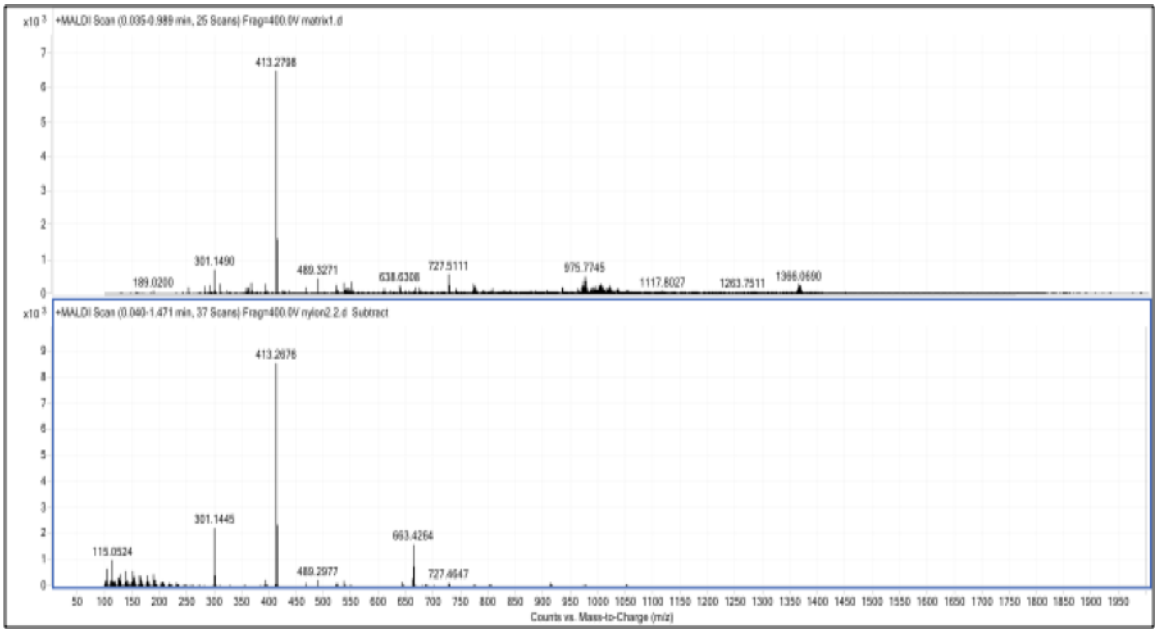

Figure 4.7. Mass spectra of DCTB (control – top) and Brahms fiber sample (with matrix peaks subtracted – bottom)

likely due to differences in ionization energy between the matrixes and sample. The next carpet sample to be analyzed was the DuPont fiber sample. Figure 4.8. is the spectra of the fiber using CHCA and figure 4.9. is the spectra of the fiber using DCTB.

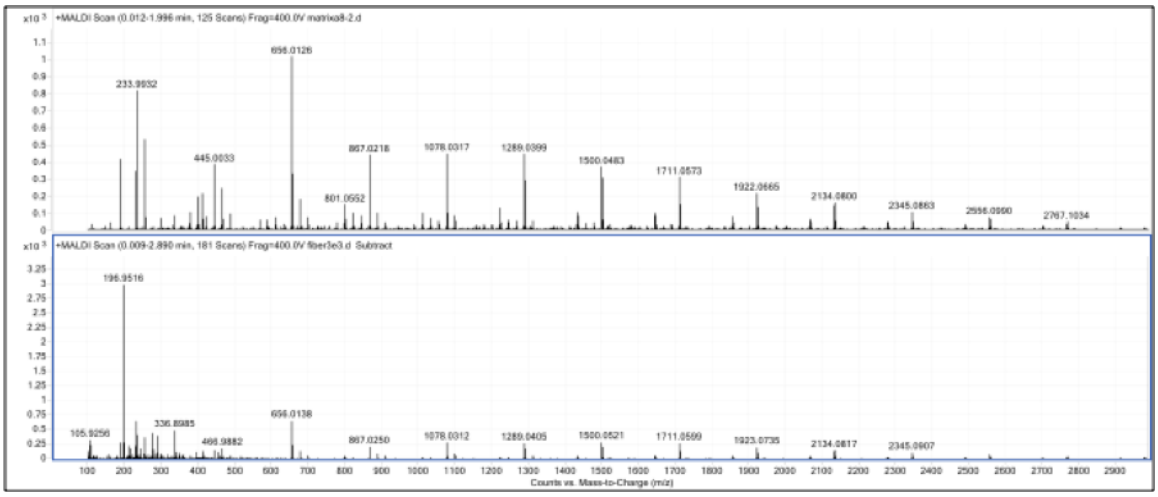

Figure 4.8. Mass spectra of CHCA (control – top) and DuPont fiber sample (with matrix peaks subtracted – bottom)

As was the case with the previous two samples the fiber has produced peaks different from the matrix and cationizing agent. The sample peaks produced peaks with good intensity.

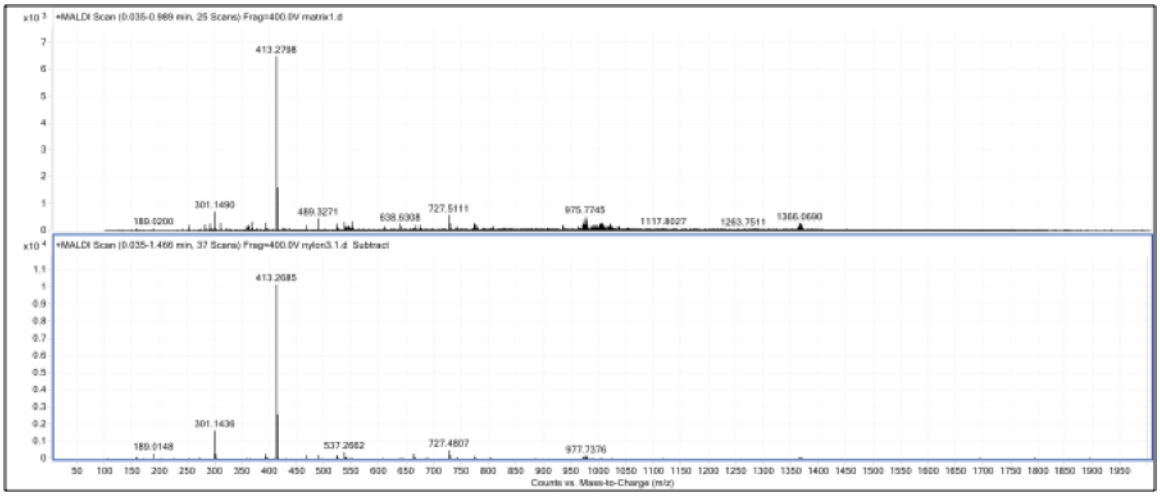

Figure 4.9. Mass spectra of DCTB (control – top) and DuPont fiber sample (with matrix peaks subtracted – bottom)

The final carpet fiber sample that was analyzed was the Stainmaster fiber sample. As with the other samples both CHCA and DCTB were used to analyze this fiber. Unfortunately, quality spectra could not be obtained using the DCTB matrix. Figure 4.10. is the spectra produced by CHCA. The spectra produced with the CHCA and

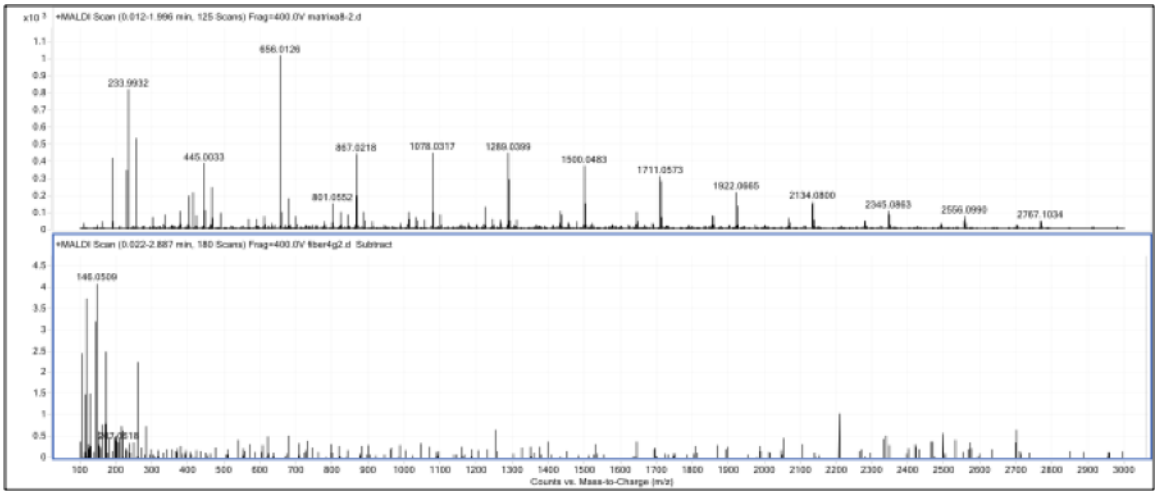

Figure 4.10. Mass spectra of CHCA (control – top) and Stainmaster fiber sample (with matrix peaks subtracted – bottom)

Stainmaster fiber sample produced sample peaks that were unique from the matrix, as seen in the bottom pane of figure 4.10. A pattern was distinguishable within the Masland, Brahms and DuPont fiber samples that were analyzed employing the use of the CHCA matrix. A repeating peak unit of ~211 amu was consecutively fragmented between the mass range of 500 – 2500 *m/z*. Each of the three fibers also portrayed very different lower-abundance peak patterns, which were distinct among each manufacturer. This indicates the presence of different chemical entities present within the separate manufactured fiber samples. Revealing that MADLI is able as is PyGCMS to distinguish the chemical additives of the fibers.

Similar results were observed whenever the Masland, Brahms and DuPont fibers were

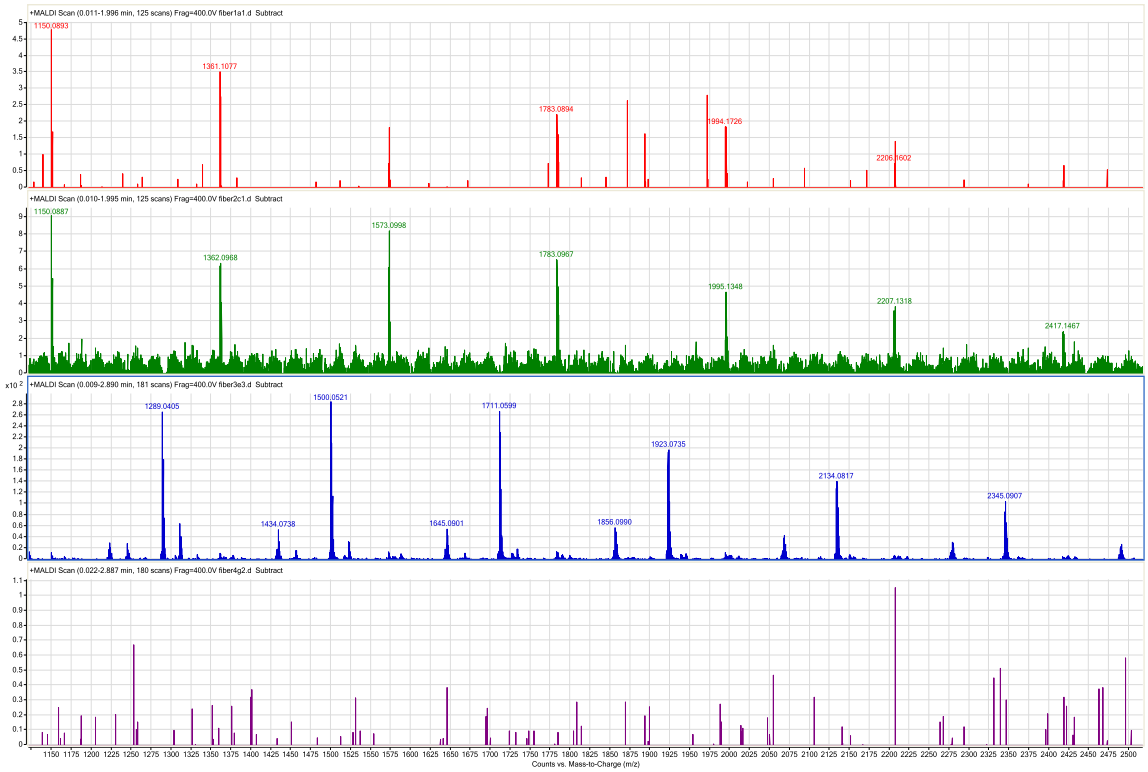

Figure 4.11. Magnified stacked spectra of Masland, Brahms, DuPont and Stainmaster fibers analyzed with CHCA matrix peaks subtracted 1150 – 2500

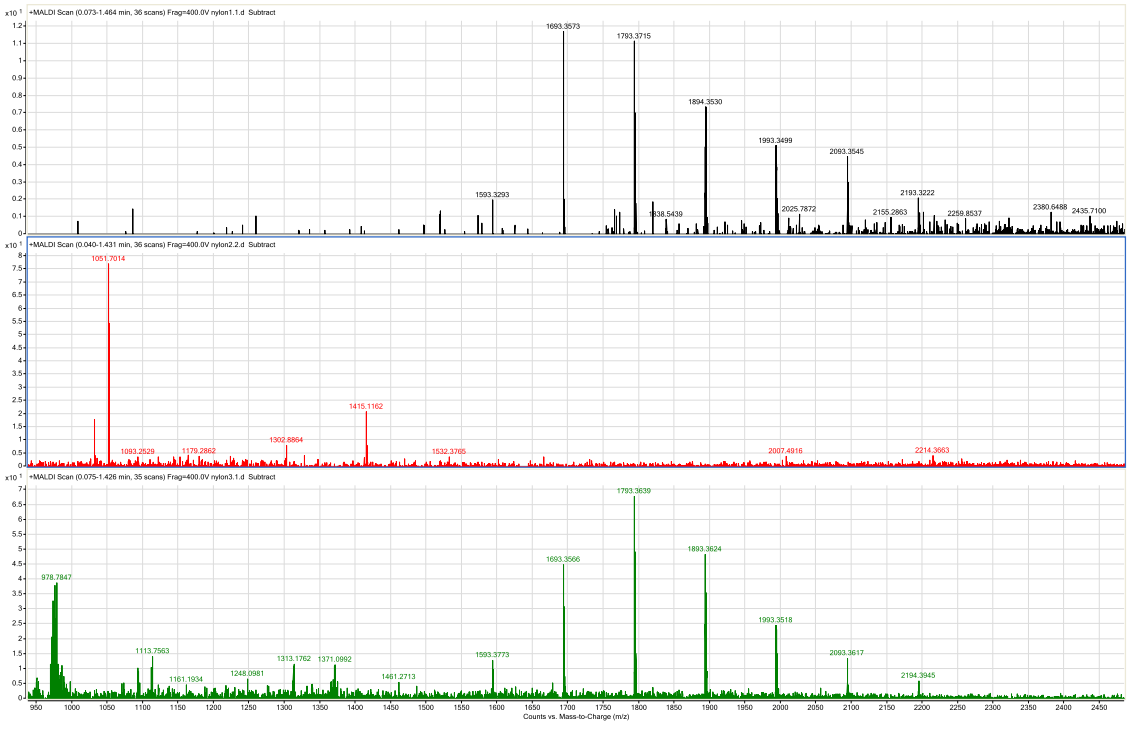

Figure 4.12. Magnified stacked spectra of Masland, Brahms and DuPont fibers analyzed with DCTB matrix peaks subtracted 950 – 2450

analyzed with DCTB as the matrix. A repeating mass unit of 100-112 amu was observed between the mass range of 100 – 2300 *m/z*, with lower-abundance peaks observed that were distinct for each manufactured nylon sample. The Stainmaster fiber portrayed a peak pattern that was unique from the other three carpet fiber samples when analyzed with both CHCA and DCTB. Further analysis must be performed to find consistency within this fiber sample and to confirm the differences observed among the different brands of carpet fibers.

4.4. Conclusion

It was determined that both CHCA and DCTB matrixes were suitable for the analysis of the different carpet fibers. The carpet fibers were analyzed and it was determined that the polymer additives could be detected using MALDI. Different carpet samples from different manufacturers were analyzed successfully. It has been discovered that both CHCA and DCTB matrixes could be applied for this analysis and each matrix provided sample peaks that differed from the other. These unique differences were useful in providing more information on the chemical additives that are used in the manufacture of carpet fibers. While the additives are considered proprietary and are not readily identifiable, these unique additives give the fibers a signature that is unique to its manufacturer. This was observed within the spectra, as each contained peaks that were different from the other nylon fibers. The analyzed fibers consistently produced spectra that were similar when a fiber from the same carpet sample was tested yet produced different spectra whenever fiber samples from the different brands of fibers were analyzed. While more work

will be needed to firmly establish this type of analysis method for carpet fiber evidence, this preliminary work demonstrates that more research has the strong potential for success.

References:

1. Kathryn L. Hatch, H. I. M., Textile dermatitis: an update. *Contact Dermatitis* **1995,***32* (6), 319-326.
2. Causin, V.; Marega, C.; Schiavone, S.; Guardia, V. D.; Marigo, A., Forensic analysis of acrylic fibers by pyrolysis-gas chromatography/mass spectrometry. *Journal of Analytical and Applied Pyrolysis* **2006,***75* (1), 43-48.
3. Herrera, M.; Matuschek, G.; Kettrup, A., Fast identification of polymer additives by pyrolysis-gas chromatography/mass spectrometry. *Journal of Analytical and Applied Pyrolysis* **2003**, 70 (1), 35-42.
4. Wang, F. C.-Y., Polymer additive analysis by pyrolysis-gas chromatography: I. Plasticizers. *Journal of Chromatography A* **2000,***883* (1-2), 199-210.
5. Wang, F. C.-Y., Polymer additive analysis by pyrolysis-gas chromatography: II. Flame retardants. *Journal of Chromatography A* **2000,***886* (1-2), 225-235.
6. Wang, F. C.-Y.; Buzanowski, W. C., Polymer additive analysis by pyrolysis-gas chromatography: III. Lubricants. *Journal of Chromatography A* **2000,***891* (2), 313-324.
7. Wang, F. C.-Y., Polymer additive analysis by pyrolysis-gas chromatography: IV. Antioxidants. *Journal of Chromatography A* **2000,***891* (2), 325-336.
8. Deedrick, D. W., Hairs, Fibers, Crime and Evidence Part 2: Fiber Evidence. *Forensic Science Communications* **2000,***2* (3).
9. Deedrick, D. W., Hairs, Fibers, Crime and Evidence Part 3: Crime and Evidence. *Forensic Science Communications* **2000,***2* (3).
10. Walch, A.; Rauser, S.; Deininger, S.-O.; Höfler, H., MALDI imaging mass spectrometry for direct tissue analysis: a new frontier for molecular histology. *Histochemistry and Cell Biology* **2008,***130* (3), 421-434.

Chapter 5.

Analysis of Glutathione

5.1. Introduction

Glutathione is a biomolecule that has recently been found to have great importance in the detoxification of the body.[1-5] Levels of glutathione within the body are being investigated to determine the implications of different levels of the two different forms of glutathione that are found within the human body, oxidized and reduced.[6-8] Glutathione has been determined to be connected with a wide variety of cells throughout the body. There have been connections drawn between glutathione and neurological disorders/neurotoxicity, cancers, tumors, liver disease, cardiovascular disease, chronic toxicity and autism among other ailments.[1, 2, 6, 8-10] Due to the wide range of diseases that glutathione has been associated with, many studies have been ongoing not only to determine the different disorders that it is linked to, but also to determine how its oxidized and reduced forms effect the ailment and what levels of glutathione are needed for successful detoxification and repair of cells.[2, 5-9, 11] It has been determined that the levels of reduced glutathione (GSH) and oxidized glutathione (GSSG) and the ratio of GSH:GSSG can indicate the current oxidative stress the body is undergoing.[4, 6] It has been determined that within healthy cells and tissues that 90% of the glutathione present is in the reduced form and the oxidized form is only present at 10% but with oxidative stress these levels can and

do change.[9] Figure 5.1. shows the chemical structure of glutathione with A. being the reduced form and B. is the oxidized form of the molecule.

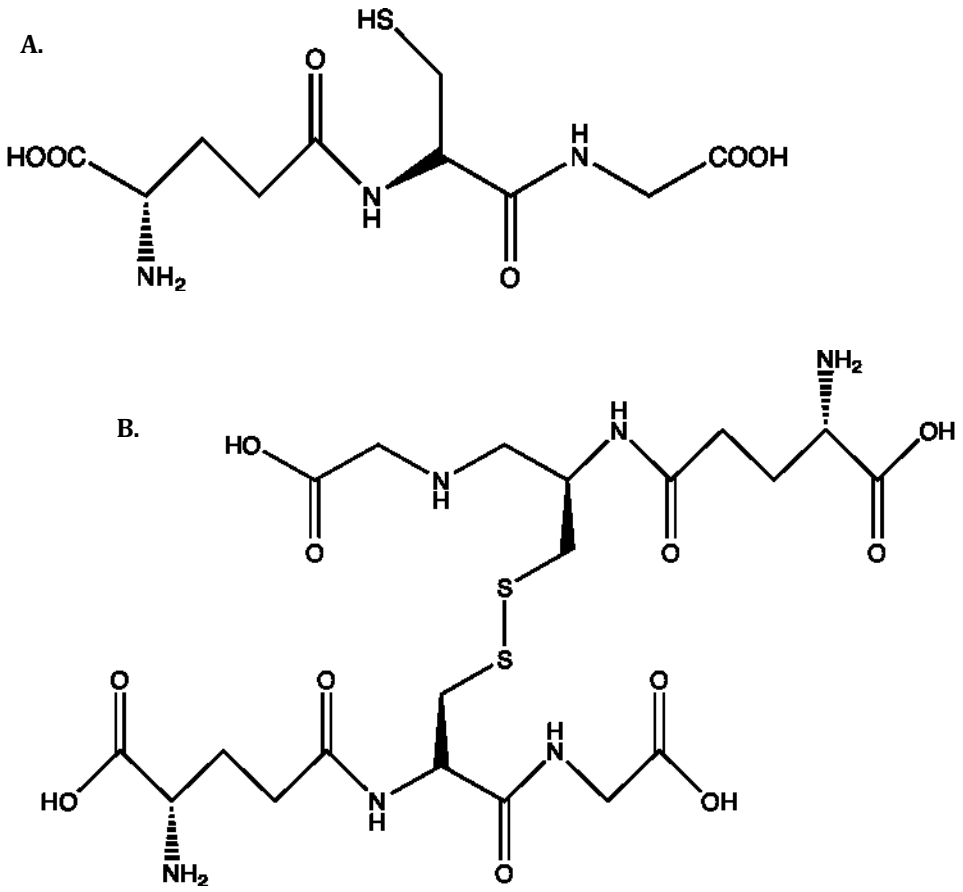

Figure 5.1. chemical structure of glutathione **A.** reduced **B.** oxidized

Because of the importance of this molecule, analysis and species determination has become necessary. In order to complete this analysis of reduced and oxidized glutathione was analyzed by AP – MALDI-TOF-MS.

5.2. Materials and Methods

5.2.1. Samples and Reagents

The matrix used for the analysis of GSH and GSSG was CHCA purchased from Fluka (Lausanne, Switzerland). This matrix was chosen due to its success in the literature

for the analysis of proteins and peptides.[12, 13] Standards of GSH and GSSG were obtained from Sigma-Aldrich (St. Louis, MO). Solvent used for analysis was HPLC grade methanol (EMD Chemicals Merk Rockland, MA).

Matrix solution was made by dissolving 9.0 mg of CHCA into 250 µL of methanol. The glutathione standards were made by combining 2.0 mg of standard sample with 250 µL of methanol. Samples were then made by adding 30 µL of GSH and 30 µL CHCA to a microcentrifuge tube. This was repeated for the GSSG standard. These samples were hand spotted onto a MALDI target and analyzed.

5.2.2. Instrumentation

All experiments were performed on an updated Agilent (Santa Clara, CA) LC/MSD/TOF 6200 equipped with a MassTech (Columbia, MD) AP – MALDI source with a nitrogen laser operating at 337 nm with a spiraling raster motion. The Agilent TOF – MS is an orthogonal high-resolution mass spectrometer with pulsed dynamic focusing. Spectra were then collected of the different samples upon the Agilent 6200 series time of flight mass spectrometer with an atmospheric pressure MALDI unit from MassTech.

Optimized parameters for sample signal were determined and they were as follows: capillary voltage was set to 3200 volts, fragmentor was 375 volts, gas temperature was 350° C with a drying gas flow of 5 L/min. The laser attenuation was set to 6 and spectra were collected over 1 min.

5.2.3. Limit of Detection Sample Preparation

Standard stock solutions of GSH standard and GSSG standard were made to a concentration of 4000 ppm. Serial dilution of each stock solution was completed to make up solutions of the following concentrations: 400 ppm, 40 ppm, 4 ppm and .4 ppm. This was done with both the GSH and GSSG standards. Samples were then made by combining 30 µL of matrix solution with 30 µL of either GSH or GSSG. This was repeated for each concentration, resulting in samples with concentrations of 200 ppm, 20 ppm, 2 ppm and .2 ppm. Samples were hand spotted onto MALDI target and the samples were run using the method that had been optimized for the analysis of glutathione.

5.3. Results and Discussion

5.3.1. Optimization Results

The GSH and GSSG standards were analyzed using AP – MALDI-TOF-MS. While it was initially unknown whether analysis of the glutathione by MADLI would produce useful results, it was soon determined that analysis of the samples were achievable. Figure 5.2. is spectra of GSH and GSSG that were optimized by adjusting the MS voltages for the best possible signal strength.

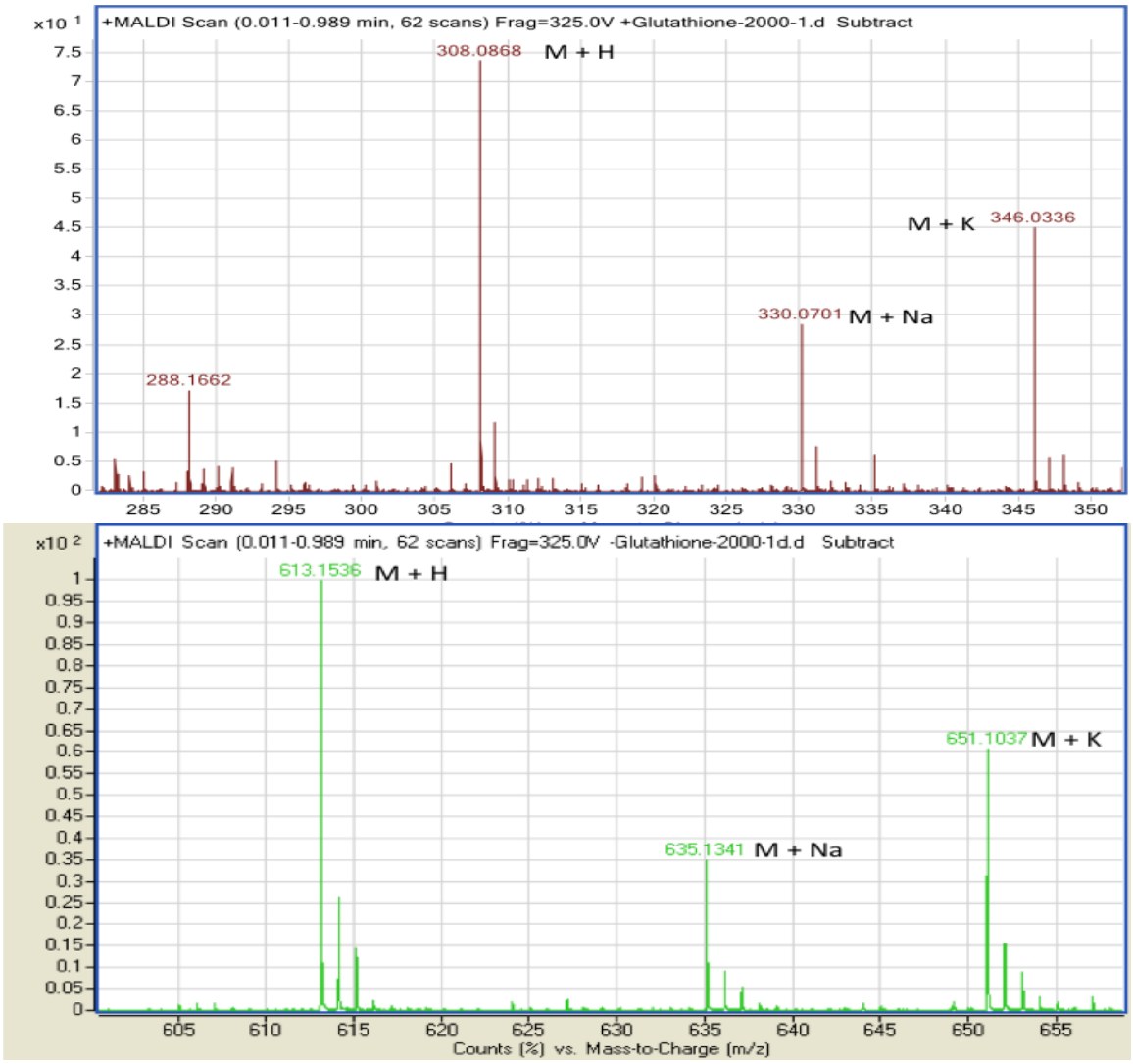

Figure 5.2. spectra of glutathione reduced (top) and oxidized (bottom)

The optimization of the method for the analysis of glutathione went smoothly and good spectra of both GSH and GSSG were obtained. Figure 5.2. are the resulting spectra. The analyte can be observed in the top spectra, the spectra of GSH, at a *m/z* of 308.0868 amu for protonated ion and at *m/z* of 330.0701 amu and 346.0336 amu for the sodiated and passiated ions of glutathione. Similarly the GSSG spectra shows the presence of protonated GSSG at the *m/z* 613.1536 amu, sodiated ion 635.1341

amu and the passiated ion at *m/z* 651.1037 amu. These results demonstrated that both GSH and GSSG could be analyzed effectively with MALDI.

5.3.2. Limit of Detection

The various concentrations of the GSH and GSSG were then analyzed using the

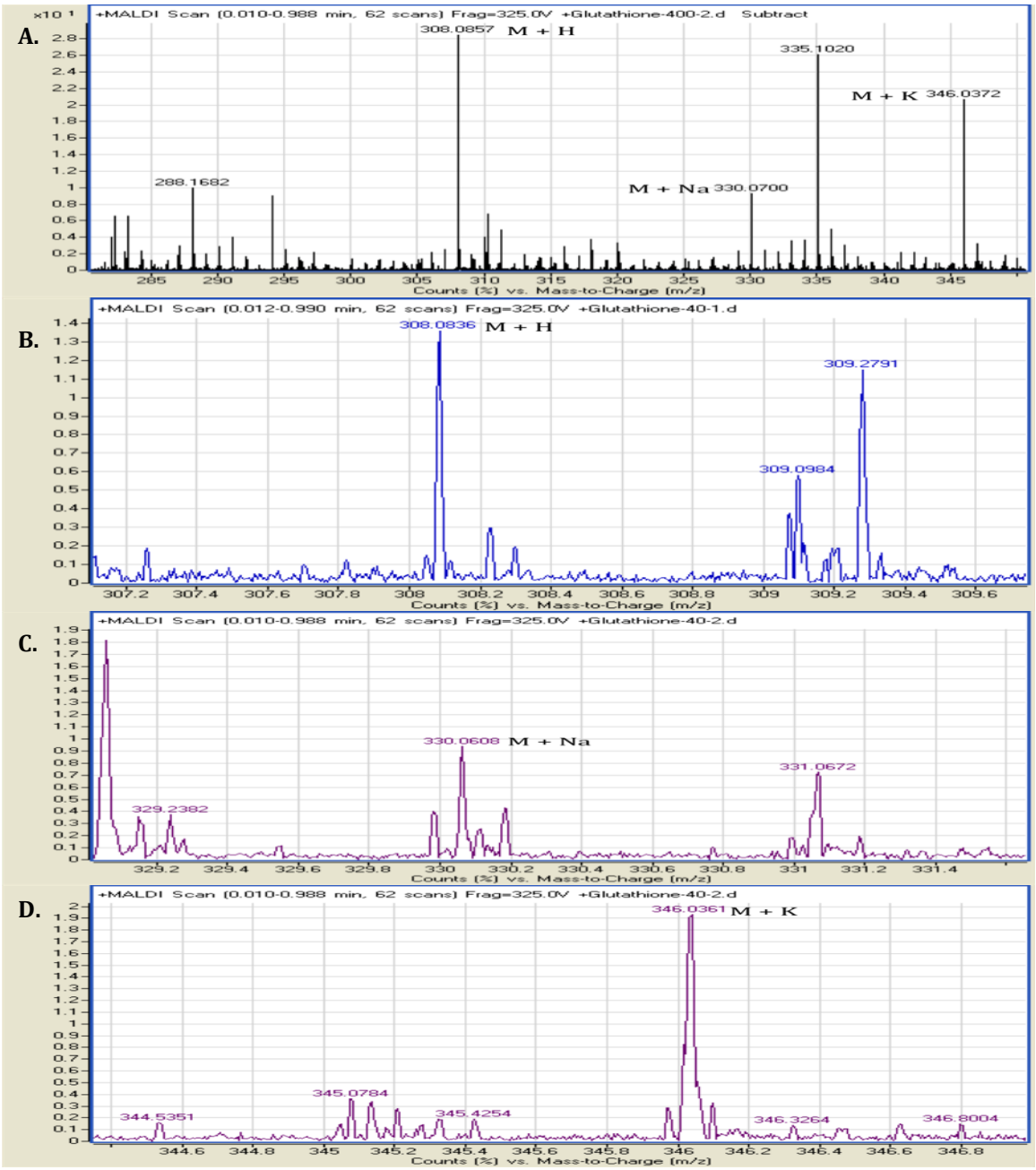

Figure 5.3. spectra of GSH **A.** GSH 200 ppm **B.** GSH 20 ppm protonated peak **C.** GSH 20 ppm sodiated peak **D.** GSH 20 ppm passiated GSH peak

previously optimized method. As with the spectra that were obtained during the method optimization, the various concentrations of the GSH ionized in protonated, sodiated and passiated forms. Figure 5.3. are spectra of GSH from 200 and 40 ppm.

As was evident with the previous detection of GSH, at the concentrations of 200 ppm and 20 ppm multiple ion peaks are visible. The analyte can be observed in the top spectra, the spectra of GSH, at a *m/z* of 308.0857 amu for protonated ion and at *m/z* of 330.0608 amu and 346.0361 amu for the sodiated and passiated ions of

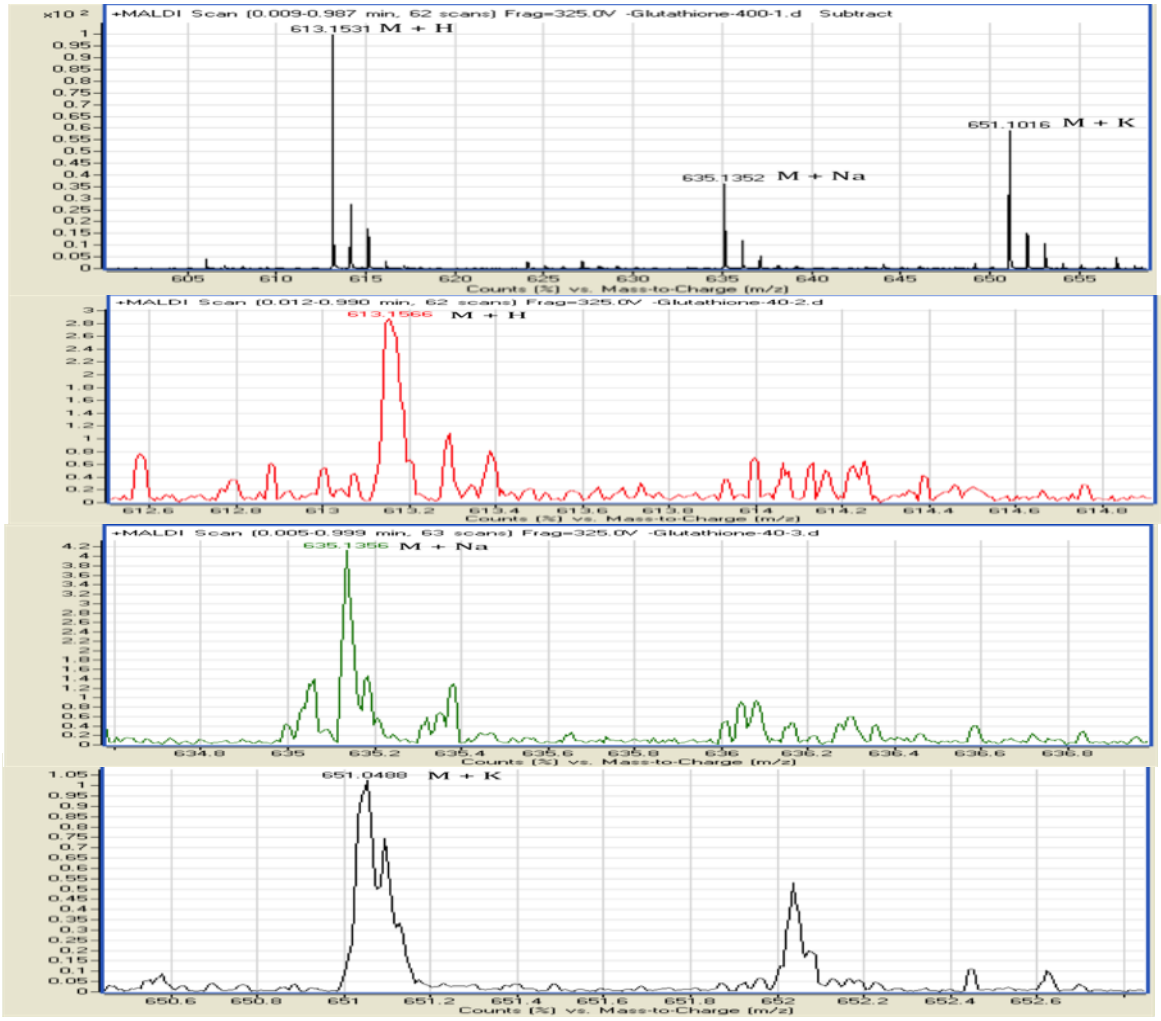

Figure 5.4. spectra of GSSG **A.** GSSG 200 ppm **B.** GSSG 20 ppm protonated peak **C.** GSSG 20 ppm sodiated peak **D.** GSSG 20 ppm passiated peak

glutathione. GSH at concentration < 20 ppm could not be distinguished from the background noise peaks leading to the conclusion that the limit of detection for the GSH was 20 ppm. For the GSSG limit of detection, the analysis was completed in the same way the GSH was done. Figure 5.4. shows the spectra that were collected for the detection limit of GSSG. As was the case with the GSH, the GSSG spectra show the presence of protonated GSSG at the *m/z* 613.1536 amu, sodiated ion 635.1341 amu and the passiated ion at *m/z* 651.1037 amu. It was determined that at concentration < 20 ppm, the sample peaks could not be distinguished from the background noise peaks leading to the conclusion that the limit of detection for the GSSG was 20 ppm, as was the case with the GSH.

5.4. Conclusion

It was determined that reduced and oxidized glutathione could be analyzed using MALDI. Good intensity spectra were obtained with protonated, sodiated and passiated glutathione present. Once the instrument parameters were optimized, limit of detection was accomplished for both forms of glutathione. It was determined that for both GSH and GSSG, 20 ppm was the limit of detection. This limit of detection study was carried out using serially diluted standard solutions. While this study was successful in that both species of glutathione were detected it has also shed light upon the fact that in order for speciated glutathione analysis of blood to be completed a procedure that involves a concentrating of the sample will be necessary. The limit of detection for GSSG is below the levels usually found in human blood.[3]

Reference:

1. Obolenskaya, M. Y.; Teplyuk, N. M.; Divi, R. L.; Poirier, M. C.; Filimonova, N. B.; Zadrozna, M.; Pasanen, M. J., Human placental glutathione S-transferase activity and polycyclic aromatic hydrocarbon DNA adducts as biomarkers for environmental oxidative stress in placentas from pregnant women living in radioactivity- and chemically-polluted regions. *Toxicology Letters* **2010,** *196* (2), 80-86.

2. Yochum, C. L.; Bhattacharya, P.; Patti, L.; Mirochnitchenko, O.; Wagner, G. C., Animal model of autism using GSTM1 knockout mice and early post-natal sodium valproate treatment. *Behavioural Brain Research* **2010,** *210* (2), 202-210.
3. Flagg, E. W.; Coates, R. J.; Jones, D. P.; Eley, J. W.; Gunter, E. W.; Jackson, B.; Greenberg, R. S., Plasma total glutathione in humans and its association with demographic and health-related factors. *British Journal of Nutrition* **1993,** *70* (03), 797-808.
4. Reed, D. J., Glutathione: Toxicological Implications. *Annual Review of Pharmacology and Toxicology* **1990,** *30* (1), 603-631.
5. Giustarini, D.; Dalle-Donne, I.; Milzani, A.; Rossi, R., Detection of glutathione in whole blood after stabilization with N-ethylmaleimide. *Analytical Biochemistry* **2011,** *415* (1), 81-83.
6. Sies, H., Glutathione and its role in cellular functions. *Free Radical Biology and Medicine* **1999,** *27* (9,Äì10), 916-921.
7. RICHIE, J. P. S., L.; ABRAHAM, P.; LEUTZINGER,Y., *Blood glutathione concentrations in a large-scale human study*. American Association for Clinical Chemistry: Washington, DC, ETATS-UNIS, 1996; Vol. 42.
8. Dalton, T. P.; Chen, Y.; Schneider, S. N.; Nebert, D. W.; Shertzer, H. G., Genetically altered mice to evaluate glutathione homeostasis in health and disease. *Free Radical Biology and Medicine* **2004,** *37* (10), 1511-1526.
9. Pastore, A.; Federici, G.; Bertini, E.; Piemonte, F., Analysis of glutathione: implication in redox and detoxification. *Clinica Chimica Acta* **2003,** *333* (1), 19-39.
10. Stempak, D.; Dallas, S.; Klein, J.; Bendayan, R.; Koren, G.; Baruchel, S., Glutathione Stability in Whole Blood: Effects of Various Deproteinizing Acids. *Therapeutic Drug Monitoring* **2001,** *23* (5), 542-549.
11. Chen, H.-I.; Chiu, Y.-W.; Hsu, Y.; Li, W.-F.; Chen, Y.-C.; Chuang, H.-Y., The Association of Metallothionein-4 Gene Polymorphism and Renal Function in Long-Term Lead-Exposed Workers. *Biological Trace Element Research* **2010,** *137* (1), 55-62.
12. Chrisey, D. B.; Pique, A.; McGill, R. A.; Horwitz, J. S.; Ringeisen, B. R.; Bubb, D. M.; Wu, P. K., Laser Deposition of Polymer and Biomaterial Films. *Chemical Reviews* **2003,** *103* (2), 553-576.
13. Vogel, A.; Venugopalan, V., Mechanisms of Pulsed Laser Ablation of Biological Tissues. *Chemical Reviews* **2003,** *103* (2), 577-644.

Chapter 6.

Biofilm analysis via AP – MALDI-TOF-MS

6.1. Introduction

It has been well documented that a biological matrix is formed by certain bacteria for its adhesion to orthopedic implants.[1-3] Published information indicates that the bacterial matrix formed involves two polysaccharides one responsible for the adhesion of cells and other biomaterial known as capsular polysaccharide/adhesin (PS/A) and a polysaccharide antigen that is responsible for intercellular adhesion known as polysaccharide intercellular adhesion (PIA).[4] PIA is crucial in the formation of biofilms, believed to be the mediator of bacterial accumulation into cellular aggregates.[5] Biofilm formation is usually characterized in two phases: initial adherence to some surface and cell proliferation with intercellular adhesion that results in the accumulation of the biofilm.[6] Because the polysaccharides are known to be a key part of biofilm formation, the need to study and characterize these molecules is important.[5, 6] In this study, the bacterial matrix will be characterized using AP – MALDI-TOF-MS.

Polysaccharides are chains of sugars/carbohydrates that contain a repeating monomer joined by glycosidic bonds.[7] Polysaccharides are contain at least 20 monosaccharide units and can contain thousands of units.[7] Some polysaccharides

are linear chains, while others can be branched.[7] Figure 6.1 is the chemical structures of selected polysaccharides.

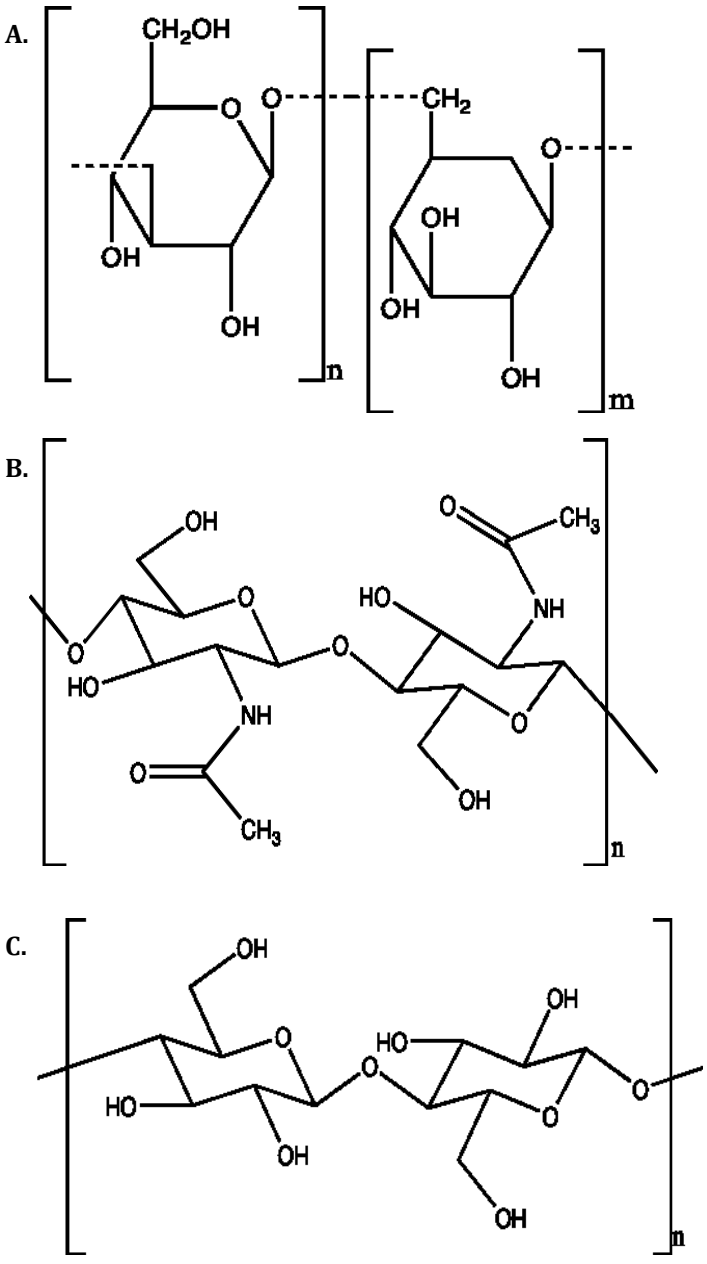

Figure 6.1. Chemical structures of polysaccharides **A.** structure of chrysolaminarin **B.** structure of chitin **C.** structure of cellulose

6.1. A. is the chemical structure of chrysolaminarin, which is regarded as one of the world's most common biopolymer. B. is the chemical structure of chitin which is a component of cell walls. C. is the chemical structure of cellulose which is known to be secreted for biofilm formation.

Bacterial infections are a significant problem with joint implants and central venous catheters[8]. It has been reported that <1% of hip replacements, <2% of knee implants become infected[9]. While this does seem like a low rate of occurrence, this equates to approximately 112,000 cases annually.[8] The number of cases per year is expected to rise as the number of surgeries for joint replacement rise due to an aging and more active population[9]. Antibiotic treatment of the implant infections is not very effective resulting in another surgery where the implant is removed but this has the potential to leave the patient with substantial disability[10]. Cost is another consideration with a joint replacement surgery costing ~$30,000 and the removal of an infected implant costs 5.2 – 7.2 times as much as the initial operation.[8, 9]

By analyzing the components of *Staphylococcus Epidermidis* that are responsible for its adhering capabilities, the materials that various implants are made out of, or coated with, can be altered to offer a surface that is resistant to the growth of a biofilm matrix. Having a surface resistant to the bacterial matrix would effectively prevent the bacterial infection from occurring in the first place which would save the patient time, prevent painful follow-up procedures and save a considerable amount of money, helping to fray the astronomical cost of the medical system.

The cell wall will be analyzed using AP – MALDI-TOF-MS. The analysis will focus on the carbohydrate components of the cell wall. This focus is to characterize the two polysaccharides that are responsible for the biofilm formation that makes this bacteria such a nuisance to orthopedic implants[4]. The two polysaccharides that have been credited with biofilm formation are polysaccharide/adhesin (PS/A) and polysaccharide intercellular adhesin (PIA)[5]. A carbohydrate standard panel will be used for characterization. These polysaccharide components will be explored to determine how these components allow biofilm formation and whether there is a certain chemical that will interact with the components to inhibit the formation of a biofilm.

6.2 Materials and Methods

6.2.1. Samples and Reagents

S. Epidermidis (ATCC strain 49134) were grown and allowed to adhere to culture plates by collaborators at Allegheny General Hospital (Pittsburgh, PA). The resulting biofilm will be obtained and an extraction and purification were completed on the cells to separate the cell wall from the entire cell. Two different samples were used, a sample of the biofilm forming species and a planktonic colony species. Two different strains were also provided, one labeled as '185' and the other labeled as '195'. Both the biofilm and the planktonic varieties of each were analyzed.

CHCA (Fluka, Lausanne, Switzerland) was the matrix used to analyze the cell wall extracts and was used as received. The solvent used for the experiment was HPLC grade methanol (EMD Chemicals, Merk Rockland, MA).

6.2.2. Instrumentation

All experiments were performed on an updated Agilent (Santa Clara, CA) LC/MSD/TOF 6200 equipped with a MassTech (Columbia, MD) AP – MALDI source with a nitrogen laser operating at 337 nm with a spiraling raster motion. The Agilent TOF – MS is an orthogonal high-resolution mass spectrometer with pulsed dynamic focusing.

Spectra were then collected of the different samples upon the Agilent 6200 series time of flight mass spectrometer with an atmospheric pressure MALDI unit from MassTech.

Instrument parameters were as follows: capillary voltage was set to 3200 volts, fragmentor was 375 volts, gas temperature was 350° C with a drying gas flow of 5 L/min. The laser attenuation was set to 6 and spectra were collected over 1 min.

6.2.3. *S. Epidermidis* Sample Preparation

To extract the cell wall from the rest of the cell, first the cell was mechanically disrupted with glass beads in a Braun disintegrator at 4° C. After removal of the glass beads, the suspension was treated with deoxyribonuclease and ribonuclease (3 µg/ml each) for 60 min. Whole cells were removed by successive centrifugations at 2,000 x g for 10 min. The cell walls were sedimented at 15,000 x g, suspended in

0.05 M tris(hydroxymethyl)aminomethane(Tris)-hydrochloride buffer (pH 7.6), and heated at 90° C for 10 min. After centrifugation at 15,000 x g and resuspension in the same buffer, the cell walls were treated with trypsin (200 μg/ml) at 37° C for 1 hr. After centrifugation at 15,000 x g the pellet was washed several times with water and finally suspended in water. This cell wall preparation was checked for the presence of whole cells with a phase contrast microscope.[11]

Once the cell wall extraction from *S. Epidermidis*was completed, samples were prepared for MALDI analysis. A matrix solution was prepared by dissolving ~ 9.0 mg of CHCA into 250 μL of methanol. Four different *S. Epidermidis* were received and analyzed. The received samples were 185 biofilm, 185 planktonic, 195 biofilm and 195 planktonic. These samples were vortexed for ~ 30 sec to ensure any settled material was re-suspended. Each sample had 30 μL pipetted from its tube into a new micro centrifuge tube and 30 μL of CHCA solution was added to each of the samples. The samples were then pipetted onto a MALDI target using a volume of ~0.5 μL.

Samples were then analyzed using positive mode AP – MALDI-TOF-MS. The laser attenuation was set to 6 and spiral motion raster was enabled. The gas temperature was held constant at 350° C with a flow of 5 L/min. The capillary voltage was set to 3050 V and the fragmentor voltage was 325 V. The sample was collected over 1 min with a mass range from 100 – 2000 amu.

6.3. Results/Discussion

6.3.1. Spectra from 185 Strain

Spectra with good signal intensity were collected. The samples were analyzed to determine differences within the cell wall extracts between the biofilm forming bacteria and the planktonic colony forming bacteria. Figure 6.2. is stacked spectra produced from 5 different 185 biofilm samples.

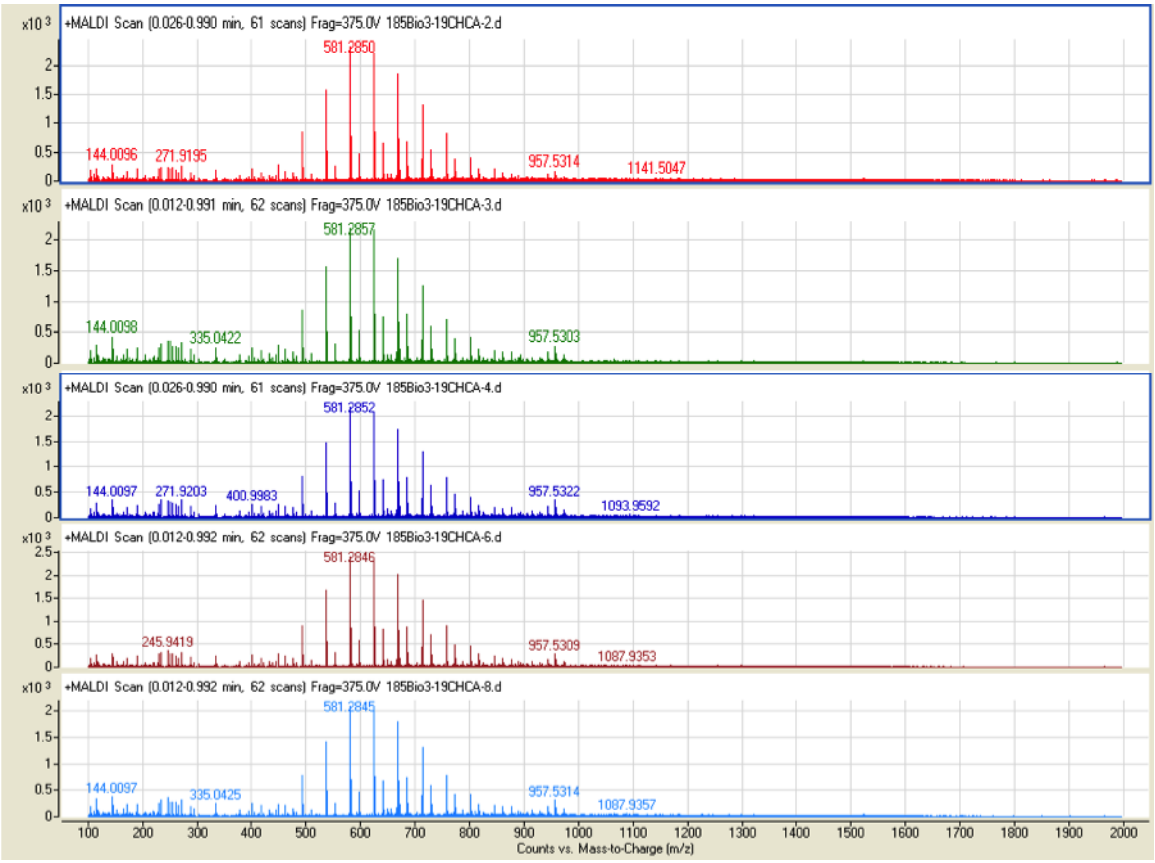

Figure 6.2. Stacked spectra of 185 biofilm

Figure 6.2. demonstrates that there was consistency within the prepared sample. Each spectrum above was collected from a different sample spot on the MALDI target. These spectra have good signal intensity without an overshadowing by

matrix peaks. Figure 6.3. stacked spectra produced from the 185 planktonic colony forming bacteria.

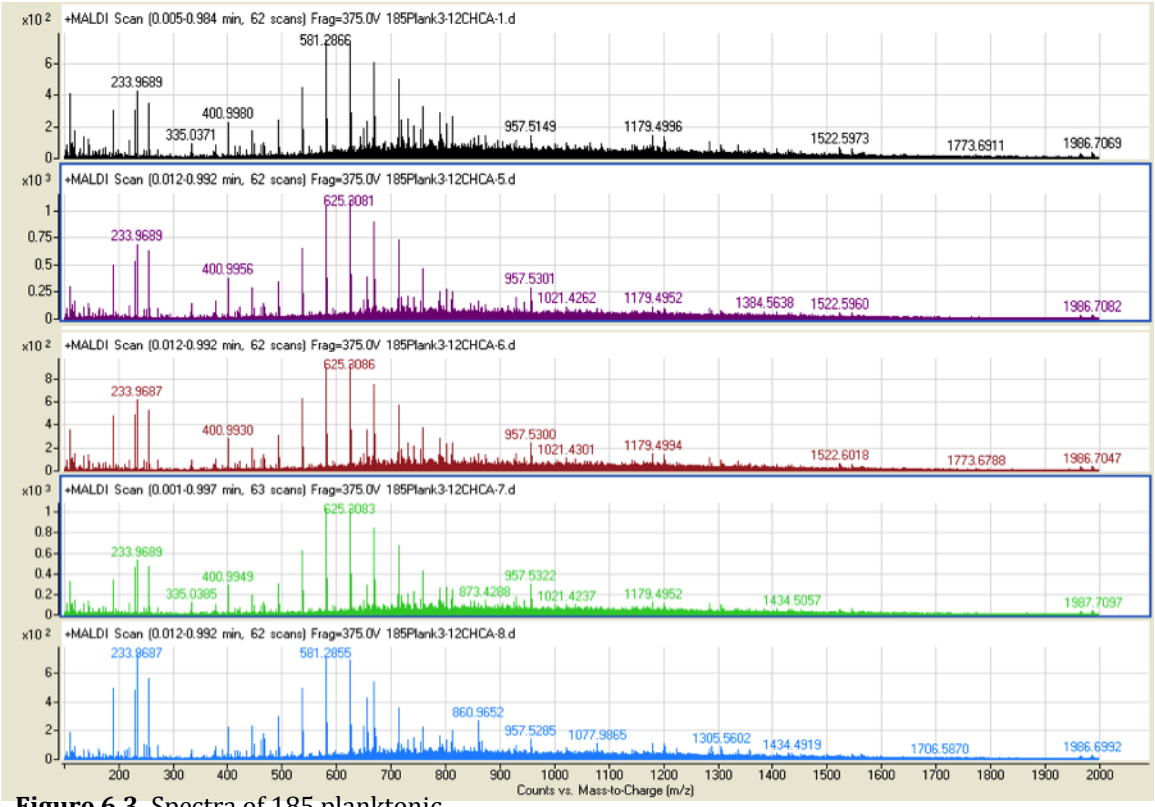

Figure 6.3. Spectra of 185 planktonic

As with figure 6.2. figure 6.3. shows that there was a consistency in the spectra produced by the 185 planktonic colony forming bacteria. As with figure 6.2., each spectrum was collected from a different spot that was deposited onto the MALDI target. These spectra had good signal intensity and the sample peaks were well distinguished from the background noise. In figure 6.4. the differences between the biofilm and planktonic samples become evident. The biofilm sample has several peaks in the region from 245 – 300 mass range that are not present within the planktonic sample. Another difference is the intense peak at a *m/z* of 116 in the biofilm spectra that is absent in the planktonic.

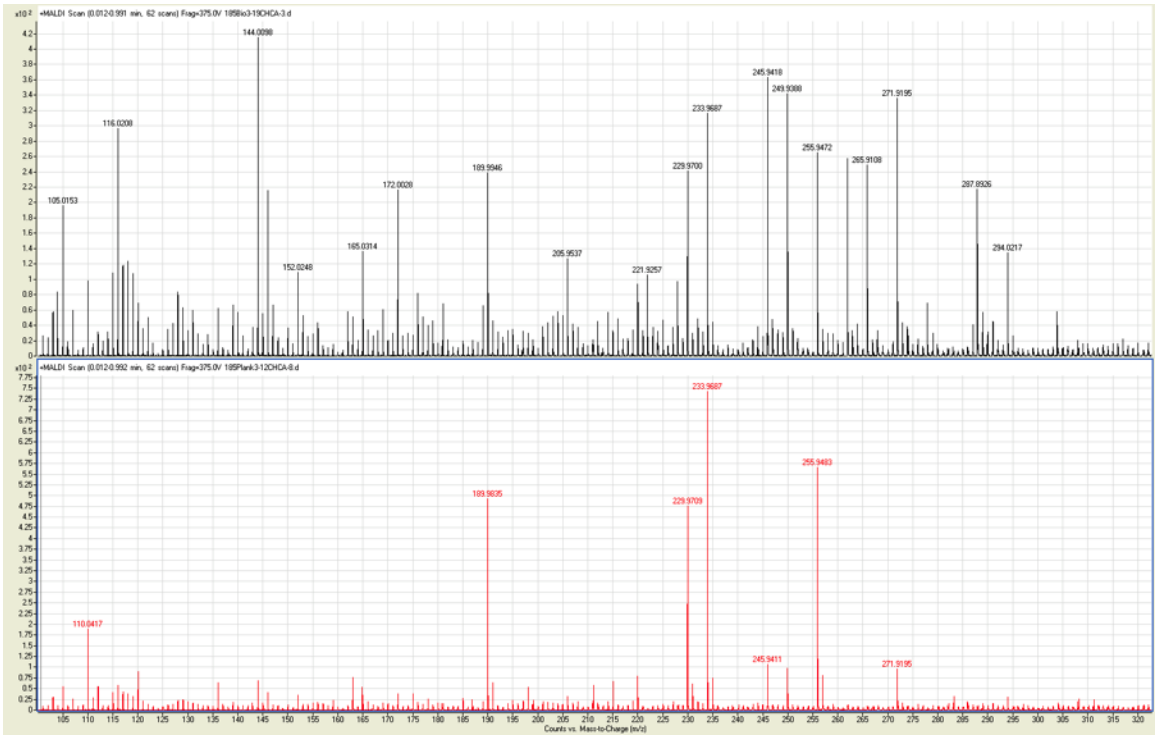

Figure 6.4. Magnified portion of spectra m/z 100 – 320 biofilm (top) planktonic (bottom)

The differences highlighted within this section between the biofilm and the planktonic forming bacteria spectra confirm that the cell wall components of the two types of bacteria are different. This data indicates that the suspicions that it is in fact the cell walls of the bacteria that vary resulting in different type of bacterial colonies being formed, either a biofilm formation or a planktonic colony formation are correct.

6.3.2. Spectra from 195 Strain

As was the case with the 185 strain of bacterial cell wall extracts, clear spectra with good intensity were collected from samples of the 195 strain of bacteria. Analysis of this strain was completed using the same methodology that was used for the 185 strain of bacteria. Figure 6.5. is a stacked spectra of the 195 biofilm forming

bacteria. The five different spectra contained in figure 6.5. show consistency among the analyzed sample. Each of these spectra were collected from different sample spots on the MALDI target. The samples showed consistent spectra indicating that the sample was uniform. Figure 6.6. is stacked spectra of 195 planktonic colony

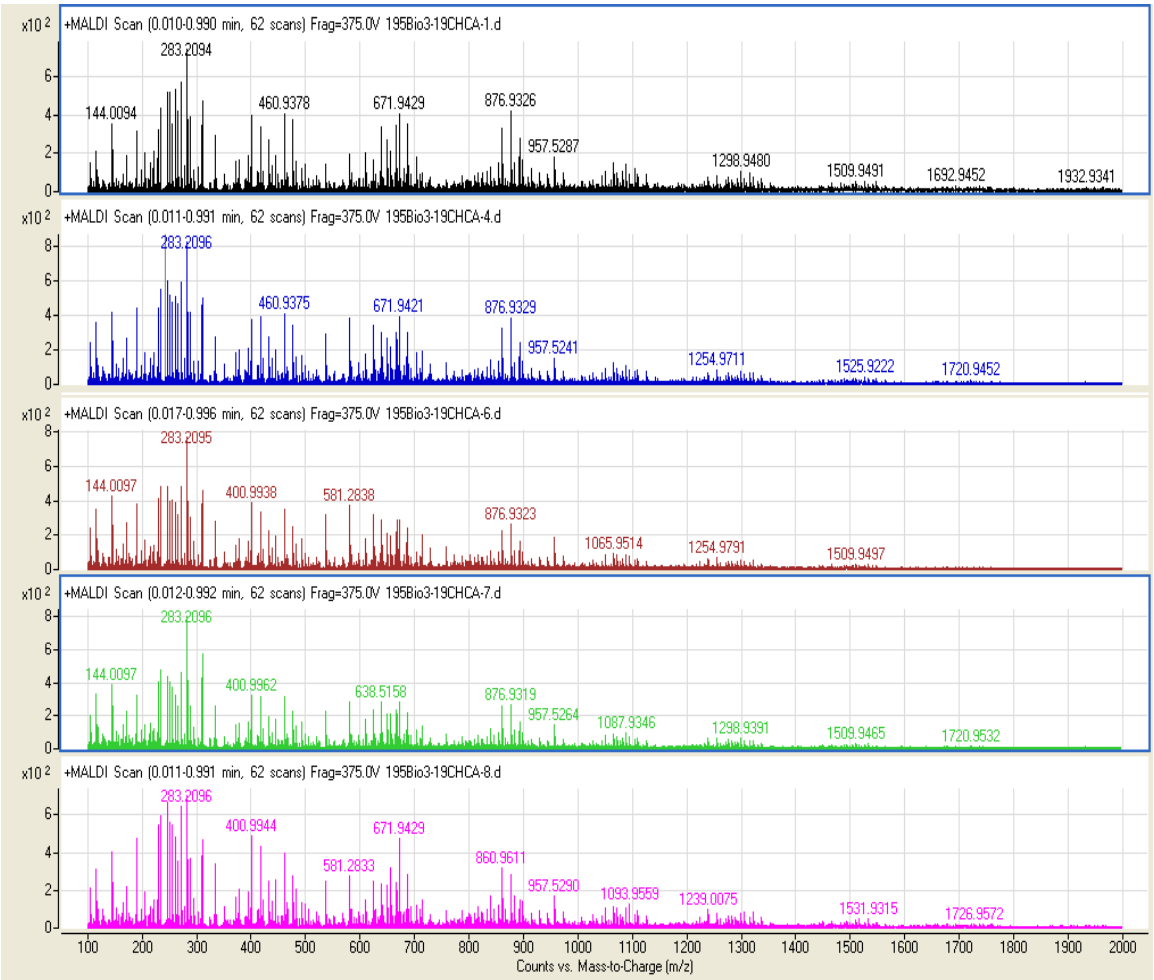

Figure 6.5. Stacked spectra of 195 biofilm

bacteria. As observed in figure 6.6. the spectra are consistent despite originating from different spots on the target. This consistency is important for accurate analysis.

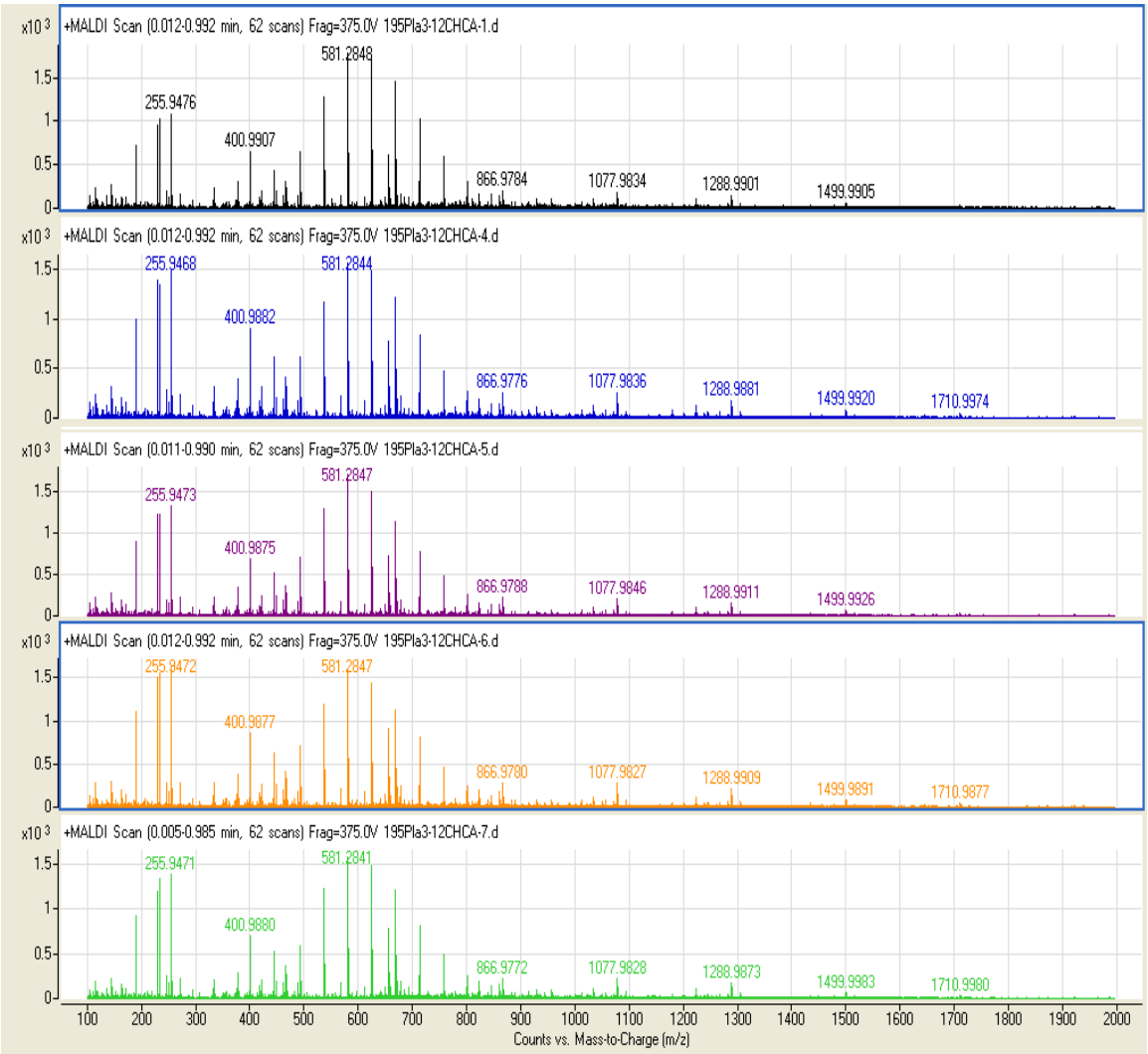

Figure 6.6. Stacked spectra of 195 planktonic

Figure 6.7. is a zoomed in section of the spectra to allow for peak comparison between the biofilm and planktonic forming bacteria cell wall extracts.

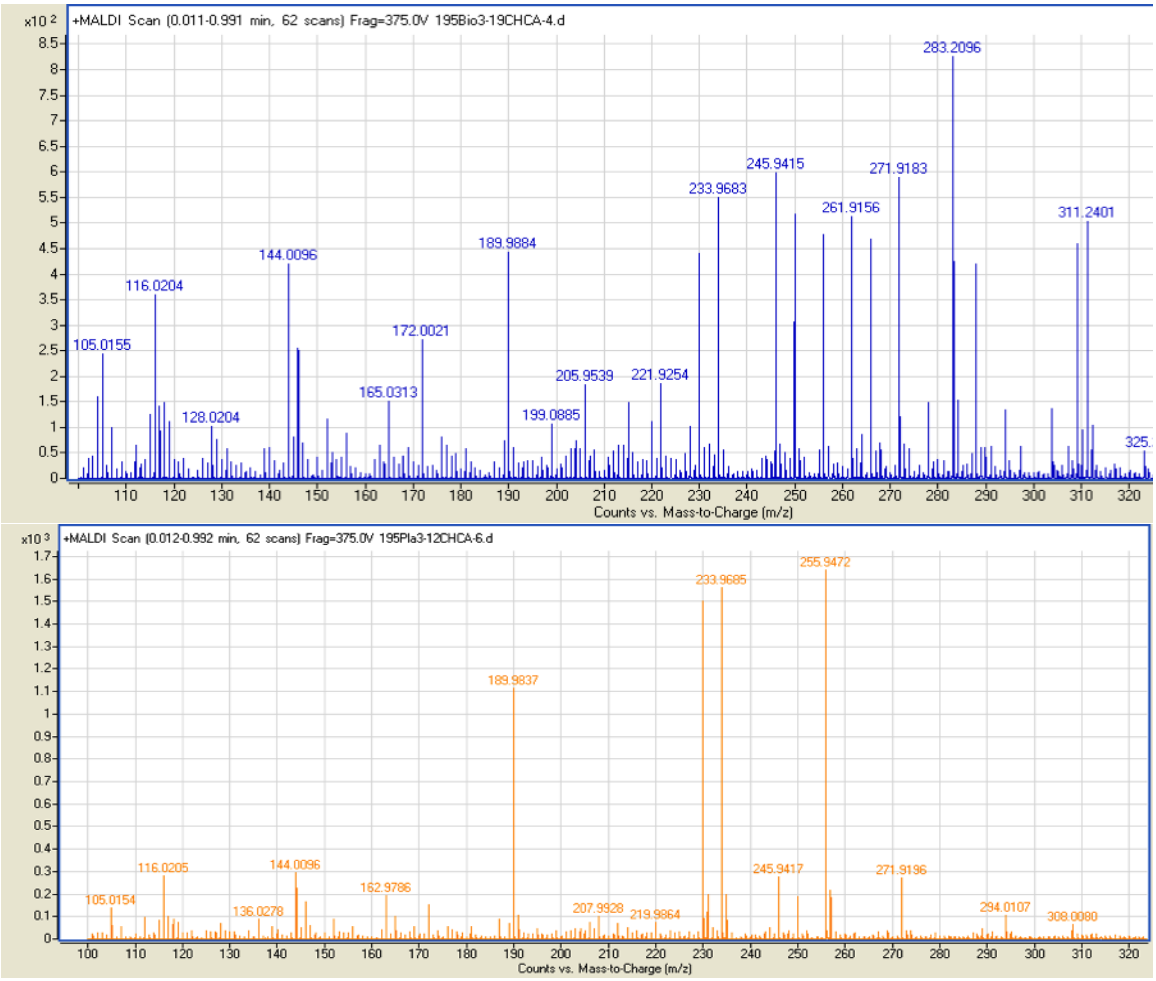

Figure 6.7. Magnified portion of spectra m/z 100 – 320 biofilm (top) planktonic (bottom)

Within the magnified portion of the spectra, *m/z* range 100 – 320, the differences between the two forms of bacteria become apparent. The range between *m/z* 160 – 315 have quite a few differences in the peaks present. Figure 6.8. is another magnified portion of spectra. This magnified portion of spectra shows dramatic

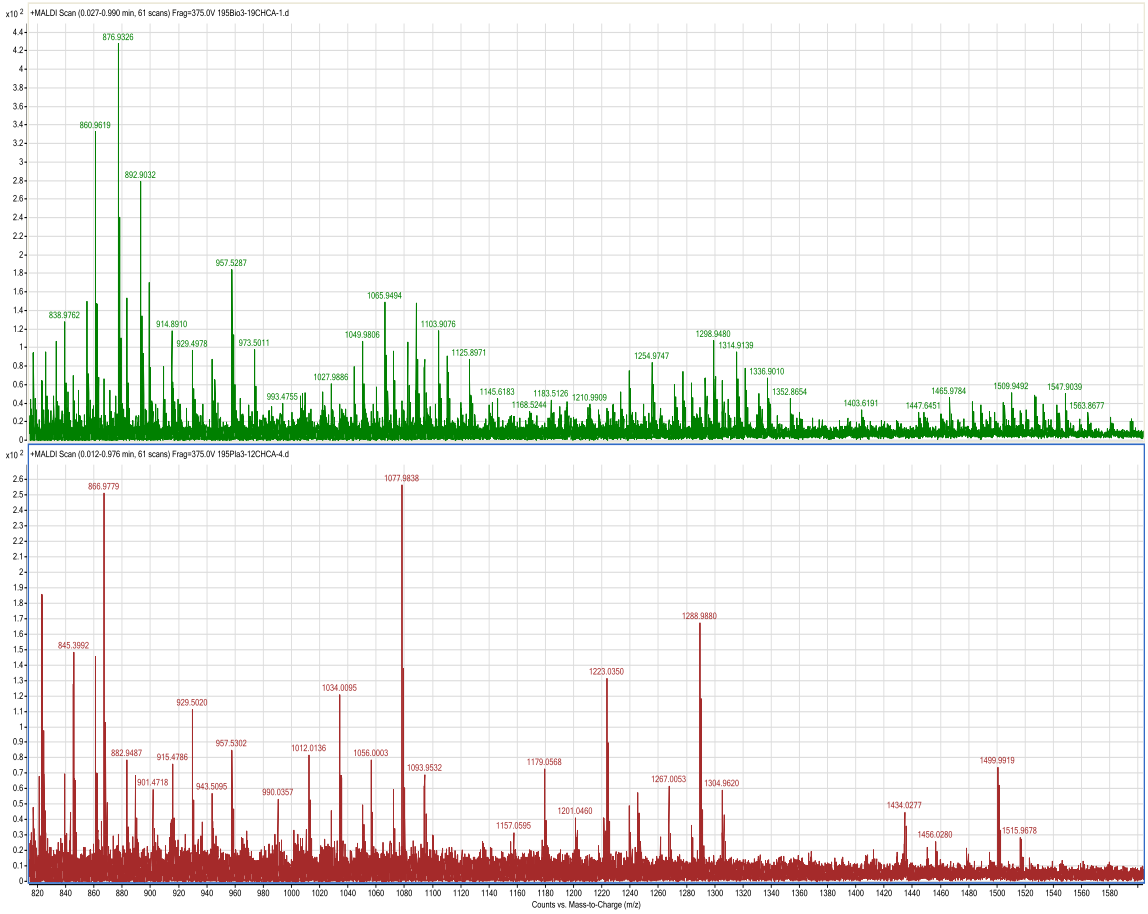

Figure 6.8. Magnified portion of spectra m/z 820 – 1585 biofilm (top) planktonic (bottom)

differences between the sample spectra. The biofilm spectra contains groupings of mulitple peaks while the planktonic spectra has a similar pattern but the peaks in each grouping are not as numerous. These groupings have even spacing of 211 amu, indicating that this is likely a polysaccharide. It is known that polysaccharide chains can contain differing end groups which would explain the grouping of spectral peaks.

Figure 6.10 is another magnified portion of the spectra from 1170 – 1380 *m/z*. Once again numerous peak differences are observable.

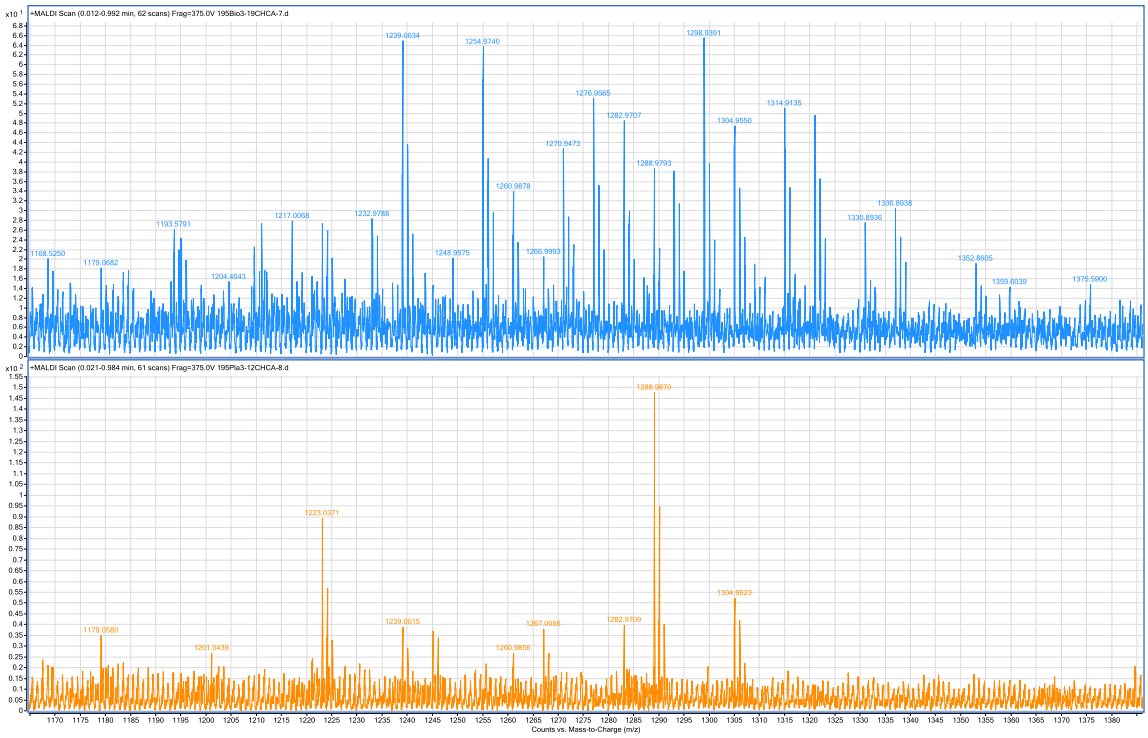

Figure 6.9. Magnified portion of spectra m/z 1170 – 1380 biofilm (top) planktonic (bottom)

As with the 185 strain of the bacteria, the 195 strain has significantly different spectra indicating that the cell walls are composed of completely different components. The spectra indicates that there is a significant future for investigating the differences within bacteria that lead them to either form biofilms or normal planktonic colonies as they grow. This information, once elucidated, can enable the development of materials that will hinder biofilm formation. It is critical to understand how a bacteria is adhering and forming onto a surface to be able to take steps to alter and prevent the formation.

6.4. Conclusion

This study was successful in the analysis of bacterial cell wall extracts. Samples were analyzed using AP – MALDI-TOF-MS to determine if there were distinguishable peaks that varied between the biofilm forming bacteria and planktonic colony forming bacteria. Clear spectra with peaks of good intensity were produced by both strains of bacteria and by biofilm and planktonic bacteria. The produced spectra were then used to compare the biofilm and planktonic bacteria of each strain. Both strains presented peaks that were not present in both biofilm and planktonic bacteria spectra indicating that there are component differences within the cell walls of the different forms of bacteria.

Investigation of the various differences between the biofilm and planktonic cell walls would be a good future direction of this project. With this work the first objective of using AP – MALDI to analyze the cell wall extracts was successful and to a great degree. This success provides promise of good results in future analyses of these samples.

References:

1. Friedrich Gotz, Staphylococcus and biofilms. *Molecular Microbiology* **2002,***43* (6), 1367-1378.
2. Christine Heilmann, O. S., Christiane Gerke, Nongnuch Vanittanakom, Dietrich Mack, Friedrich Gotz,, Molecular basis of intercellular adhesion in the biofilm-forming *Staphylococcus epidermidis*. *Molecular Microbiology* **1996,***20* (5), 1083-1091.
3. Christensen, G. D.; Simpson, W. A.; Bisno, A. L.; Beachey, E. H., Adherence of slime-producing strains of Staphylococcus epidermidis to smooth surfaces. *Infect. Immun.* **1982,***37* (1), 318-326.
4. Sadovskaya, I.; Vinogradov, E.; Flahaut, S.; Kogan, G.; Jabbouri, S., Extracellular Carbohydrate-Containing Polymers of a Model Biofilm-Producing Strain, Staphylococcus epidermidis RP62A. *Infect. Immun.* **2005,***73* (5), 3007-3017.
5. McKenney, D.; Hubner, J.; Muller, E.; Wang, Y.; Goldmann, D. A.; Pier, G. B., The ica Locus of Staphylococcus epidermidis Encodes Production of the Capsular Polysaccharide/Adhesin. *Infect. Immun.* **1998,***66* (10), 4711-4720.
6. Costa, A.; Henriques, M.; Oliveira, R.; Azeredo, J., The role of polysaccharide intercellular adhesin (PIA) in Staphylococcus epidermidis adhesion to host tissues and subsequent antibiotic tolerance. *European Journal of Clinical Microbiology & Infectious Diseases* **2009,***28* (6), 623-629.
7. Lehninger, A. L.; Nelson, D. L.; Cox, M. M., *Lehninger Principles of Biochemistry*. W.H. Freeman: 2005.
8. Darouiche, R. O., Treatment of Infections Associated with Surgical Implants. *N Engl J Med* **2004,***350* (14), 1422-1429.
9. Uckay, I.; Pittet, D.; Vaudaux, P.; Sax, H.; Lew, D.; Waldvogel, F., Foreign body infections due to *Staphylococcus epidermidis*. *Annals of Medicine* **2008,***99999* (1), 1 - 11.
10. Jean-Claude Theis, S. G., Jonathan White,, FACTORS AFFECTING IMPLANT RETENTION IN INFECTED JOINT REPLACEMENTS. *ANZ Journal of Surgery* **2007,***77* (10), 877-879.
11. Jetten, A. M.; Vogels, G. D., Nature and Properties of a Staphylococcus epidermidis Bacteriocin. *J. Bacteriol.* **1972,***112* (1), 243-250.

Chapter 7.

Conclusions

7.1 Sample Deposition's Effect on MALDI Quantitation

It was found that the sample deposition method used not only significantly influences the intensity and reproducibility of the signal produced, but also influences the outcome of analyte quantitation. In all of the three analytes used it was found that ESD was superior for accurate and precise quantitation. In two samples, the meperidine and the rapamycin it was discovered that the hand spotting method produced more accurate results than the nanospotter method but in the case of the glyphosate the nanospotter was found to produce more accurate results than the hand spotting. This would also explain the error within the quantitation of the samples because good signal intensity is essential for an accurate sample quantitation and the standard deviation for the samples demonstrates the spot to spot variability. The data is clear that the ESD method is the superior method of the three methods tested for accurate and precise quantitation of these analytes. ESD with IDMS was also found to consistently produce quantitation errors that were significantly lower than other previously published studies.

7.2. Synthetic Polymer Analysis

This study of synthetic polymers has provided a great deal of information about analyzing synthetic polymers using AP – MADLI-TOF-MS. It was determined that for the analysis of PEG 550 the MAC ratio that gives the best sample signal intensity is one that has a moderately higher matrix and cationizing agent concentration but the poorest intensity was observed whenever the ratio consisting of a matrix and cationizing agent concentration was much greater than the amount of analyte. PEG 1430 and 2064 both preferred a MAC ratio using equal amounts of matrix analyte and cationizing agent and performed poorly whenever a ratio that used a greater concentration of matrix and cationizing agent than analyte. The fact that both PEG 1430 and 2064 favored and hindered by the same ratios could be due to them having larger M_n's. The analysis of PS 870 showed a preference for a MAC ratio that kept the matrix and analyte at the same concentration but contained significantly less cationizing agent. Poor signal was obtained whenever a ratio with matrix and cationizing agent significantly lower than the analyte was used. PS 1300 had most intense signal with equal amounts of matrix and analyte with slightly lower cationizing agent added and the ratio that resulted in the weakest signal was a ratio that used equal amounts of matrix and analyte but had significantly lower volume of cationizing agent. The PS 2100 signal was best when equal amounts of matrix and analyte with significantly less cationizing agent was used, which was unique from the other PS samples. PS 2100 had the lowest sample signal whenever a ratio was used that contained barely any of the cationizing agent. Among the PS samples, each

M_n had different ratios that it found to produce the most intense and weakest signal. These results confirmed the suspicion that the ratio of matrix:analyte:cationizing agent would have significant impact upon the resulting signal intensity. Overall it seemed that both the PEG and the PS was best analyzed whenever the amount of matrix and analyte were combined close to the same values. The amount of cationizing agent that was added to the samples seemed to have a considerable impact upon the spectral intensity. The PEG required more of the cationizing agent, NaTFA, and the best spectra resulted whenever the amount of cationizing agent was approximately the same as the amounts of the matrix and analyte within the sample solution. The PS had a different trend from the PEG. The PS had better signal whenever the amount of the cationizing agent, AgTFA, was approximately half (or less) the amount of matrix and analyte that was added to the solution. The PS required the amount of matrix to be kept high, while the amounts of the cationizing agent had to be balanced at different amounts that were less than equal to the amounts of the other sample components, but greater than 0. The ratio of sample components must be carefully selected to achieve the desired signal intensity.

Peak shifting was also discovered to occur as the MAC ratio was changed. This alteration of spectra can be attributed to MSE. While MALDI MS provides invaluable information regarding the physical structure of synthetic polymers, this study highlights the importance of proper sample preparation in order to produce spectra that not only elucidates structure but also accurately represents the synthetic polymer's physical properties.

More investigation is required to determine whether the trend seen here would still be present whenever the samples were analyzed by vacuum MALDI-TOF-MS. Another approach for further investigation could be to explore whether a matrix such as DHB would produce the same effects. While there are definitive conclusions that can be made about the research that has been done, there is always the potential to unlock more answers by following up this research project with another to fully analyze the trends and effects that are occurring.

7.3 Analysis of In-tact Carpet Fibers

It was determined that both CHCA and DCTB matrixes were suitable for the analysis of the different carpet fibers. The carpet fibers were analyzed and it was determined that the polymer additives could be detected using MALDI. Different carpet samples from different manufacturers were analyzed successfully. It has been discovered that both CHCA and DCTB matrixes were able to be applied for this analysis and each matrix provided sample peaks that differed from the other. These unique differences were useful in providing more information on the chemical additives that are used in the manufacture of carpet fibers. While the additives are considered proprietary and are not readily identifiable, these unique additives give the fibers a signature that is unique to its manufacturer. This was observed within the spectra, as each contained peaks that were different from the other nylon fibers. The analyzed fibers consistently produced spectra that were similar when a fiber from the same carpet sample was tested yet produced different spectra whenever fiber samples from the different brands of fibers were analyzed. While more work will be needed to firmly establish this type of analysis method for carpet fiber

evidence, this preliminary work demonstrates that more research has the strong potential for success.

7.4 Glutathione Analysis

It was determined that reduced and oxidized glutathione could be analyzed using MALDI. Good intensity spectra were obtained with protonated, sodiated and passiated glutathione present. Once the instrument parameters were optimized, limit of detection was accomplished for both forms of glutathione. It was determined that for both GSH and GSSG, 20 ppm was the limit of detection. This limit of detection study was carried out using serially diluted standard solutions. While this study was successful in that both species of glutathione were detected it has also shed light upon the fact that in order for speciated glutathione analysis of blood to be completed a procedure that involves a concentrating of the sample will be necessary. The limit of detection for GSSG is below the levels usually found in human blood.

7.5. Analysis of Biofilm Forming Bacteria

This study was successful in the analysis of bacterial cell wall extracts. Samples were analyzed using AP – MALDI-TOF-MS to determine if there were distinguishable peaks that varied between the biofilm forming bacteria and planktonic colony forming bacteria. Clear spectra with peaks of good intensity were produced by both strains of bacteria and by biofilm and planktonic bacteria. The produced spectra were then used to compare the biofilm and planktonic bacteria of each strain. Both

strains presented peaks that were not present in both biofilm and planktonic bacteria spectra indicating that there are component differences within the cell walls of the different forms of bacteria.

Investigation of the various differences between the biofilm and planktonic cell walls would be a good future direction of this project. With this work the first objective of using AP – MALDI to analyze the cell wall extracts was successful and to a great degree. This success provides promise of good results in future analyses of these samples.